Chronic Dietary Supplementation of Branched-Chain Amino Acids Does Not Attenuate Muscle Torque Loss in a Mouse Model of Duchenne Muscular Dystrophy

Justin E. Sperringer

Dissertation submitted to the faculty of the Virginia Polytechnic Institute and State University in partial fulfillment of the requirements for the Doctor of Philosophy in Human Nutrition, Foods, & Exercise

Advisory Committee:

Committee Chair – Susan Hutson

Committee Co-Chair – Matthew Hulver

Robert Grange

Dongmin Liu

Samer El-Kadi

August 2nd, 2019

Blacksburg, VA

Keywords: Duchenne Muscular Dystrophy; dystrophin; dystrophin glycoprotein complex; amino acids; branched-chain amino acids; leucine; isoleucine; valine; mTOR; skeletal muscle; muscle function

Chronic Dietary Supplementation of Branched-Chain Amino Acids Does Not Attenuate Muscle Torque Loss in a Mouse Model of Duchenne Muscular Dystrophy

Justin E. Sperringer

Academic Abstract

Duchenne Muscular Dystrophy (DMD) is an X-linked recessive, progressive muscle-wasting disease characterized by mutations in the *dystrophin* gene. Duchenne muscular dystrophy is the most common and most severe form of inherited muscle diseases, with an incidence of 1 in 3,500 male births[1,2]. Mutations in the dystrophin gene result in non-functional dystrophin or the complete absence of the protein dystrophin, resulting in necrosis and fibrosis in the muscle, loss of ambulation, cardiomyopathies, inadequate or failure of respiratory function, and decreased lifespan. Although there has been little research for effective nutritional strategies, dietary intervention may be effective as an adjuvant treatment. In this study, wild type (WT) and *mdx* animals were provided either a control or elevated branched chain amino acid (BCAA) diet nocturnally for 25 weeks to determine if the elevated BCAAs would attenuate muscle torque loss.

Twenty-five weeks of chronic, elevated BCAA supplementation had no impact on muscle function measures. Interestingly, *mdx* and WT animals had the same torque responses in the low stimulation frequencies (1 Hz – 30 Hz) compared to higher stimulation frequencies. Tetanus was reached at a much lower stimulation frequency in *mdx* animals compared to WT animals (100 Hz vs +150 Hz). The *mdx* mouse consistently had more cage activity in the light cycle X- and Y-planes. Interestingly, animals on the BCAA diet increased X-, Y-, and Z-plane activity in the dark cycles at four weeks while animals on the control diet more Z-plane activity at 25 weeks, although not significant. All three BCAAs were elevated in the plasma at 25 weeks, although only Leu was significantly elevated. The BCAAs had no effect on. The diaphragm and skeletal muscle masses were larger in *mdx* animals, and WT animals had a significantly larger epididymal fat pad. The active state of BCKDC determined by phosphorylation of the E1α enzyme was greater in WT animals in white skeletal muscle, but not red skeletal muscle. Protein synthesis effectors

of the mTORC1 signaling pathway and autophagy markers were similar among groups. Wild type animals had increased mTORC1 effectors and animals on the BCAA diet had decreased autophagy markers, although not significant.

Although BCAAs did not affect muscle function, fibrosis, or protein synthesis effectors, this study illustrates the functionality of *mdx* muscles over time. It would be interesting to see how the different muscle fiber types are affected by DMD, noting the differences between the diaphragm, heart, red muscle, and white muscle fibrosis markers. Although there was no increase in mTORC1 effectors with an elevated BCAA diet, it would be interesting to determine muscle protein synthesis, myofibrillar protein synthesis, and total protein turnover in the *mdx* mouse with an elevated BCAA diet, although the dietary intervention started when mice arrived at 4 weeks of age, earlier intervention may be beneficial early in the disease process.

Chronic Dietary Supplementation of Branched-Chain Amino Acids Does Not Attenuate Muscle Torque Loss in a Mouse Model of Duchenne Muscular Dystrophy

Justin E. Sperringer

General Audience Abstract

Duchenne Muscular Dystrophy (DMD) is an X-linked recessive, progressive muscle-wasting disease characterized by mutations in the *dystrophin* gene. Duchenne muscular dystrophy is the most common and most severe form of inherited muscle diseases, with an incidence of 1 in 3,500 male births[1,2]. Mutations in the dystrophin gene result in non-functional dystrophin or the complete absence of the protein dystrophin, resulting in necrosis and fibrosis in the muscle, loss of movement and walking ability, cardiomyopathies, inadequate or failure of respiratory function, and decreased lifespan. Although there has been little research for effective nutritional strategies, dietary intervention may be effective as an adjuvant treatment and palliative care. The branched chain amino acids (BCAAs) are known to directly stimulate muscle protein synthesis by direct activation of the mechanistic target of rapamycin complex 1 (mTORC1). This study aimed to illustrate the differences between diseased and healthy mice and determine if BCAAs can reduce muscle torque loss.

Twenty-five weeks of chronic, elevated BCAA supplementation had no impact on muscle function measures. Interestingly, *mdx* and WT animals had the same torque responses in the low stimulation frequencies (1 Hz – 30 Hz) compared to higher stimulation frequencies. Tetanus was reached at a much lower stimulation frequency in *mdx* animals compared to WT animals (100 Hz vs +150 Hz). The *mdx* mouse consistently had more cage activity in the light cycle X- and Y-planes. Interestingly, animals on the BCAA diet increased X-, Y-, and Z-plane activity in the dark cycles at four weeks while animals on the control diet more Z-plane activity at 25 weeks, although not significant. All three BCAAs were elevated in the plasma at 25 weeks, although only Leu was significantly elevated. The BCAAs had no effect on. The diaphragm and skeletal muscle masses were larger in *mdx* animals, and WT animals had a significantly

larger epididymal fat pad. The active state of BCKDC determined by phosphorylation of the E1α enzyme was greater in WT animals in white skeletal muscle, but not red skeletal muscle. Protein synthesis effectors of the mTORC1 signaling pathway and autophagy markers were similar among groups. Wild type animals had increased mTORC1 effectors and animals on the BCAA diet had decreased autophagy markers, although not significant.

Although BCAAs did not affect muscle function, fibrosis, or protein synthesis effectors, this study illustrates the functionality of *mdx* muscles over time. It would be interesting to see how the different muscle fiber types are affected by DMD, noting the differences between the diaphragm, heart, red muscle, and white muscle fibrosis markers. Although there was no increase in mTORC1 effectors with an elevated BCAA diet, it would be interesting to determine muscle protein synthesis, myofibrillar protein synthesis, and total protein turnover in the *mdx* mouse with an elevated BCAA diet, although the dietary intervention started when mice arrived at 4 weeks of age, earlier intervention may be beneficial early in the disease process.

Table of Contents

Dedication

First and foremost, I would like to express how truly grateful and thankful I am for my family. This degree would not be possible without their continued, unwavering support. They were with me every step of the way, kept me motivated, and grounded. I would like to express how grateful I am for my advisor, Dr. Susan Hutson. Without her guidance, academic, and personal support, this degree would not be possible. She is always there for support and pushes me to do my best. I am especially grateful and thankful to have had Dr. Adele Addington as my mentor and teacher – no one could ask for a better person or mentor. I would like to thank my committee for their patience, support, and assistance. I thank the entire faculty and staff of the Department of Human Nutrition, Foods, & Exercise. I want to thank Dr. Donna Westfall-Rudd, Dr. Matthew Hulver, Dr. Deborah Good, Dr. Robert Grange, Dr. Janet Rankin, Dr. Jay Williams, and the College of Agriculture and Life Sciences Graduate Teaching Scholars program for their assistance in academic teaching and advising. I would also like to thank Mrs. Haiyan Zhang for her mentoring and assistance.

Abbreviations

4E-BP1 – eIF4E binding protein 1

AAs – amino acids

ACE – angiotensin converting enzyme

Akt – protein kinase B

ALT – alanine aminotransferase

ANOVA – analysis of variance

AST – aspartate aminotransferase

β-Ala – beta alanine

BCAAs – branched chain amino acids

BMD – Becker muscular dystrophy

CAMKII – Ca+2-calmodulin-dependent protein kinase II

CGH – comparative genomic hybridization

Cit – citrulline

CK – creatine kinase

CMDs – congenital muscular dystrophies

CRISPR/Cas9 – clustered regularly interspaced short palindromic repeats/CRISPR-associated protein 9

DGC – dystrophin glycoprotein complex

DMD – Duchenne muscular dystrophy

ECM – extracellular matrix

EGCG – epigallocatechin gallate

eIF4E – eukaryotic initiation factor 4E

EMA – European Medicines Agency

FDA – Food & Drug Administration

GAP – GTPase activating protein

GEF – guanine nucleotide exchange factor

Grb2 – Growth factor receptor-bound protein 2

HDR – homology-directed repair

HPLC – high performance liquid chromatography

HOP – hydroxyproline

IGF-1 – insulin-like growth factor 1

LGMDs – limb-girdle muscular dystrophies

MAP/MAPK – mitogen-activated protein kinase

MDC1A – merosin-deficient congenital muscular dystrophy type 1A

MG53 – Mitsugumin 53

MLPA – multiplex ligation-dependent probe amplification

MMEJ – microhomology end joining

MTJ – myotendinous junction

mTORC1 – mechanistic target of rapamycin complex 1

MuSK – muscle-specific kinase

NDA – new drug application

NMJ – neuromuscular junction

NHEJ – non-homologous end joining

NMR – nuclear magnetic resonance

nNOS – neuronal nitric oxide synthase

Orn – ornithine

PGC-1α – PPARγ coactivator-1 alpha

PI3K – phosphoinositide 3-kinase

PIP2 - phosphatidylinositol 4,5-bisphosphate

PKA – protein kinase A

PKC – protein kinase C

PKG – protein kinase G

PP2A – protein phosphatase 2A

PPARγ – peroxisome proliferator-activated receptor gamma

PVDF – polyvinylidene difluoride

Rag – ras-related GTP binding

RT-PCR – reverse transcriptase polymerase chain reaction

RVD – repeat variable di-residues

S6K1 – p70 ribosomal S6 kinase 1

SEM – standard errors of the means

TALEN – transcription activator-like effector nucleases

Tau – taurine

TGF-β – transforming growth factor-β

TIF-IA – transcription initiation factor IA

TNF-α – tumor necrosis factor-α

TSC – tuberous sclerosis complex

UGC – utrophin glycoprotein complex

v-ATPase – vacuolar H^+-ATPase

WT – wild type

ZFN – zinc finger nucleases

List of Figures

CHAPTER TWO

CHAPTER THREE

SUPPLEMENTARY FIGURES

CHAPTER ONE

Introduction

Duchenne muscular dystrophy (DMD) is an X-linked recessive, progressive muscle-wasting disease characterized by mutations in the *dystrophin* gene[1,2]. Duchenne muscular dystrophy is the most common and most severe form of inherited muscle diseases, with an incidence of 1 in 3,500 male births[1,2]. Mutations in the dystrophin gene result in non-functional or the absence of the protein dystrophin, resulting in necrosis and fibrosis in the muscle, loss of ambulation, cardiomyopathies, inadequate or failure of respiratory function, and decreased lifespan[1,2]. There is no cure for DMD, with most treatment options focused on improving quality of life through symptom treatment and palliative care[3].

Glucocorticoids are the only pharmacological treatment for DMD to slow the decline of muscular strength and function, primarily through reducing inflammation[4,5]. Gene therapies are now at the forefront of DMD treatment. Microdystrophins, truncated versions of the *dystrophin* gene that contain essential domains of the dystrophin protein, have been shown to restore dystrophin expression and stabilize clinical symptoms in dog models of DMD and are currently in clinical trials[6]. Inhibition of myostatin, an inhibitor of muscle growth, has had limited success in human studies improving the six-meter walk test (6MWT), reducing fibrosis, and inducing hypertrophy[7].

Stop codon read-through agents and exon-skipping agents have been studied with mixed results, with gene editing strategies emerging as the new avenue of research[4]. The CRISPR/Cas9 genome editing system has shown promising results in editing the genome and restoring dystrophin in *mdx* mice and human cell lines, significantly improving dystrophin expression, histology, and muscle function[8,9]. The system is not at the clinical stage for DMD and undesired insertions and deletions can occur in off-target sites[10-12].

Although there has been little research for nutritional strategies, dietary intervention may be effective as an adjuvant treatment and palliative care[3]. The branched-chain amino acids (BCAAs; Leu, Ile, Val),

particularly Leu, have been shown to increase protein synthesis through the activation of the mechanistic target of rapamycin complex 1 (mTORC1)[13-15].

It was hypothesized that the chronic elevated BCAAs would attenuate muscle function and strength loss by stimulating muscle protein synthesis through mTORC1 effectors. Specifically, maximal torque production and torque production at increasing stimulation frequencies will be improved in animals on the BCAA diet. Tissue fibrosis was expected to be reduced in animals on the BCAA diet. Plasma and tissue BCAAs are expected to be elevated in animals on the BCAA diet. It is also expected that autophagy markers will be reduced in *mdx* animals on the BCAA diet.

CHAPTER TWO

Duchenne Muscular Dystrophy

Clinical description

The initial observations in patients subsequently diagnosed with DMD are muscular weakness and abnormal motor function, such as the inability to rise from the floor (Gower's grade), with the patient "climbing" to the standing position[5,16]. Delayed onset of walking, frequent falling, and difficulty running and climbing stairs are some of the initial symptoms of DMD[5]. Most DMD patients are diagnosed with the disease around five years of age through genetic testing[5,16,17]. The inability or a delay in the ability to use language has also been identified in screening for DMD[5,18].

Patients with DMD present with an increased serum creatine kinase (CK) and an increase in serum alanine aminotransferase (ALA) and aspartate aminotransferase (AST)[5]. Newborn screening is limited to CK assays on dried blood samples over time as signs and symptoms of the disease develop with age[19]. Dried blood spots are obtained from a heel or finger prick that is blotted onto a filter paper that allows small volume sampling and for the ease of sampling, transporting, and analysis of blood samples that maintain the stability of DNA, RNA, and proteins within the sample[20]. Normal CK levels are <200 U/L, with DMD patients having CK levels up to 100 times the normal levels[17]. Similarly, ALT and AST can be over 10 and over 20 times the normal levels (7 – 55 U/L & 8 – 60 U/L, respectively)[21]. High levels of serum ALT and AST are not limited to DMD, as high levels are also biomarkers of other diseases, such as hepatocellular disease and pancreatitis[21,22]. Abnormal CK levels, which are indicative of cardiac injury and skeletal muscle injury, with concomitant increases in serum ALT and AST are indicative of myopathies[21,22].

Diagnosis

Deletion of one or more exons in the *dystrophin* gene is the cause of DMD in approximately 65% of all patients and duplication of one or more exons accounting for 6% – 10%; missense, nonsense, splice

variants, insertions and deletions, and small inversions account for the remainder of the cases[23]. Complex rearrangements of the gene and deep intronic changes to the gene are also observed but constitute a small fraction of DMD cases[23-25]. Multiplex ligation-dependent probe amplification (MLPA) is the most commonly used tool for the diagnosis of deletion/duplication mutations in DMD, as it can quantify all 79 exons in the *dystrophin* gene[23,26].

Comparative genomic hybridization (CGH) is an oligonucleotide-based array that identifies the presence of copy number variants, large DNA segments of variable copies in comparison to a reference genome, in the entire *dystrophin* gene[23]. This method also maps the intronic 3' and 5' flanking regions of *dystrophin*, allowing CGH to detect complex rearrangements, intron alterations, and specific mutation break-points[23-25]. By using multiple probes in CGH, it guarantees mutations are detected and reduces false-positive results due to short nucleotide polymorphisms[23]. Complex rearrangements and deep intronic mutations, harmful DNA variants located over 100 base pairs away from exon-intron junctions that often lead to pseudo-exon inclusion attributed to the activation of non-canonical splice sites, splice variants, changes in splicing regulatory elements, and non-coding RNA genes, may not be identified using CGH, requiring muscle RNA analysis via RT-PCR for diagnosis[23,27,28].

Dystrophin

The *dystrophin* gene is the largest known, covering 2.5 Mb of genomic DNA and consisting of 79 exons[29-31]. The full-transcript mRNA encodes the 3,685-amino acid dystrophin protein of 427 kDa[29,30]. In Becker Muscular Dystrophy (BMD), mutations in the *dystrophin* gene result in a semi-functional dystrophin protein, while DMD results in non-functional dystrophin or complete loss of the protein[29,32]. Dystrophin is an intracellular rod-shaped protein, localized to the inner surface of the sarcolemma and is highly expressed at costameres, proteins that anchor the sarcomere to the cell membrane, particularly at the myotendinous junction (MTJ) and the neuromuscular junction (NJM)[29,31,32]. With its subcellular location within the muscle

fiber and the high expression of dystrophin in areas of cell-to-cell contact, it is thought that dystrophin protects the muscle during mechanical stress as well as being involved in cellular signaling (Figure 1)[29,31,32].

Expression of dystrophin is controlled by three different promoters – brain, muscle, and Purkinje, which consist of unique first exons spliced to a common set of 78 exons[30]. Expression of the brain promoter primarily expresses dystrophin in the hippocampus and cortical neurons of the brain, the Purkinje promoter in cerebellar Purkinje cells and skeletal muscle, and the muscle promoting expression in skeletal, cardiac, and smooth muscle with low expression in brain astroglia[30,33].

The dystrophin protein binds with intracellular and extracellular membrane proteins to form a glycoprotein complex that is thought to protect muscle from mechanical stress (Figure 1)[29-32]. The carboxyl end of dystrophin contains a Cys-rich domain with a similar sequence to that of α-actinin, and two Ca^{2+} binding motifs (WW & ZZ domains)[31]. The WW domain is implicated in binding to β-dystroglycan and the ZZ domain in stabilizing the interaction between dystrophin and β-dystroglycan[31]. The central rod domain consists of several spectrin-like repeats with breaks in the pattern that form four "hinges", thought to be triple helical to provide structural integrity and flexibility and assist in actin binding[31,32]. The amino terminus of dystrophin, known as the actin binding domain, functions to link cytoskeletal f-actin to dystrophin[31,32].

The DGC also functions as a scaffold for many signaling proteins, including nNOS, PIP2, calmodulin, and grb2[34]. The DGC has also been implicated in ERK signaling, MAPK signaling, epidermal growth factor receptor-mediated signaling, and insulin signaling[34]. Additionally, the DGC is required for maintaining Ca^{+2} homeostasis as well as neurotransmitter and ion channel clustering at the NMJ[34]. See Table 1 for a list of known muscle and neuronal signaling proteins, channels, and kinases associated with the DGC (Table 1).

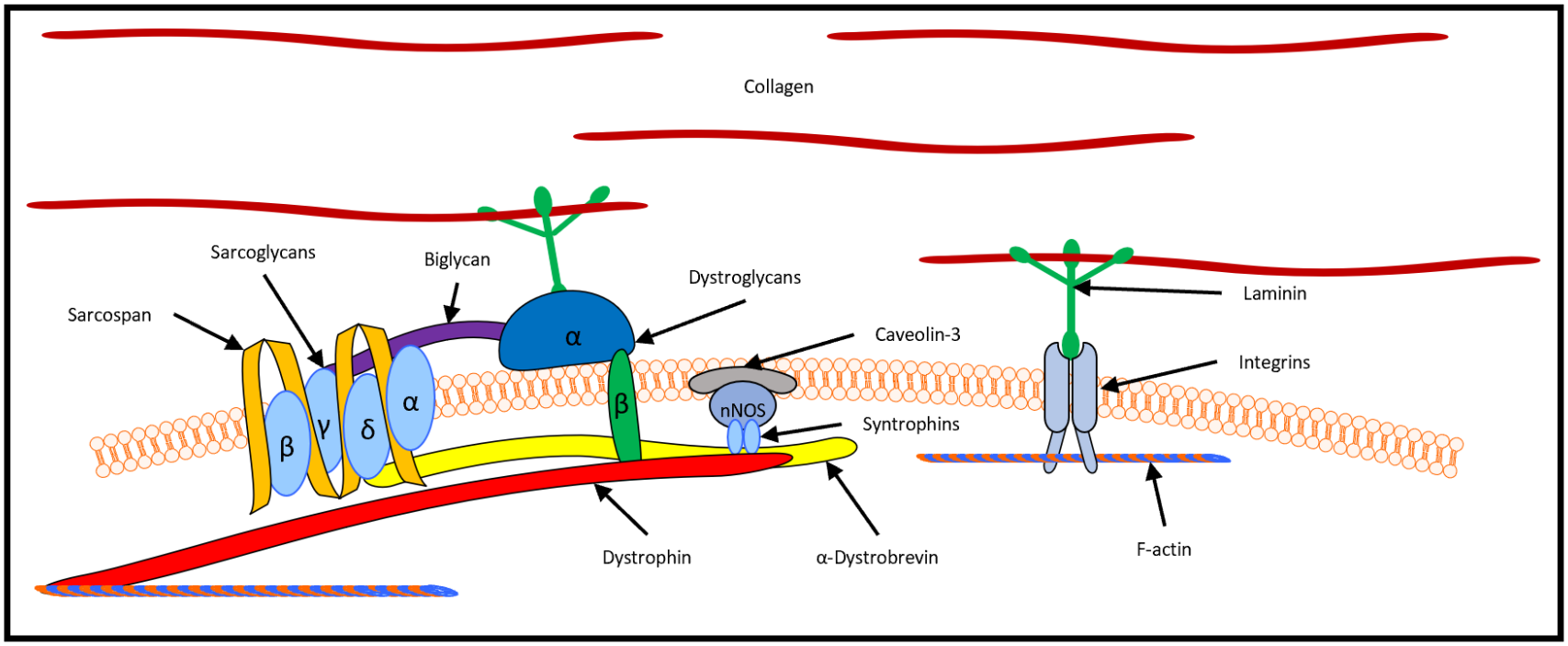

Figure 1 – Diagram of the Dystrophin Glycoprotein Complex and protein interactions[29,32,35].

Proteins & Kinases	DGC Binding Site	Function	Tissue
Calmodulin	Dystrophin	Ca^{+2} binding & signaling protein	Skeletal & cardiac muscle; Brain
nNOS	Dystrophin & α-syntrophin	Ca^{+2} & calmodulin-dependent NO synthesis	Skeletal muscle
α-Catulin	α-dystrobrevin-1	Multipurpose scaffolding protein for G protein signaling pathways	Skeletal muscle
ABCA1	Syntrophins	Cholesterol/lipid transporter	Schwann cells
Kir2.1 & Kir4.1	Syntrophins	K^{+2} channels	Skeletal & cardiac muscle; Astroglia
Aquaporin-4	α-syntrophin	Water channel	Skeletal muscle; Astroglia
Mixed-lineage leukemia 5 (MLL5)	α-syntrophin	Regulate MyoG expression	Skeletal myoblasts
Myocilin	α-syntrophin	Modulator of muscle hypertrophy pathway	Skeletal muscle
Nav 1.4 & Nav 1.5	α-syntrophin	Na^{+} channels	Skeletal & cardiac muscle
PTEN	α-syntrophin	Phosphatase and tensin homolog	Skeletal myoblasts
Stress-activated kinase 3, ERK6 & p38γ	α-syntrophin	Mitogen-activated protein kinase	Skeletal muscle
TRPC1 & TRPC4	α-syntrophin	Non-voltage-gated cation channels	Skeletal muscle
ARMS (EphA4 receptor-associated protein)	β2-syntrophin	Substrate for ephrin receptors	Skeletal muscle
SAST	β2-syntrophin	Syntrophin-associated Ser/Thr kinase related to MAST	Brain
MAST205	β2-syntrophin	Microtubule-associated Ser/Thr kinase	Skeletal & cardiac muscle; Brain
Diacylglycerol kinase zeta	γ1- & α-syntrophin	Metabolizes diacylglycerol to phosphatidic acid	Skeletal muscle
Src kinase	β-dystroglycan	Non-receptor Tyr kinase	Skeletal muscle
Tks5	β-dystroglycan	Adapter protein involved in many signaling pathways	Myoblasts
α_{1D}-Adrenergic receptor	α- & β-syntrophin	G protein receptor regulator of blood pressure	Vascular smooth muscle
MAP1A/MAP1B LC1	α-syntrophin	Microtubule-associated proteins light chain 1	Schwann cells; Brain
Cavin-1	Unknown	Central organizer of caveolae	Cardiac muscle
Ahnak1	Unknown	Scaffold protein associated with Ca^{+2}-channel β-subunit	Cardiac muscle
Cypher/ZASP	Unknown	Sarcomeric Z-line AKAP associated with L-type Ca^{+2}-channels	Cardiac muscle
CryAB	Unknown	Heat shock protein	Cardiac muscle

Table 1 – Table of the dystrophin glycoprotein complex and protein interactions in muscle and brain[36].

Dystrophin glycoprotein complex

Dystrophin is a part of a larger membrane complex that spans the sarcolemma, named the Dystrophin Glycoprotein Complex (DGC; Figure 1)[29,31]. The DGC consists of sarcoplasmic, transmembrane, and extracellular proteins and functions to link the extracellular matrix (ECM) to the cytoskeleton of cardiac and skeletal muscle fibers[29,31]. The complex can be further divided into three core subcomplexes – dystrophin-dystroglycan subcomplex, sarcoglycan-sarcospan subcomplex, and dystrobrevin-syntrophin subcomplex[31].

Utrophin

Utrophin is a homologue of dystrophin that is structurally similar and has similar functions as dystrophin, although it is ubiquitously expressed unlike dystrophin[31]. In non-diseased skeletal muscles, utrophin is present at the NMJ and is co-localized with acetylcholine receptors and stabilizing the synaptic cytoskeleton[31]. Dystrophin and utrophin are expressed in a reciprocal manner – in dystrophic-deficient muscle, utrophin expression increases and is directed at the costameres[31]. The amino terminal has calponin homology domain with actin binding properties that binds to cytoskeletal f-actin[31]. Utrophin is approximately 7% shorter than dystrophin and contains carboxyl-terminal WW domain and ZZ zinc finger binding domains homologous to dystrophin and interact with components of the DGC[31].

Dystrophin-dystroglycan subcomplex

The absence of α-dystroglycan is embryonically lethal, although disruption of the dystroglycans in mature skeletal muscle results in sarcomere instability and degeneration of the muscle fiber[29,37]. α-dystroglycan is an extracellular protein on the cell surface that binds to β-dystroglycan and the laminins in the ECM (Figure 1)[31,32]. Dystrophin is linked to laminin-2 in the ECM through interactions with α- and β-dystroglycan[31,32]. β-dystroglycan is a transmembrane protein that binds to dystrophin at the WW and ZZ domains and is implicated in RhoGTPase signaling[31,38].

Sarcoglycan-sarcospan subcomplex

Loss of dystrophin results in the destabilization of the sarcoglycan subcomplex at the sarcolemma, resulting in a "leaky" sarcolemma[29,39]. Sarcospan is a transmembrane protein tightly associated with the sarcoglycans, forming the sarcoglycan-sarcospan sub-complex (Figure 1)[31]. Mutations in the α, β, λ, and δ-sarcoglycan genes result in the limb-girdle muscular dystrophies (LGMD) type 2D, 2E, 2C, and 2F, respectively[29,39]. The LGMDs are autosomal dominant (six forms) and autosomal recessive (10 forms) muscular dystrophies characterized by pelvic and shoulder girdle muscle wasting, with a wide spectrum of phenotype severity[39]. Patients are usually diagnosed with LGMDs in the second or third decade in life[39].

The sarcoglycans and sarcospan are tightly-associated transmembrane proteins that are thought to be essential in the proper assembly and function of the DGC and in cellular signaling (Figure 1)[29,31]. The sarcoglycan subcomplex is linked extracellularly to α-dystroglycan through the binding of biglycan to α- and λ-sarcoglycan[29,31]. The sarcoglycan complex interacts with cytoskeletal filamin-C through λ- and δ-sarcoglycan as well as core signaling proteins biglycan, α-dystrobrevin, and sarcospan[29,31].

Dystrobrevin-syntrophin subcomplex

Loss of α-dystrobrevin results in congenital heart disease and no myopathies have been associated with syntrophin nor neuronal nitric oxide synthase (nNOS) ablation, although ablation of either the syntrophin or nNOS have abnormal NMJs[29,40-42]. α-dystrobrevin forms a subcomplex of the DGC with nNOS in addition to the syntrophins (α1 & β1; Figure1)[29,32]. Although there is only a minor cardiac and skeletal muscle disease phenotype in α-dystrobrevin knockout mice, nNOS is displaced from the sarcolemma into the sarcoplasm, thought to be the result of the loss of α-dystrobrevin and syntrophin interaction[29,43]. Sarcolemma integrity is greatly improved in *mdx* mice with nNOS overexpression[29]. The *mdx* mouse (C57BL/10ScSn-Dmd^{mdx}/J) is the most common animal model for DMD, with a C-to-T transition that results in a premature stop codon in exon 23[44].

Intracellularly, dystrophin binds cytoskeletal f-actin as well as intermediate filaments and sarcomere proteins through the dystrobrevins (Figure 1)[29,31]. α-dystrobrevin binds directly to intermediate filament proteins synemin, dysbindin, and syncolin[29]. α-dystrobrevin is connected to the Z-disc of the sarcomere through the binding of syncolin to desmin[29]. Synemin is important for linking both intermediate filaments (desmin & vimentin) and proteins within the sarcomere (desmin & α-actinin) to the sarcolemma at the costameres[29]. Syntrophins also create signal transduction complexes through directly binding dystrophin and associating with numerous kinases, ion channels, and signaling molecules in the DGC[29,40].

Signaling associated with the DGC

Mutations in the DGC and utrophin affects cellular signaling as well as the NMJ. Utrophin accumulates at the postsynaptic side of the NMJ and with dystroglycan interacting with structural and signaling components on the NMJ, agrin, laminin, and rapsyn as well as clustering with acetylcholine receptors[34,36,45]. Agrin is released from motor neurons to activate postsynaptic muscle-specific kinase (MuSK), leading to a signaling cascade to cluster acetylcholine receptors[34,36,45]. Rapsyn, an effector of MuSK, physically links the acetylcholine receptor to the utrophin glycoprotein complex (UGC), which is required for the stabilization of the acetylcholine receptors as proper maturation of the NMJ[34,36,45].

β-dystroglycan binds multiple adaptor proteins essential in skeletal muscle differentiation, specifically through RhoGTPases[34,36,45]. The C-terminus of β-dystroglycan also binds Grb2, an important adaptor protein for recruiting additional components of the mitogen-activated protein (MAP) kinase pathway[34,36,45]. Phosphorylation of β-dystroglycan at the C-terminus Tyr892 residue has been implicated in regulating the interactions between dystrophin and caveloin-3 for the recruitment of c-Src and Fyn proteins to the sarcolemma, that are implicated in phosphorylating syntrophin of the DGC[34,36,45]. β-dystroglycan has also been shown to associate with GTPase dynamin 1 to regulate endocytosis[36].

The sarcoglycans play an essential role in the DGC-mediated signaling through biglycan, sarcospan, and α-dystrobrevin[36]. Biglycan interacts with many cytokines and growth factors associated with

dystropathologies, including transforming growth factor-β (TGF-β) and tumor necrosis factor-α (TNF-α), as well as bone morphogenic proteins[36]. Biglycan also regulates $nNOS_{\mu}$ along with the sarcoglycan complex, α-dystrobrevin, and syntrophin[36]. Sarcospan is a regulator of Akt pathways[36]. The dystrobrevins have been implicated in signal transduction pathways, as α-dystrobrevin knockout mice develop muscle degeneration, with nNOS displaced from the sarcolemma and resultant abnormal nNOS signaling[34,45]. The DGC and dystrobrevin are also associated with the signaling molecules calmodulin, Ca^{+2}-calmodulin-dependent protein kinase II (CaMKII), protein kinase A (PKA), phosphoinositide 3-kinase (PI3K), Growth factor receptor-bound protein 2 (Grb2), son of sevenless, Ras, and nNOS as well as Ser/Thr protein kinase phosphorylation sites on protein members within the DGC[34,36,45]. Indeed, dystrobrevin is a target of PKA at the NMJ and is implicated in synaptic plasticity, learning, and memory[34,36,45].

The PI3K/Akt signaling pathway is essential for muscle growth and hypertrophy downstream of the DGC. Disruption of dystroglycan and laminin binding via antibody blockade results in decreased PI3K-mediated phosphorylation of protein kinase B (Akt) and subsequent increase in apoptosis[34,36,45]. This is thought to be due to the laminin-dependent interaction of the DGC with G-proteins[34,36,45]. Laminin-deficient muscles are pro-apoptotic and is thought to contribute to dystrophic phenotypes[34,36,45]. Inhibition of apoptotic signaling by Bcl-2 overexpression and Bax inactivation have been shown to ameliorate dystrophy in laminin-α2-deficient animal models, implicating the DGC and associated proteins to apoptotic and survival signaling[34,36,45]. Alterations to the integrin-mediated signaling pathways can also alter Akt and MAP kinase activity[34,36,45]. In the presence of laminin, dystrophin associated with syntrophin to mediate the downstream Rac1 signaling, which is implicated in regulating cell growth, cytoskeletal reorganization, and activation of protein kinases[34,36,45].

Generally, nNOS generates NO for several signaling pathways involved in apoptosis, ischemia protection, and regulation of vascular tone[34,36,45]. Nitric oxide plays a role in modulating UGC function at the NMJ and acts as an antero- and retrograde modulator of synaptic transmission; agarin induces increased NO and cGMP that stimulates PKG and inhibits PKC that increases the interaction of dystrophin and utrophin with

actin, stabilizing the acetylcholine receptors at the NMJ[34,36,45]. Nitric oxide also targets the Src family of protein kinases that phosphorylate the β-subunit of the acetylcholine receptor to promote the binding of rapsyn and association with acetylcholine receptors[34,36,45].

Ca^2 levels are elevated in dystrophic muscle as a result of disruption to the sarcolemma and abnormal activation of Ca^{+2} leak channels[34,36,45]. The increased intracellular Ca^{+2} may be a cause of the disease pathology due to apoptosis and oxidative stress leading to Ca^2-dependent proteolysis via the activation of Ca^2-dependent proteases and calpains[34,36,45]. Calmodulin physically interacts with dystrophin, and syntrophin, and calmodulin activity is reduced in dystrophic muscle[34,36,45]. Calmodulin is a Ca^{+2}-binding protein that regulates many Ca^{+2}-dependent processes and is a cellular Ca^{+2} sensor[34,36,45]. Calmodulin is thought to regulate the binding of dystrophin and utrophin to actin and CaMKII phosphorylates dystrophin and syntrophin, and the dystrophin-syntrophin interaction is inhibited upon phosphorylation via CaMKII[34,36,45]. Additionally, CaMKII and dystrophin have been shown to be essential for maintaining neurotransmitter release at the NMJ[34,36,45].

Molecular mechanism of DMD and myopathies associated with the DGC

Complete loss or a non-functional dystrophin protein disrupts the connection between the cytoskeleton and the ECM, resulting in decreased sarcolemmal integrity[29]. The decreased structural integrity of the muscle fiber increases the susceptibility of muscle to damage caused by normal muscular contractions[29]. Repeated cycles of degeneration and regeneration eventually lead to the exhaustion of muscle satellite cell pools and results in necrosis and fibrosis of the muscle[29]. Loss of dystrophin can significantly affect other components of the DGC and contribute to the dystrophic phenotype[29]. Disruption of the cytoskeletal-ECM connection, disruption of the integrin-mediated linkage of cytoskeletal-ECM connection, disruption of the ECM, aberrant glycosylation of DGC proteins, impaired signaling, defective sarcolemmal repair, and cytoskeletal defects all contribute to the dystrophic phenotype[29,32].

The primary cause for a disruption of the cytoskeletal-ECM link is the absence or non-functioning protein dystrophin and the proteins of the DGC[29,32]. The linkage of dystrophin and the ECM is through the binding of α- and β-dystroglycan that bind laminin-2 in the ECM to connect the cytoskeleton through the sarcolemma with the basement membrane[29,32]. The sarcoglycans and sarcospan provide additional support to the DGC and sarcolemma, and mutations in individual sarcoglycan genes result in LGMDs[29,32]. Additionally, defects with one sarcoglycan subunit results in the loss of one or more of the remaining sarcoglycan subunits, resulting in destabilization of the DGC and decreased sarcolemmal integrity[29,32].

Disruption or loss of the integrin-mediated link between the cytoskeleton and the ECM also contributes to sarcolemmal integrity[29,32]. α7β1 integrin functions similarly to the DGC by connecting the actin cytoskeleton to the ECM and mutations in the α7 chain causes CMDs[29,32]. α7β1 is involved in cell adhesion, proliferation, and differentiation in developing myoblasts and is expressed throughout the sarcolemma for attachment to the basal lamina in mature myofibers[29,32]. α7β1 is thought to be complimentary to the DGC, also being localized at costameres, NMJs, and MTJs[29,32]. Indeed, loss of the DGC results in increases in α7β1 integrin at the sarcolemma to reinforce the link between the sarcolemma and basal lamina[29,32].

Disruption of the ECM, a network of collagen, glycoproteins, and proteoglycans essential for cellular attachment and a scaffold for cellular signaling, has also been shown to contribute to myopathies[29,32]. Mutations in the laminin-α2, one of the subunits of the muscle-specific laminin that interacts with the DGC through the dystroglycans and α7β1 integrin, result in merosin-deficient congenital muscular dystrophy type 1A[32]. Additionally, α7β1 integrin is secreted as a complex with α-dystroglycan to interact with the protein entactin, an integral component of the basement membrane, to bind collagen and build the ECM[32]. Detachment of the ECM and cell membrane induces anoikis, an apoptotic pathway that occurs when cells detach from the ECM[32].

Structural and posttranslational defects in the DGC can also weaken the sarcolemma and result in myopathies, particularly the hypoglycosylation of α-dystroglycan[29,32]. Extensive O-glycosylation is

required for α-dystroglycan to bind ECM proteins, such as laminin-2, to link dystrophin and the DGC to the ECM[32]. This results in decreased binding of ECM proteins that results in destabilization of the sarcolemma that result in CMDs Walker-Warburg syndrome, muscle-eye-brain disease, and Fukuyama CMD[32]. However, disorders are often a result of mutations in the dystroglycans with posttranslational modifications a small fraction of cases[32].

Although many signaling pathways can or are affected by impaired signaling at the DGC, NO signaling is particularly affected (see *Signaling associated with the DGC* section)[29,32]. α-dystrobrevin, syntrophins, and nNOS are all part of the DGC and regulate signal transduction at the sarcolemma[29,32]. Nitric oxide is synthesized from L-Arg by nNOS to for the synthesis of the potent vasodilator cGMP to increase localized blood flow to the area[32]. Complete loss of dystrophin displaces nNOS from the sarcolemma and results in functional ischemia, although many muscular dystrophies also displace nNOS from the sarcolemma, illustrating a link between myopathies and impaired nNOS signaling[32]. Interestingly, ablation of α-dystrobrevin in mice develop muscular dystrophy and cardiomyopathies as a result of compromised nNOS signaling, as nNOS is displaced from the sarcolemma and resultant decreased production of NO[32].

Due to repeated damage to muscles, sarcolemmal repair can be affected in dystropathologies. Dysferlin is essential in the Ca^{+2}-dependent repair pathway, promoting the fusion of intracellular vesicles with each other and the sarcolemma[29,32]. Mutations in the dysferlin gene result in LGMD2B, Miyoshi myopathy, and distal anterior compartment myopathy[32]. In Mitsugumin 53 (MG53)-caveolin-3-dysferlin-mediated sarcolemmal repair from contraction-induced injury, oxidized extracellular influx oligimerizes MG53 on intracellular vesicles for translocation and nucleation with the damaged site[32]. Interaction of MG53 with caveolin-3 results in rapid sarcolemmal repair facilitated by dysferlin in the presence of Ca^{+2} [32]. Dysferlin ablation in mice develop progressive muscular dystrophies with an intact DGC but have defective sarcolemmal repair[32]. The annexins (A1, A2, etc…) also interact with dysferlin, which are phospholipid binding proteins that dock interacting proteins at the cell membrane in a Ca^{+2}-dependent manner[32]. Upon

damage, A6 accumulates at the damaged site independent and simultaneously with dysferlin and docked intracellular vesicles for the recruitment of A1 and A2 to the repair site for sarcolemmal repair[32].

Cytoskeletal F-actin, intermediate filaments, and microtubule defects have also been associated with myopathies. Desmin is an essential intermediate filament protein that connects neighboring Z-discs as well as anchoring myofibrils to organelles to maintain spatial organization of the cell, with mutations in desmin resulting in LGMD1D with dilated cardiomyopathy[32]. Plectin, a membrane protein that links the components of the cytoskeleton, binds both the actin binding domain of dystrophin and β-dystroglycan at the costameres, and mutations result in LGMD2Q without a skin manifestation[32]. This results in greater distances between the sarcolemma and myofibrils with misaligned Z-lines[32].

Current treatments

Clinical trials for DMD treatments discussed below can be found at https://clinicaltrials.gov/. Clinical trials can be searched for based on status of the study (e.g. recruiting and not yet recruiting & all studies), condition or disease (e.g. Duchenne muscular dystrophy), specifying terms (e.g. NCT number, drug name, investigator name, etc…), and country. See Table 2 for a list of clinical trials and their status (Table 2).

	Intervention(s)	Status	Study Title	NCT Number
1	rAAVrh74.MCK.GALGT2	Active, not recruiting	Gene Transfer Clinical Trial to Deliver rAAVrh74.MCK.GALGT2 for Duchenne Muscular Dystrophy	NCT03333590
2	Vamorolone & Prednisone	Recruiting	A Study to Assess the Efficacy and Safety of Vamorolone in Boys With Duchenne Muscular Dystrophy(DMD)	NCT03439670
3	Vamorolone	Enrolling by invitation	Long-term Extension Study to Assess Vamorolone in Boys With Duchenne Muscular Dystrophy (DMD)	NCT03038399
4	RO7239361	Recruiting	Clinical Trial to Evaluate the Efficacy, Safety, and Tolerability of RO7239361 in Ambulatory Boys With Duchenne Muscular Dystrophy	NCT03039686
5	DS-5141b	Active, not recruiting	Study of DS-5141b in Patients With Duchenne Muscular Dystrophy	NCT02667483
6	N/A	Recruiting	A Registered Cohort Study on Duchenne Muscular Dystrophy	NCT04012671
7	N/A	Not yet recruiting	Prognostic Factors Affecting Duchenne Muscular Dystrophy	NCT03372655
8	Casimersen & Golodirsen	Enrolling by invitation	An Extension Study to Evaluate Casimersen or Golodirsen in Patients With Duchenne Muscular Dystrophy	NCT03532542
9	Tamoxifen	Recruiting	Tamoxifen in Duchenne Muscular Dystrophy	NCT03354039
10	SRP-5051	Recruiting	A Phase 2 Study for Dose Determination of SRP-5051, Then Dose Expansion in Patients With Duchenne Muscular Dystrophy Amenable to Exon 51-Skipping Treatment	NCT04004065
11	Edasalonexent	Enrolling by invitation	An Open-Label Extension Study of Edasalonexent in Boys With Duchenne Muscular Dystrophy	NCT03917719
12	Physical Activity Registration	Not yet recruiting	Physical Activity Level of Norwegian Boys With Duchenne Muscular Dystrophy	NCT03947112
13	Visit Frequency	Recruiting	A Natural History Study In Chinese Male Patients With Duchenne Muscular Dystrophy	NCT03760029
14	Eteplirsen	Not yet recruiting	A Study to Evaluate Safety, Tolerability, and Efficacy of Eteplirsen in Patients With Duchenne Muscular Dystrophy	NCT03985878
15	Canakinumab Injection	Recruiting	Single Escalating Dose Pilot Trial of Canakinumab (ILARIS®) in Duchenne Muscular Dystrophy	NCT03936894
16	N/A	Recruiting	The Burden of Access in Duchenne Muscular Dystrophy in the US	NCT03951675
17	rAAVrh74.MHCK7.micro-dystrophin	Active, not recruiting	Systemic Gene Delivery Clinical Trial for Duchenne Muscular Dystrophy	NCT03375164
18	Suvodirsen	Active, not recruiting	A Randomized, Double-blind, Placebo-controlled, Efficacy and Safety Study of WVE-210201 (Suvodirsen) in Ambulatory Patients With Duchenne Muscular Dystrophy	NCT03907072
19	Idebenone	Recruiting	Phase III Study With Idebenone in Patients With Duchenne Muscular Dystrophy (SIDEROS-E)	NCT03603288
20	Ataluren	Recruiting	A Study to Assess Dystrophin Levels in Participants With Nonsense Mutation Duchenne Muscular Dystrophy (nmDMD) Who Have Been Treated With Ataluren	NCT03796637
21	NS-065/NCNP-01	Active, not recruiting	Extension Study of NS-065/NCNP-01 in Boys With Duchenne Muscular Dystrophy(DMD)	NCT03167255
22	PF-06939926	Enrolling by invitation	A Study to Evaluate the Safety and Tolerability of PF-06939926 Gene Therapy inDuchenne Muscular Dystrophy	NCT03362502
23	Stem Cells	Recruiting	Bone Marrow-Derived Autologous Stem Cells for the Treatment of Duchenne Muscular Dystrophy	NCT03067831
24	Givinostat	Recruiting	Clinical Study to Evaluate the Efficacy and Safety of Givinostat in Ambulant Patients WithDuchenne Muscular Dystrophy	NCT02851797
25	Pamrevlumab	Active, not recruiting	Trial of Pamrevlumab (FG-3019), in Non-Ambulatory Subjects With Duchenne Muscular Dystrophy (DMD)	NCT02606136
26	Myoblast Transplantation	Recruiting	Transplantation of Myoblasts to Duchenne Muscular Dystrophy (DMD) Patients	NCT02196467
27	Prednisone & Deflazacort	Active, not recruiting	Finding the Optimum Regimen for Duchenne Muscular Dystrophy	NCT01603407
28	Testosterone	Active, not recruiting	Testosterone Therapy for Pubertal Delay in Duchenne Muscular Dystrophy	NCT02571205
29	N/A	Recruiting	Duchenne Muscular Dystrophy Heart Study	NCT03443115
30	Idebenone	Recruiting	A Phase III Double-blind Study With Idebenone in Patients With Duchenne Muscular Dystrophy (DMD) Taking Glucocorticoid Steroids	NCT02814019
31	N/A	Active, not recruiting	Longitudinal Study of the Natural History of Duchenne Muscular Dystrophy (DMD)	NCT00468832
32	Physical Exercise	Not yet recruiting	Regular Physical Exercise in Duchenne Muscular Dystrophy	NCT03963453
33	rAAVrh74.MCK.GALGT3	Active, not recruiting	Gene Transfer Clinical Trial to Deliver rAAVrh74.MCK.GALGT2 for Duchenne Muscular Dystrophy	NCT03333590
34	Vamorolone & Prednisone	Recruiting	A Study to Assess the Efficacy and Safety of Vamorolone in Boys With Duchenne Muscular Dystrophy(DMD)	NCT03439670
35	Vamorolone	Enrolling by invitation	Long-term Extension Study to Assess Vamorolone in Boys With Duchenne Muscular Dystrophy (DMD)	NCT03038399
36	RO7239362	Recruiting	Clinical Trial to Evaluate the Efficacy, Safety, and Tolerability of RO7239361 in Ambulatory Boys With Duchenne Muscular Dystrophy	NCT03039686
39	Edasalonexent	Active, not recruiting	Phase 1/2 Study in Boys With Duchenne Muscular Dystrophy	NCT02439216
40	N/A	Not yet recruiting	Natural History of Duchenne Muscular Dystrophy	NCT03882827

Table 2 – List of clinical trials for DMD therapies

41	Cosyntropin	Recruiting	A Study to Assess the Efficacy and Safety of MNK-1411 in Duchenne Muscular Dystrophy	NCT03400852
42	Assessment Tools	Recruiting	Outcome Measures in Duchenne Muscular Dystrophy: A Natural History Study	NCT02780492
43	Givinostat	Recruiting	Givinostat in Duchenne's Muscular Dystrophy Long-term Safety and Tolerability Study	NCT03373968
44	N/A	Active, not recruiting	Double Push Acoustic Radiation Force (DP ARF) Ultrasound for Monitoring Degeneration inDuchenne Muscular Dystrophy	NCT01506518
45	Ataluren	Active, not recruiting	A Study to Assess Dystrophin Levels in Participants With Nonsense Mutation Duchenne Muscular Dystrophy (nmDMD)	NCT03648827
46	N/A	Recruiting	Regression of Hamstring Flexibility and Performance in Children With Duchenne Muscular Dystrophy	NCT03589612
47	SRP-4045 & SRP-4053	Recruiting	Study of SRP-4045 and SRP-4053 in DMD Patients	NCT02500381
48	Ifetroban	Not yet recruiting	Oral Ifetroban in Subjects With Duchenne Muscular Dystrophy	NCT03340675
49	Assistive Device	Recruiting	Use of Dynamic Arm Supports to Promote Activities of Daily Living in Individuals With DMD	NCT03531788
50	Eteplirsen	Recruiting	Study of Eteplirsen in Young Patients With DMD Amenable to Exon 51 Skipping	NCT03218995
51	P-188 NF	Recruiting	Safety and Efficacy of P-188 NF in DMD Patients	NCT03558958
52	SGT-001	Recruiting	Microdystrophin Gene Transfer Study in Adolescents and Children With DMD	NCT03368742
53	Genetic Characterization	Active, not recruiting	Characterization of Clinical Skeletal and Cardiac Impairment in Carriers of DMD and BMD	NCT02972580
54	Assistive Device	Recruiting	Prevention of Scoliosis in Patients With Duchenne Muscular Dystrophy Using Portable Seat Device	NCT03611244
55	N/A	Recruiting	The Duchenne Registry	NCT02069756
56	Bisoprolol Fumarate	Recruiting	Bisoprolol in DMD Early Cardiomyopathy	NCT03779646
57	Nebivolol	Active, not recruiting	Nebivolol for the Prevention of Left Ventricular Systolic Dysfunction in Patients With Duchenne Muscular Dystrophy	NCT01648634
58	Observations	Active, not recruiting	Cardiac Involvement in Patients With Duchenne/Becker Muscular Dystrophy	NCT02470962
59	MRI & Biomarkers	Recruiting	Magnetic Resonance Imaging and Biomarkers for Muscular Dystrophy	NCT01484678
60	Assessment Tools	Recruiting	Effects of Fear of Falling on Physical Performance and Quality of Life in Children With Duchenne Muscular Dystrophy	NCT03507530
61	N/A	Recruiting	Peak Cough Flow and Cough Clearance in Patients With Muscular Dystrophy	NCT02034305
62	Ataluren	Recruiting	Registry of Translarna (Ataluren) in Nonsense Mutation Duchenne Muscular Dystroph	NCT02369731
63	Givinostat	Recruiting	Clinical Study to Evaluate the Efficacy and Safety of Givinostat in Ambulant Patients With Becker Muscular Dystrophy	NCT03238235
64	N/A	Active, not recruiting	Becker Muscular Dystrophy - A Natural History Study to Predict Efficacy of Exon Skipping	NCT01539772
65	MRI & Biomarkers	Recruiting	Validating Cardiac MRI Biomarkers and Genotype-Phenotype Correlations for DMD	NCT02834650
66	Ataluren	Enrolling by invitation	Study of Ataluren in Previously Treated Participants With Nonsense Mutation Dystrophinopathy (nmDBMD)	NCT01247207
67	Tamoxifen	Active, not recruiting	Treatment Effect of Tamoxifen on Patients With DMD	NCT02835079
68	Biomarkers	Recruiting	Evaluation of Muscle miRNA as Biomarkers in Dystrophinopathies	NCT02109692
69	Ataluren	Recruiting	Long-Term Outcomes of Ataluren in Duchenne Muscular Dystrophy	NCT03179631
70	Muscle Biopsy	Recruiting	Endomysial Fibrosis, Muscular Inflammatory Response and Calcium Homeostasis Dysfunction in Duchenne Muscular Dystrophy	NCT01823783
71	CAP-1002	Active, not recruiting	A Study of CAP-1002 in Ambulatory and Non-Ambulatory Patients With Duchenne Muscular Dystrophy	NCT03406780
72	Physiotherapy	Enrolling by invitation	Effectiveness of a Multimodal Physiotherapy Program With Virtual Reality Glasses inDuchenne and Becker.	NCT03879304
73	BLS-M22	Not yet recruiting	Safety Study of BLS-M22 in Healthy Volunteers	NCT03789734
74	Spironolactone & Prednisolone	Recruiting	Spironolactone Versus Prednisolone in DMD	NCT03777319
75	Biomarkers	Recruiting	Molecular Analysis of Patients With Neuromuscular Disease	NCT00390104
76	Biomarkers	Recruiting	Biomechanical and Morphological Changes in Dystrophic Muscle	NCT02472990
77	RO7239361	Active, not recruiting	Study of an Investigational Drug, RO7239361 (BMS-986089), in Ambulatory Boys With DMD	NCT02515669
78	Assistive Device	Recruiting	User-centred Assistive System for Arm Functions in Neuromuscular Subjects	NCT03127241
79	Virtual Reality	Not yet recruiting	Feasibility of Virtual Reality in Children With Neuromuscular Disease, Effectiveness of Virtual Reality and Biofeedback	NCT03689660
80	Biomarkers	Recruiting	Biomarker for Duchenne Disease (BioDuchenne)	NCT02994030
81	N/A	Recruiting	Acceptance and Commitment Therapy for MuscleDisease	NCT02810028

Table 2 (continued) – List of clinical trials for DMD therapies

Pharmacological treatments

Although the mechanism by which corticosteroids increase strength in DMD is unknown, the inhibition of proteolysis, stimulation of myoblast proliferation, stabilization of the sarcolemma, increases in myogenic repair, and decrease in intracellular Ca^{2+} are known beneficial effects of corticosteroid therapy[16]. Glucocorticoids and corticosteroids are the only pharmacological treatment for DMD that has been shown to slow the decline of muscular strength and function, as well as aid in the stabilization of respiratory function and decrease the risk of scoliosis[4,10,23]. Prednisone, prednisolone, and deflazacort are the three most commonly used corticosteroids[4,10,23]. Behavioral changes (anxiousness/depression, attention problems, aggression, etc…), weight gain, excessive hair growth, and the development of Cushing-like features (fatty tissue deposits in the face and between shoulders, slow wound healing, fragile skin, etc…) are possible adverse effects of corticosteroid use[16]. Drug combinations of prednisone, prednisolone, deflazacort, and vamorolone are currently in clinical trials (e.g. NCT03439670, NCT01603407 & NCT03439670) (Table 2).

Idebenone and vamorolone are anti-inflammatory drugs that are currently in clinical trials (e.g. NCT03038399, NCT03603288, & NCT02814019; Table 2)[4,10]. Idebenone is a benzoquinone with antioxidant properties while vamorolone is a glucocorticoid[4,10]. Idebenone has been implicated in reducing inflammation in patients who do not respond well to glucocorticoids, particularly in delaying respiratory complications and failure[4,10]. Vamorolone is a corticosteroid that functions similarly to prednisone with fewer side-effects as well as increasing muscular strength in *mdx* mice[4,10]. Eplerenone, a mineralocorticoid/aldosterone receptor antagonist, in conjunction with ACE inhibitors can attenuate the decline in left ventricular systolic function, although not currently in clinical trials for DMD[10,46]. Raman et. al.[47,48] found that 25 mg eplerenone treatment daily for two years for preclinical cardiomyopathy in young DMD patients had significantly improved left ventricular contractility while treatment in older DMD patients maintained contractile functioning without worsening nor improvement.

Angiotensin-converting enzyme (ACE) inhibitors and β-blockers may help in delaying cardiomyopathies, such as myocardial dysfunction and necrosis and arrhythmias in DMD patients[10,49]. ACE inhibitors work by preventing the conversion of angiotensin I to angiotensin II, a vasoconstrictive peptide hormone, increasing blood flow to cardiac muscle[50]. Beta-blockers are β-adrenergic receptor blocking agents, resulting in a reduction in heart rate and lowering blood pressure[51]. Mineralocorticoid/aldosterone receptor antagonists prevent the binding of aldosterone and other steroid hormones (e.g. corticosteroids; lower affinity) to their respective receptors[51].

Clinical trials with tadalafil and sildenafil, phosphodiesterase-5A (PDE5A) inhibitors, have failed to improve ambulation (6 m walk test)[52,53]. Chronic tadalafil, treatment of 1 mg/kg/day for 16 months has been shown to reduce histopathological features in dystrophic muscle, reduced calpain-mediated proteolysis, and preserved cardiac function[52,53]. PDE inhibitors prevent hydrolysis of cGMP, prolonging cGMP bioavailability in the nNOS signaling pathway to increase blood flow to the working muscles[52]. No clinical trials for tadalafil and sildenafil are currently ongoing.

Histone deacetylase and myostatin inhibitors aim to inhibit myostatin to increase muscle regeneration and hypertrophy[4,10]. Givinostat, a myostatin inhibitor, has been shown to increase muscle regeneration and decreased fibrosis in DMD patients[4,54]. Patients are currently being recruited for givinostat clinical trials (NCT03373968 & NCT03238235)[55]. Clinical trials into domagrazumab have been terminated due to lack of efficacy and the emergence of treatment-emerging adverse effects by week 49 (NCT02310763) (Table 2)[55].

Pamrevlumab is an inhibitor of connective tissue growth factor (CTGF/CCN2) that has been shown to decrease fibrosis and skeletal muscle damage in *mdx* mice[4,56]. Repeated cycles of degeneration and regeneration of muscle in DMD patients results in fibrosis and collagen deposition in the muscle, replacing functioning myofibers with non-functional fibrotic tissue[31,57]. This results in decreased muscular strength and function as patients age. Pamrevlumab is currently in clinical trials (NCT02606136) (Table 2)[4,55].

Genetic strategies for DMD

Packaging of microdystrophins into viral vectors have been shown to improve skeletal and cardiac muscle function and ameliorate muscle pathology to the less-severe form Becker Muscular Dystrophy (BMD), where there is some functional dystrophin protein[58-61]. Human studies have had limited success; Bowles and colleagues administered a microdystrophin vector into the biceps of 6 DMD boys aged 5 – 11 years old, with muscle biopsies showing only two of the six patient having limited transgene expression of dystrophin over the two year study[58,62,63]. In the study consisted of a two-week baseline screening, two-day inpatient period for injecting 1.2 mL of the vector in three equivalent boluses spaced 0.5 cm apart along the longitudinal orientation of the biceps and acute toxicity monitoring and followed over two-year outpatient follow-up. Blood and urine were collected at days 8, 15, 30, 43, 53, 60, 90, and 120 as well as at 6, 9, 12, 18, and 24 months. Two of the patients with no detectable levels of dystrophin developed elevated T-cell responses to endogenous and transgene dystrophin epitopes, indicating gene expression with no detectable functional protein[62]. rAAVrh74.MHCK7, SGT-001, & PF-06939926 are micro-dystrophin therapies currently undergoing clinical trials[10,55,64]. Sarepta Therapeutics (rAAVrh74.MHCK7 & GALGT2; NCT03375164), Solid Biosciences (SGT-001; NCT03368742), and Pfizer Pharmaceuticals (PF-06939926; NCT03362502) are currently developing microdystrophin therapies and in clinical trials (Table 2).

Approximately 10% - 15% of DMD cases are the result of a nonsense mutation resulting in a premature stop codon in the mRNA[4,10]. Aminoglycoside antibiotics have been shown to read through premature nonsense codons to restore dystrophin expression[58,65]. Gentamycin therapy has been shown to restore dystrophin expression and resist muscle damage in *mdx* mice[58,66]. Human studies have shown mixed results[58]. Intravenous injection of gentamycin into DMD patients once daily for two weeks failed to detect full-length dystrophin[58,67]. Administration of gentamycin for six months saw significant increases in dystrophin levels[58,68]. No clinical trials for gentamycin treatment for DMD are currently ongoing.

Ataluren is a non-aminoglycoside stop codon read-through agent with no antibiotic properties that has been tested in multiple disease models, particularly in cystic fibrosis and dystrophinopathies[4,10]. Aminoglycoside antibiotics and ataluren bind to ribosomal RNA subunits and interfere with the ribosome's ability to recognize premature stop codons to allow for normal translation[4,10,66]. In clinical trials, Ataluren provided no significant improvements in the 6MWT in clinical trials[58,69,70]. There are currently three clinical trials that are recruiting (NCT03796637 & NCT02369731) or are active and not recruiting patients (NCT03648827) (Table 2). The U.S. Food and Drug Administration (FDA) denied Ataluren's new drug application (NDA) as of October 2017 due to lack of efficacy[4,55]. The European Medicines Agency (EMA) granted conditional marketing for treating patients two years old or less with a nonsense DMD mutation[58].

Exon skipping agents correct the reading frame of the *dystrophin* gene to produce truncated functional dystrophin protein by targeting the exon with antisense oligonucleotides (ASOs) by modifying the pre-mRNA splicing, resulting in the milder BMD phenotype[58]. Eteplirsen, a phosphorodiamidate morpholino oligomer (PMO), and drisapersen, a 2'-*O*-methyl-phosphorothioate oligonucleotide (2'*O*MePS), are oligonucleotides that target exon 51, an exon attributed to approximately 14% of the mutations resulting in DMD[58]. Early Phase I clinical trials of eteplirsen showed an increase in dystrophin by 11% - 21% in Phase I trials[4,71]. Clinical trials are currently ongoing for eteplirsen (NCT03985878 & NCT03218995). Similarly, drisapersen, showed promising results by showing partial restoration of dystrophin (17% - 35%) after single-dose injection in the tibialis anterior muscle, but subsequent trials failed to show significant differences in the six-minute walk test (6MWT)[10,72,73]. Eteplirsen has not demonstrated clinical efficacy, however patients show a decreased rate of the loss of ambulation; recent studies have shown an attenuation in respiratory decline[58,74,75]. Drisapersen has also failed to show clinical efficacy. No clinical trials are currently ongoing for drisapersen. Recently, NS-065/NCNP-01 (viltolarsen) has been showed to skip exon 53 in all DMD patients[58]. NS-065/NCNP-01 (NCT03167255), SRP-4053 (golodirsen), SRP-4045 (casimersen), stereopure ASO, and DS-5141b (suvodirsen) are additional exon skipping agents that are currently in ongoing clinical studies (NCT03532542, NCT02500381, & NCT03907072)[58].

Cellular strategies

Satellite cells, muscle stem cells, develop into myoblasts to contribute nuclei for repair and regeneration of muscle. Both satellite cell and myoblast injection have shown some expression of donor-derived dystrophin, although there was no muscle function amelioration[58,76-78]. Muscle- and blood-derived CD133+ stem cells are capable of migration to myofibers for muscle regeneration, and restoration of satellite cell pools and both are currently under investigation for muscle regeneration in dystropathologies[58]. Mesangioblasts, vasculature-associate stem cells, have been demonstrated to recover dystrophin expression and muscle function in DMD dogs[58,79]. Clinical trials into intra-atrial mesangioblast transplantation failed to show improvements in muscle function[58,80]. Similarly, pericytes which are contractile connective tissue cells surrounding the microvasculature capable of differentiation into myogenic cells have shown promising results in scid-*mdx* mice; human DMD pericytes with human mini-dystrophin transplanted non scid-*mdx* mice resulted in myofiber expression of dystrophin[58,81]. Additionally, transplantation of human iPS-derived myogenic cells into *mdx* mice produce human-derived dystrophin and improved muscle strength[58]. Patients for clinical trials for bone marrow-derived autologous stem cells are currently being recruited (NCT03067831).

Genome editing strategies

Transcription activator-like effector nucleases (TALEN), Zinc Finger Nucleases (ZFN), and CRISPR/Cas9 are synthetic nucleases that create site-specific double-strand breaks for non-homologous end joining (NHEJ) or homologous recombination to edit the genome[4,10,12]. TALEN is a flexible and specific nuclease that uses the TALE domain repeat variable di-residue (RVDs), tandem repeats of 34 AAs with variations at the 12th and 13th AAs, conjugated with FokI nuclease (together as TALEN) to target specific DNA sequences[12]. However, the assembly and cloning process takes two to three weeks for one TALEN[12]. ZFNs are a conjugation of three or four zinc finger domains with FokI that target specific sequences of DNA and delete or insert small nucleotide sequences to adjust the reading frame[12]. Full DNA binding of zinc finger

domains to each other does not always have full binding activity[12]. Target sequences are limiting for ZFN, as they can prefer certain sequences over others[12]. Neither TALENs or ZFNs are currently studied for DMD, and are not in clinical trials[55].

CRISPR/Cas9 is currently at the forefront of genome-editing therapies for genetic diseases, such as DMD and cystic fibrosis. The CRISPR/Cas9 system uses an engineered RNA-guided nuclease to create a double-strand break at the target locus adjacent to a short protospacer motif sequence[82]. Different Cas enzymes from various bacteria are used for the function of CRISPR I and III – VI systems[83]. SpCas9 (*Streptococcus pyrogenes*) and SaCas9 (*Staphylococcus aureus*) are the most widely used Cas9 enzymes[83]. Double-strand breaks can be repaired using NHEJ, homology-directed repair (HDR), and microhomology end joining (MMEJ). Although NHEJ is effective in repairing the double-strand breaks in most cell types, HDR and MMEJ repair is thought to be restricted to proliferating cells[82]. HDR uses either sister chromatid or exogenous DNA as a template for repair for precise modifications at the target site[82]. MMEJ uses a homologous sequence of 5 – 25 base pairs that flank the original break in the DNA for ligation, deleting the regions between the microhomologies[82].

Long *et al.* injected a CRISPR/Cas9 system with an ssHDR template into *mdx* mouse zygotes at the 1-cell stage and implanted the zygote into pseudopregnant mice and observed significant dystrophin expression, with pups having 83% NHEJ or 41% HDR correction at seven to nine weeks of age in skeletal muscle[82-84]. Amoasii and colleagues delivered an AAV9 vectors containing SpCas9 along with an exon 51-targeting gRNA into the TA muscle of one month old ΔE50-DMD dogs and evaluated at six weeks post injection to reframe exon 51 or disrupt the acceptor site for the skipping of exon 51 to adjust the *dystrophin* gene reading frame for restoration of dystrophin[83,85]. Targeting of exon 51 of in the ΔE50-DMD dogs observed 52 – 67% of WT dystrophin levels as well as improving histopathology and restoration of β-dystroglycan; no significant editing at off-target sites were noted[83,85]. In follow up work by Amoasii and colleagues, systemic delivery of AAV9 vectors containing SpCas9 and gRNA and analyzed eight weeks post injection observed dystrophin restoration in various skeletal muscles through immunostaining of various skeletal muscles[83].

Dystrophin was restored to approximately 5 – 70% of WT animals. Interestingly, one dog given a much larger dose had approximately 92% of dystrophin restored to WT levels in the heart[85].

Ousterout and colleagues[11] deleted exons 45 – 55, which account for approximately 60% of DMD cases, using multiplex CRISPR/spCas9 by using two sgRNAs flanking exon 51 to form truncated dystrophin protein and restoring dystrophin expression in DMD patient-derived myoblasts[10,11]. However, gene editing occurred at three off-target sites that were detectable in immortalized cell lines[12]. Due to concerns about off-target editing, in silico prediction of off-target sites with deep sequencing as well as whole-genome sequencing are used to evaluate possible off-target sites[82]. Dosage titration of Cas9 and guide RNA, paired Cas9 nickases, truncated guide RNAs, and high-fidelity or enhanced Cas9 are recent approaches used to minimize off-target editing[82]. Olson and colleagues[82] restored dystrophin protein expression and the corresponding force generation in three-dimensional engineered heart muscle. The researchers concluded that correcting 30% - 50% of the cardiomyocytes will restore a non-disease phenotype[82]. One consideration for genome editing techniques is the problem of editing off-target sites. Recently, Olson and colleagues used SpCas9 and restored approximately 90% of dystrophin protein expression in all muscles & heart of mice with exon 44 deletion within one month of a single systemic dose[9].

Nutritional strategies to promote muscle protein synthesis

The branched-chain amino acids (BCAAs), Leu, Ile, and Val are nutritionally essential AAs required for protein synthesis and other metabolic functions[13,86]. BCAAs are unique amongst the AAs, as they pass initially through the liver largely unaltered and are delivered to peripheral tissues, particularly skeletal muscle, for initial catabolism[86]. Leu has been shown to stimulate protein synthesis by activation of the mechanistic target of rapamycin (mTOR; Figure 2)[14,15,87]. Nutritional strategies for DMD patients have focused primarily on undernutrition/malnutrition, overweight and obesity, and adequate amounts of micronutrients as well as swallowing and gastrointestinal considerations[49]. There is limited research

regarding BCAAs for increasing protein synthesis in DMD patients, with the majority of BCAA and protein synthesis research in human resistance training[3,88].

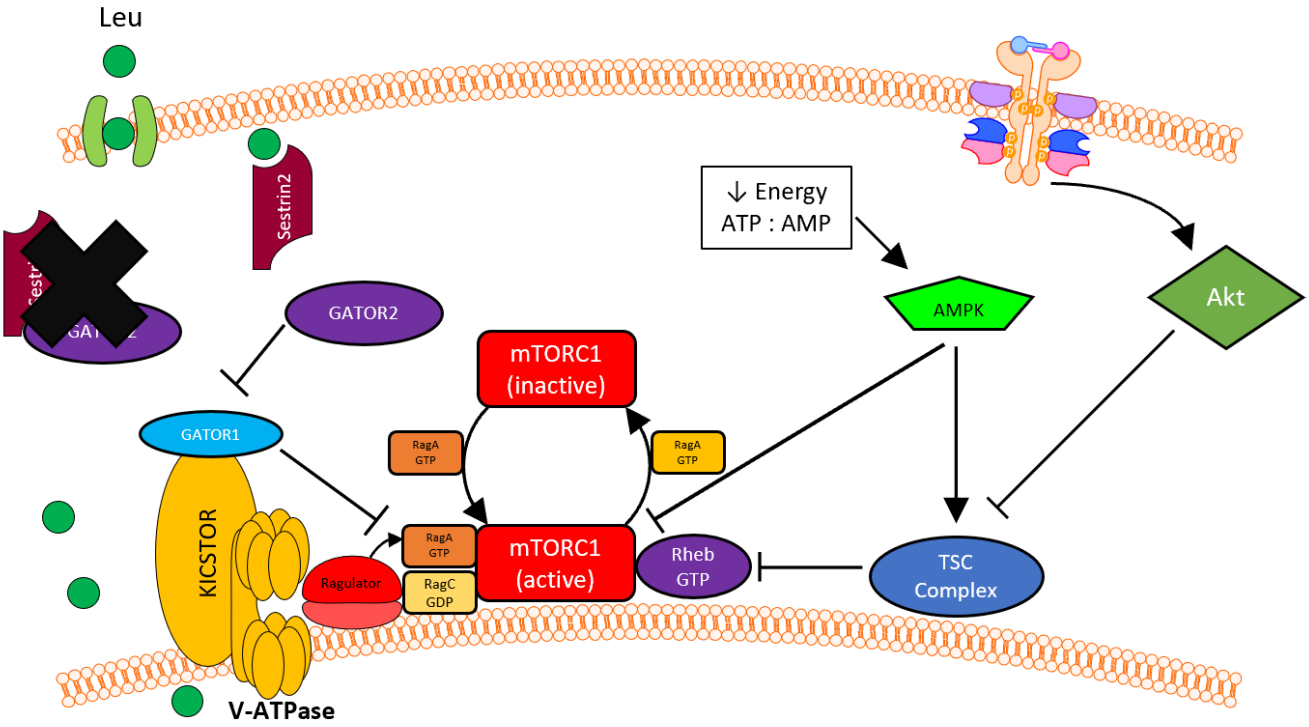

Figure 2 – Diagram of Leu activation of mTORC1[87,89-92]. Leucine activates mTORC1 through lysosomal and cytosolic actions. Leucine enters the lysosome to activate the v-ATPase. The v-ATPase promotes the GEF activity of Ragulator toward RagA/B. ATP-bound RagA/B recruits mTORC1 to the lysosomal surface for interaction with Rheb for mTORC1 activation. Cytosolic Leu binds to Sestrin2 for the dissociation of the Sestrin2-GATOR2 complex for the activation of mTORC1. GATOR2 also inhibits GATOR1, and inhibitor of RagA/B ATP loading.

mTORC1

The mTOR complexes are Ser/Thr protein kinases that control cell growth and proliferation and are classified by the sensitivity of the kinase to the compound rapamycin, a potent inhibitor of mTOR and cell growth and proliferation; mTORC1 is rapamycin-sensitive and mTORC2 is rapamycin-insensitive, although rapamycin can inhibit mTORC2 at high concentrations (Figure 2)[93-95]. mTORC1 regulates cell growth and metabolism and is implicated in autophagy, energy metabolism, lysosome biogenesis, and lipid biosynthesis[90,96]. mTORC2 controls cellular proliferation and survival, most prominently in insulin/PI3K signaling through the phosphorylation and activation of Akt[92].

mTORC1 promotes protein synthesis by phosphorylation of p70 ribosomal S6 Kinase 1 (S6K1) and eukaryotic initiation factor 4E (eIF4E) binding protein 1 (4E-BP1)[87,96]. Stimulation of S6K1 results in increased mRNA biogenesis, cap-dependent translation and elongation, and translation of ribosomal proteins[87,96]. Phosphorylation of 4E-BP1 prevents its binding to eIF4E to promote cap-dependent translation. Ribosome biogenesis is also stimulated by mTORC1 through protein phosphatase 2A (PP2A) and transcription initiation factor IA (TIF-IA)[96]. mTORC1 also has been shown to be involved in mitochondria biogenesis and metabolism by controlling the transcription activity of peroxisome proliferator-activated receptor-γ (PPARγ) coactivator 1 (PGC-1α) by direct alteration of its binding to other transcription factors, such as yin-yang 1 (YY1)[96].

mTORC1 activation requires a bipartite mechanism of activation, requiring both AAs and growth factors. Growth factors, such as insulin-like growth factor 1 (IGF-1), regulate mTORC1 through the tuberous sclerosis complex's (TSC) GTPase-activating protein (GAP) activity toward Rheb, a powerful stimulator of mTORC1 activity (Figure 2)[96,97]. Recent research has illustrated that Leu sensing of mTORC1 is through two distinct mechanisms, with one mechanism located in the cytosol and one within the lysosomal lumen[91]. Historically, Leu sensing and activation of mTORC1 initiated from within the lysosome though an unknown mechanism; within the lysosomal lumen, Leu activates the vacuolar H^+-ATPase (v-ATPase), which in turn activates Ragulator's guanine nucleotide exchange factor (GEF) activity toward RagA[91,97,98]. GTP binding

to RagA recruits mTORC1 to the lysosomal surface, where it then interacts with Rheb for activation (Figure 2)[91,98,99]. Recently, Sestrin2 and GATOR2 have been implicated in the cytosolic signaling of the mTORC1 pathway[91]. In Leu deprived conditions, Sestrin2 binds and likely inhibits GATOR2, a GAP for RagA or RagB (Figure 2)[91]. Leucine binding to Sestrin2 results in GATOR2 dissociation from Sestrin2 and resulting in the inhibition of GATOR1, an inhibitor of GAP activity toward RagA or RagB for the translocation of mTORC1 to the lysosomal surface[91]. Leucyl-tRNA synthetase (LRS) has also been established as a Leu sensor in the mTORC1 pathway, charging Leu to the cognate tRNA, where LRS functions as a GAP toward RagA or RagB.

Nutritional strategies as adjuvant therapy

Epigallocatechin gallate (EGCG), a compound extracted from green tea, as well as the AAs Tau, Gln, Ala, and Arg have been studied for the treatment of DMD[3,100,101]. Indeed, Deflazacort in conjunction with Gln and Arg improves N retention and maintains protein balance in DMD patients[3,100]. Few studies have examined Leu supplementation (or BCAAs) in DMD patients[3]. In 1982, Stewart et. al. administered the branched-chain α-ketoacids, α-ketoisocaproate, α-ketoisovalerate, and α-keto-β-methylvalerate (KIC, KIV, and KMV, respectively), in a 4:1:1 ratio of 0.45 g/kg/day in an isonitrogenous diet decreased muscle protein degradation, determined by 3-methylhistidine excretion, by approximately 14% in DMD patients[102]. Recently, Srivastava et al. noted that serum BCAAs and acetate were significantly increased in DMD as well as Tyr in BMD, and both DMD and BMD having significantly decreased serum Gln[77].

The goal of this study was to determine if the dystrophic phenotype in *mdx* mice could be ameliorated and muscular strength increased with chronic dietary supplementation of the BCAAs. It was hypothesized that high concentrations of the BCAAs during and after the meal would increase protein synthesis by upregulating mTORC1 effectors S6 and 4E-BP1 to preserve muscle function in *mdx* mice. Muscles are both specialized and adaptable and signaling pathways direct development or direct the response to stressors, such as exercise[103]. Murine muscles are composed of four different fiber types (I, IIa, IIx, & IIb) with

different functional properties based on force production, shortening velocity, and resistance to fatigue. Type I and IIa fibers are characterized by having lower absolute force and decreased shortening velocity, but greater resistance to fatigue compared to IIx and IIb fibers[103]. In diseased muscle (e.g. muscular dystrophy), contractile properties usually differ from non-diseased muscle. Muscle function assays provide support for the functional efficacy of treatment for the attenuation or rescue of muscle function[103]. *In vivo* assays measure the functionality of muscles within live animals, maintaining the viability of the muscle in the native environment. The BCAAs did not preserve muscle function in *mdx* mice and no statistically significant increases in mTORC1 effectors were noted.

CHAPTER THREE

Methods

Figure 3 shows a timeline of the study (Figure 3). Food consumption was measured daily by weight difference. Body mass was collected every 2 or 3 days for the duration of the study. Body composition and *in vivo* muscle function measured every four weeks.

Animals

All animal experiments were approved by the Institutional Animal Care and Use Committee at Virginia Tech. Mice had free access to water and were provided food from 1600 EST to 0800 EST. The *mdx* mouse (C57BL/10ScSn-Dmd^{mdx}/J) is the most common animal model for DMD, with a C to T transition that results in a premature stop codon in exon 23. Mice were purchased from the Jackson Laboratory and arrived at four weeks of age. They were separated into four groups of 10 mice (n = 40) based on genotype and diet (Wild type control diet, wild type BCAA diet, *mdx* control diet, & *mdx* BCAA diet; WT C, WT BCAA, *mdx* C, & *mdx* BCAA) and quarantined for two days. Mice were individually housed and placed in the TSE LabMaster (now PhenoMaster) system for metabolic and activity monitoring for four days. Following the metabolic and activity monitoring, mice were singly caged and food consumption monitored daily. Mice were euthanized by CO_2 asphyxiation followed by cervical dislocation.

Diets

Animals were fed nutritionally adequate, isonitrogenous diets for the duration of the study (Table 3). Diets were obtained from Research Diets, Inc. and based on the AIN-93G (D10012G) rodent diet, designed to elevate the BCAAs and keep the diets isonitrogenous (Table 3). Control (A14061002) diet contains L-Leu at 12 g/kg, L-Val at 8 g/kg, and L-Ile at 8 g/kg. The BCAA (A14061001) diet contains L-Leu at 27.64 g/kg, L-Val at 13.82 g/kg, and L-Ile 13.82 g/kg. Food was provided between 1600 hours EST to 0800 EST.

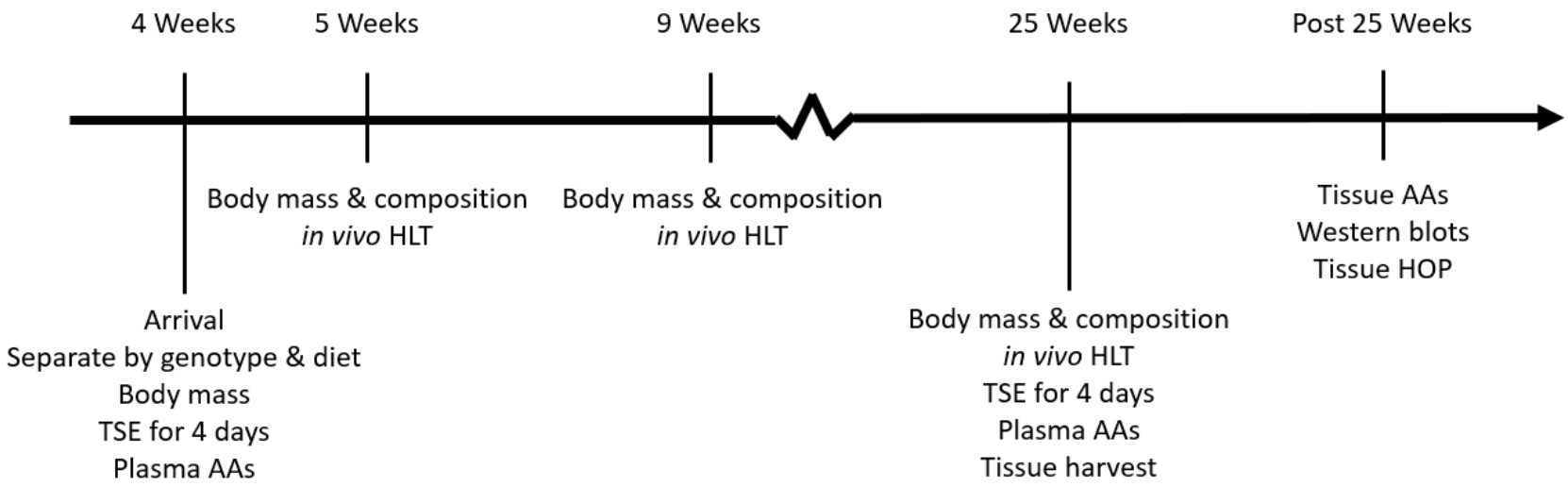

Figure 3 – Timeline of the study.

Diet	A14061002			A14061001	
	Control			BCAA	
	g %	kcal %		g %	kcal %
Protein	15.60	16.60		18.80	19.40
Carbohydrate	67.70	71.70		66.60	68.80
Fat	4.90	11.80		5.10	11.80
Total		100.00			100.00
kcal/g	3.87			3.87	
Ingredient					
L-Arg	8.27			8.27	
L-His-HCl-H_2O	6.00			6.00	
L-Ile	8.00			13.82	
L-Leu	12.00			27.64	
L-Lys-HCl	14.00			14.00	
DL-Met	6.00			6.00	
L-Phe	8.00			8.00	
L-Thr	8.00			8.00	
LTrp	2.00			2.00	
L-Val	8.00			13.82	
L-Ala	10.00			10.00	
L-Asn-H2O	10.00			10.00	
L-Asp	0.00			0.00	
L-Cys	4.00			4.00	
L-Glu	10.00			10.00	
L-Gln	10.00			10.00	
Gly	10.00			10.00	
L-Pro	10.00			10.00	
L-Ser	10.00			10.00	
L-Tyr	4.00			4.00	
Total L-AAs	158.27	633.08		185.55	742.20
Corn Starch	300.00	1200.00		280.00	1120.00
Maltodextrin 10	125.00	500.00		125.00	500.00
Sucrose	250.00	1000.00		242.00	968.00
Cellulose	50.00	0.00		50.00	0.00
Soybean Oil	50.00	450.00		50.00	450.00
Mineral Mix S10001	35.00	0.00		35.00	0.00
Sodium Bicarbonate	7.50	0.00		7.50	0.00
Vitamin Mix V1001	10.00	40.00		10.00	40.00
Choline Bitrartrate	2.00	0.00		2.00	0.00
Diammonium Citrate	24.15	0.00		0.00	0.00
FD&C Yellow Dye #5	0.00	0.00		0.00	0.00
FD&C Red Dye #40	0.00	0.00		0.05	0.00
FD&C Blue Dye #1	0.05	0.00		0.00	0.00
Total					
Nitrogen (g)	25.10			25.10	

Table 3 – Diet composition

Body composition

Nuclear magnetic resonance (NMR) is a non-invasive technique used to determine the lean mass, fat mass, and fluid content of an individual. Mice were weighed, assigned randomly to a dietary group, and subjected to NMR using the Bruker LF90 NMR/MRI System for body composition. Body mass was measured every two or three days and body composition measured every four weeks in triplicate prior to *in vivo* muscle function testing (Figure 4). Upon arrival, mice were weighed, separated by genotype and diet, and placed in the TSE LabMaster (now PhenoMaster) system for four days, then subject to NMR/MRI for body composition measurements.

Whole-body calorimetry and activity monitoring

The TSE LabMaster System is a modular system for metabolic and activity monitoring in mice. Respiratory exchange ratio (RER) is the ratio of CO_2 produced to O_2 consumed ($RER = VCO_2/VO_2$). The RER is used to determine fuel utilization, as carbohydrates, proteins, and fats produce varying amounts of CO_2 upon oxidation. Complete carbohydrate oxidation results in an RER value of 1.0 (e.g. $6\ O_2 + C_6H_{12}O_6 \rightarrow 6\ CO_2 + 6\ H_2O + 34$ ATP; $6\ CO_2/6\ O_2$ = RER of 1.0). Complete fat oxidation results in an RER value of 0.7 (e.g. 16-carbon fatty acid: $23\ O_2 + C_{16}H_{32}O_2 \rightarrow 16\ CO_2 + 16\ H_2O + 129$ ATP; $16\ CO_2/23\ O_2$ = RER of 0.7), and mixed fuel and protein oxidation with RER values of 0.85. Ventilated gas (O_2 & CO_2), cage activity (x, y, & z axes) were measured simultaneously for the duration mice were in the TSE system. Mice acclimated in the TSE system for two days prior to initiation of the measurements. Measurements of ventilated gases were used to calculate 24- and 48-hour energy expenditure RER. Reference Oxygen and CO_2 provided in the TSE system were 20.9% O_2 and 0.05% CO_2, with an air flow rate of 0.4L/min. Data were collected every 20 minutes for the duration of time spent in the system. Energy expenditure data were expressed relative to fat free mass. Energy expenditure (kJ/h) was calculated using the formula $VO_2 \times [3.815 + (1.232 \times RER)] \times 4.1868$ (Weir[104]) and normalized to the lean mass determined by NMR. Animals were individually housed in the TSE for 96 hours – the first 48 hours were for acclimation to the TSE and the

average values of the last 48 hours used for analysis. To calculate hourly activity, the average of two-hour bouts of activity from the last 24-hour period was plotted.

in vivo hind limb torque

in vivo isometric hind limb torque of the plantar-flexor muscles was assessed every four weeks from mouse five weeks of age until 25 weeks of age. Mice were anesthetized with approximately 4% isoflurane and 1.5% O_2 at a rate of 1 L/min (VetEquip Impac5 vaporizer) and placed supine on a thermoregulated platform (35°C; 809B *in situ* mouse stimulation apparatus – Aurora Scientific). Anesthesia was maintained by approximately 2% isoflurane and 1.5% O_2 at a rate of 1 L/min via nosecone. The right hind limb was shaved and sterilized with isopropyl alcohol prior to securing the foot to the foot pedal and servomotor (300C-LR Dual-Mode servomotor – Aurora Scientific). The knee was immobilized as close to 90° flexion as possible by a plunger and U-bracket on the 809B platform (flexion limited by the size of U-bracket and mouse size; approximately 110° – 130° flexion). Isometric muscle contractions were elicited through stimulation of the tibial nerve via needle electrodes (Grass technologies platinum subdermal electrodes E2 – 10 mm long & gauge 30) controlled by Dynamic Muscle Control software version 5.41 (Aurora Scientific). The current was adjusted (30 – 50 mA) until maximal torque was produced. Tetanus measurements were achieved by 150 Hz stimulation. Torque frequency analysis was performed by a series of stimulations at 1, 10, 30, 50, 65, 80, 100, 120, 150, and 180 Hz separated by 30 sec. Torque measurements were obtained for absolute torque production, torque normalized to body mass, and torque normalized to fat free mass. Normalized torque data is not shown. Torque data was analyzed using Dynamic Muscle Analysis software versions 3.2 and 5.211 (Aurora Scientific).

Western immunoblots

Western blots separate proteins based on their denatured state, measuring protein migration velocity through acrylamide gel as a function of the size, shape, and charge of the protein. Freeze-clamped tissues were ground by mortar and pestle continually cooled by liquid N_2. Fifty to 100 mg of ground tissue were

aliquoted into 1.5 mL microcentrifuge tubes and stored at -80°C until extraction. Ground tissue was extracted with 500 µL to 1 mL of extraction buffer from a freshly-made stock solution containing: 5.9 mL ultrapure H_2O, 8 mL 50 mM HEPES, 640 µL 10% CHAPS, 16 µL 1 M DTT, 800 µL 20x Cocktail inhibitor (from 1.04 mL stock of 200 µL 0.1 M EDTA, 200 µL 0.125 M EGTA, 200 µL 0.5 M benzamidine, & 440 µL ddH_2O), 160 µL Calbiochem Protease Inhibitor Cocktail Set III, 160 µL 50 mM TPP, 174 mg β-glycerophosphate, 5.32 µL microcystin, 160 µL 100mM Na_3VO_4, 67.2 mg KF, and 160 µL 100 mM 2-chloroisocaproate. Tissue extracts were sonicated 3 times at 60 pulses using a Branson Sonifier 250 (model P/S BIO) with re-freezing and thawing. Samples were then centrifuged at 14000 RPM for 10 minutes, and the supernatant was transferred to new 1.5 mL microcentrifuge tubes and stored at -80°C until use. Reducing agent compatible BCA protein assay read at 562 nm was used to determine the protein content of the extract. Loading samples were prepared by diluting the tissue extracts with ultrapure H_2O and 4x sample buffer from a stock solution (2 mL 1 M Tris Base pH 6.8, 0.8 g SDS, 0.04 g bromophenol blue, 4 mL glycerol, & 4 mL H_2O), aliquoted for single use, and stored at -80°C until the samples were loaded onto the acrylamide gel.

Samples were then thawed the day of the blot and 2 µL of β-mercaptoethanol was added to the samples before heating in boiling H_2O for 5 minutes. Antibodies for S6, p-S6, 4E-BP1, and p-4E-BP1 were purchased through Cell Signaling Technologies and run on 15% acrylamide SDS PAGE gels. Antibodies for E1α and p-E1α were provided by Dr. David Chen at UTSW and run on 10% acrylamide SDS PAGE gels. Antibodies for atrogin 1 were purchased from Abcam and run using 10% acrylamide SDS PAGE. Gels were run at 150 V and then transferred to polyvinylidene difluoride (PVDF) membranes at 80 V in Towbin Buffer (1.5 L diH_2O, 60.6 g Tris Base, 21.6 g Gly, 300 mL methanol, & 15mL 10% SDS) for 30 minutes. Ice was present in the transfer blot module around the membrane cassettes, with cold H_2O flow from a faucet passing through tubing contained within an ice bucket and into the blot module to maintain cold temperature for transfer. The blot module was placed on a stir plate with a magnetic stir rod to circulate the continually cooled Towbin buffer within the blot module. Membranes were rocked gently on a platform

rocker during all incubation periods. Membranes were stained in Ponceau S for 5 minutes and cleared with water for imaging as a total protein standard. Liver samples used pan actin as a loading control in S6 and 4E-BP1 blots and Ponceau S for atrogin1 blots. Ponceau S was washed clear of the membrane by 0.2% TBST and the membrane blocked for 30 minutes in 5% bovine serum albumin (BSA) at room temperature. Primary antibodies were diluted with 5% BSA and incubated overnight at 4°C. Membranes were washed of the primary antibodies with 0.2% TBST, followed by incubation with the secondary antibody diluted in 5% BSA at room. Secondary antibodies were cleared with 0.2% TBST and membranes developed in 1:10 diluted Femto chemiluminescent for 5 minutes. Blot images were developed using x-ray film and bands quantified using Image J software. Primary antibodies for S6, p-S6, 4E-BP1, p-4E-BP1, and Pan Actin were obtained from Cell Signaling Technologies and E1α and p- E1α from Dr. David Chuang at University of Texas at Dallas. Atrogin1 (Anti-Fbx32) was obtained from Abcam. Donkey-anti-rabbit-IgG-HRP conjugate secondary antibody was obtained from Jackson ImmunoResearch Laboratories.

Plasma & tissue amino acid analysis – HPLC

Plasma and tissue AA contents were quantified using high-performance liquid chromatography (HPLC) after fluoraldehyde o-phthalialdehyde (OPA) derivatization as described by Wu and Knabe[105]. Amino acid standards were purchased from Sigma (2.5 µmol/mL), and an additional 7 amino acids were added to the mix (2.5 µmol/mL; glutamine, asparagine, tryptophan, taurine, β-alanine and non-protein AAs citrulline, ornithine).

Plasma or ground muscle tissue was deproteinized with 1.5 M $HClO_4$ for 10 minutes, followed by neutralization with 2 M K_2CO_3. The supernatant (0.1 mL) was mixed with 0.1 mL of a 1.2% benzoic acid solution (prepared with saturated $K_2B_4O_7$) and brought to a total volume of 0.8 mL with HPLC-grade H_2O. Standards were subjected to the same protocol with final concentrations ranging from 0.01 to 1.875 nmol/mL. The sample solution (25 µL) was mixed with 25 µl of *o*-phthaldialdehyde reagent (50 mg of *o*-phthaldialdehyde in 1.25 ml of methanol to which 11.2 ml of 0.04 M sodium borate buffer, pH 9.5, 50 µl

of β-mercaptoethanol, and 0.4 ml of Brij-35 were added). After mixing, the solution was incubated for 2 min in the WATERS 2695 HPLC system before injection and separation of the *o*-phthaldialdehyde derivatives. Separation was made by gradient elution from a Supelcosil LC-18 column (15 cm × 4.6 mm, 3 μM; Sigma) with a mobile phase of 86% *solvent A* (0.1 M sodium acetate, pH 7.2, containing 9% methanol and 0.5% tetrahydrofuran) and 14% of *solvent B* (100% methanol). The gradient used excitation and emission wavelengths that are described in Wu and Knabe[105]. Detection was made with a JASCO FP-152 fluorescence detector.

Hydroxyproline assay

Collagen is the one of the most abundant proteins in mammals and forms flexible, non-elastic fibers to provide tensile strength. In DMD, collagen replaces functional muscle fibers after repeated bouts of injury, resulting in fibrosis. Hydroxyproline (HOP) is a non-essential amino acid that is a major structural component of collagen. Proline (Pro) and HOP are key in the stability of collagen, permitting sharp twists of the collagen triple helix. Collagen and elastin are the only two mammalian proteins with HOP, and assays that determine HOP content are used as indicators of collagen in tissues.

The hydroxyproline assay was adapted from the McNally Lab protocol at the University of Chicago[106]. Freeze-clamped tissues were ground in a mortar and pestle continually cooled by liquid N_2. Fifty milligrams of tissue were used. All solutions were made fresh the day of use. One milliliter (two 0.5 mL additions of HCl to ensure all tissue was removed) of 6 M HCl was added to the ground tissue microfuge tubes and transferred to a glass tube and capped with a Teflon-lined screw cap. Tubes were placed in a dry heating sand block at 105 - 110°C overnight (approximately 16 – 18 hours) in the fume hood. Samples were removed from the heating block. Samples were cooled prior to transferring 20 μL to new microfuge tubes (performed in triplicate). Hydroxyproline standards were made the day of, and 20 μL of 5 M NaOH was added to each standard and sample. Reagent A was made immediately prior to use by combining 2 mL chloramine T solution and 6 mL acetate citrate buffer (ACB) in a 1:4 volume to volume ratio. One hundred

and fifty microliters of isopropanol and 75 µL of Reagent A were added the tube vortexed and incubated at room temperature for one hour. Reagent B was made immediately prior to use, combining 20 mL Ehrlich's Reagent and 86 mL isopropanol. Ehrlich's reagent contains: 6g p-dimethylaminobenzaldehyde, 200mL 100% ethanol, and 1.35 mL H_2SO_4. One milliliter of Reagent B was added to each sample and incubated at 55°C for 1 hour. Samples were then cooled and centrifuged at 5000 RPM for 1 minute. Two hundred microliters of each standard or sample were loaded into a 96-well plate and measured at an absorbance of 558 nm. Data were reported as µg HOP/tissue weight.

Statistical analysis

All data were analyzed using GraphPad Prism 7.04 statistics and graphing software. A regular 2-way ANOVA with no repeated measures was used for genotype and diet. Multiple comparisons were determined from Tukey's multiple comparisons test with a 95% confidence interval ($p = 0.05$) to determine which group means were significantly different from each other. Two-way ANOVA compares the mean differences between groups split on two independent factors, here genotype and diet. This test determines if there is an interaction between the independent factor and dependent factor. A regular 3-way ANOVA was used for food consumption and body mass over the course of the study. A 3-way ANOVA determines if there is an interaction between three independent variables on single continuous dependent variable. Statistical error is listed as standard errors of the means.

Results

Body composition

Mice arrived at four weeks of age, with *mdx* mice already visually distinguishable from the WT mice; *mdx* mice had significantly less body mass ($p < 0.01$) (Figure 4 A). Body mass was measured every three or four days and *mdx* mice consistently exhibited lower body mass ($p < 0.01$) (Figure 4 A). From arrival until day four, *mdx* were significantly smaller than their WT counterpart and until day 18 when comparing *mdx* animals to WT BCAA animals (Figure 4 A). Body mass was no different from day 21 to day 95, where *mdx* mice again exhibited lower body mass for the duration of the study (Figure 4 A). Wild type animals on the BCAA weighed less than WT animals on the control diet, however multiple comparisons failed to reach significance (Figure 4 A).

Body composition was measured every four weeks for the duration of the study (Figure 3 & Figure 4 B – G). Body composition at five weeks showed a genotype effect, with WT animals having significantly more lean mass ($p < 0.01$) and fat mass than ($p < 0.01$) (Figure 4 B – G). At week nine, there was a shift in lean mass, with *mdx* animals having significantly more lean mass ($p < 0.05$), 13 weeks ($p < 0.01$), 17 week ($p < 0.01$), 21 weeks ($p < 0.01$), and 25 weeks ($p < 0.01$) (Figure 4 B – G). Wild type animals had significantly more fat mass at every time point ($p < 0.01$) (Figure 4 B – G). Animals on the BCAA diets had more fat mass than animals on the control diet at 21 and 25 weeks (both $p < 0.05$), although only noticeable between WT C and WT BCAA animals (Figure 4 B – G).

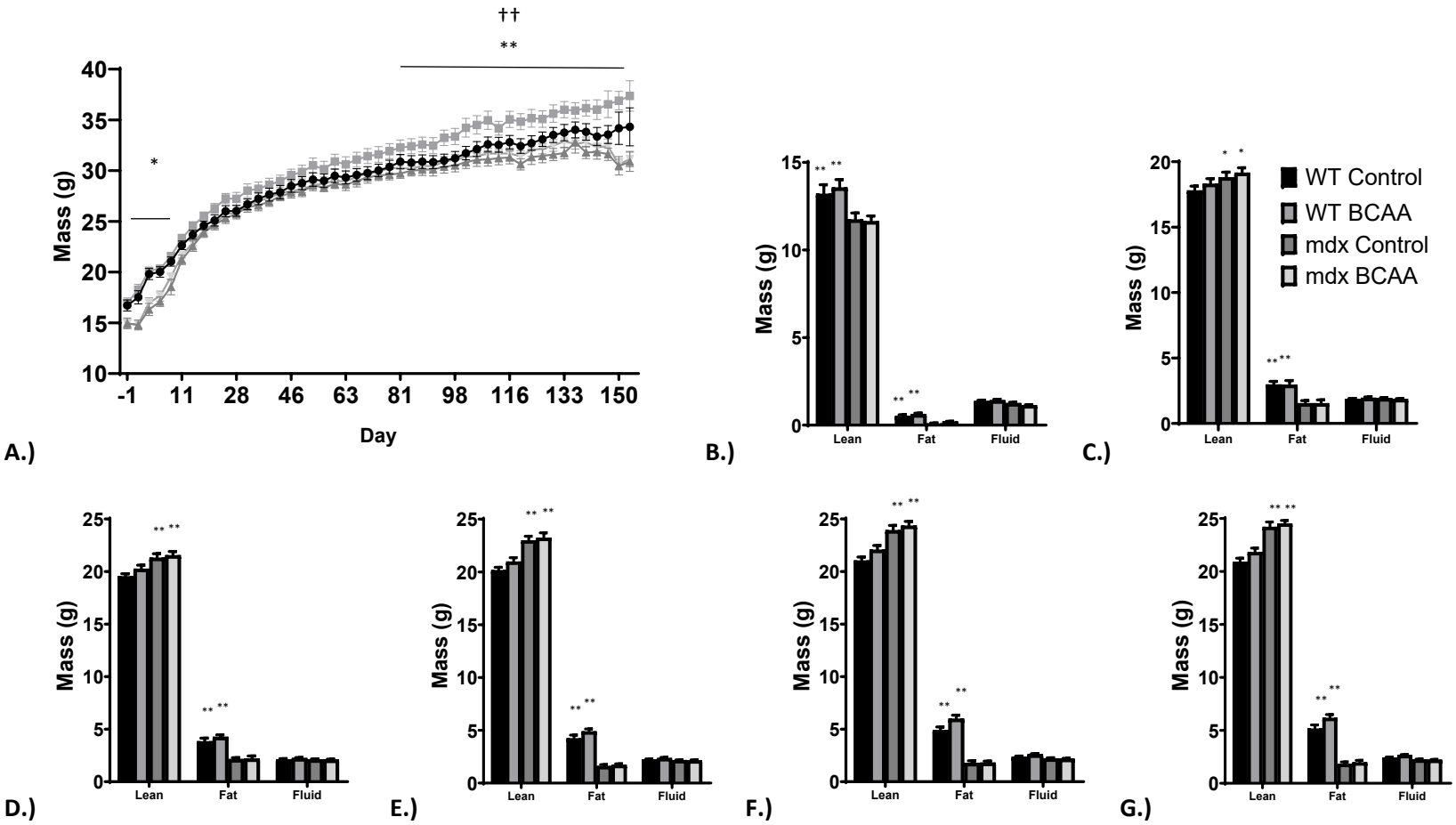

Figure 4 – Body composition measurements for lean mass, fat mass, and fluid mass over 25 weeks. Measurements were performed using the Bruker LF90 NMR/MRI system as described under Methods. Body composition was obtained every four weeks for the duration of the study. A.) Body mass over the duration of the study, Body composition at B.) 5 weeks of age, C.) 9 weeks of age, D.) 13 weeks of age, E.) 17 weeks of age, F.) 21 weeks of age, G.) 25 weeks of age. Symbols are: ● WT control, ▫ WT BCAA, ▲ mdx Control, & ▽ mdx BCAA. Genotype effect: * $p < 0.05$; ** $p < 0.01$. Data presented as standard errors of the means.

Metabolic monitoring

While in the TSE system, metabolic fuel utilization was measured using the respiratory exchange ratio (RER). An RER value of 1.0 indicates 100% carbohydrate use as fuel, 0.85 for mixed fuel use (carbohydrate, protein, & fat), and 0.7 indicates 100% fat oxidation. Mice are nocturnal feeders, and there was a distinct difference in RER during the dark cycles with mice shifting to a higher percentage of carbohydrate oxidation (Figure 6 A – C). Although there were some genotype and diet differences noted at four weeks in individual cycles (Supplementary Figure 1), WT animals and animals on the control diet consistently had higher RER values in the dark cycles, light cycles, and average RER (Figure 5 A – C). At 25 weeks, fuel utilization was different between groups (Figure 5 D – F). RER values were similar to those at four weeks, though there were some individual diet and genotype effects noted in both dark and light cycles (Supplementary Figure 1). Both WT animals and animals on the control diet consistently had higher RER values than their *mdx* and BCAA diet counterparts ($p < 0.05$) (Figure 5 D – F). This suggest that WT animals use more carbohydrates as fuels than *mdx* mice. The lower RER in animals on the BCAA diet may be a result of more protein oxidation due to the significant increase in BCAAs. Another possibility is the difference in protein, carbohydrate, and fat gram percentage and kcal percentage of the diets, with the BCAA diet having more protein, L-amino acids, fat, and less carbohydrates.

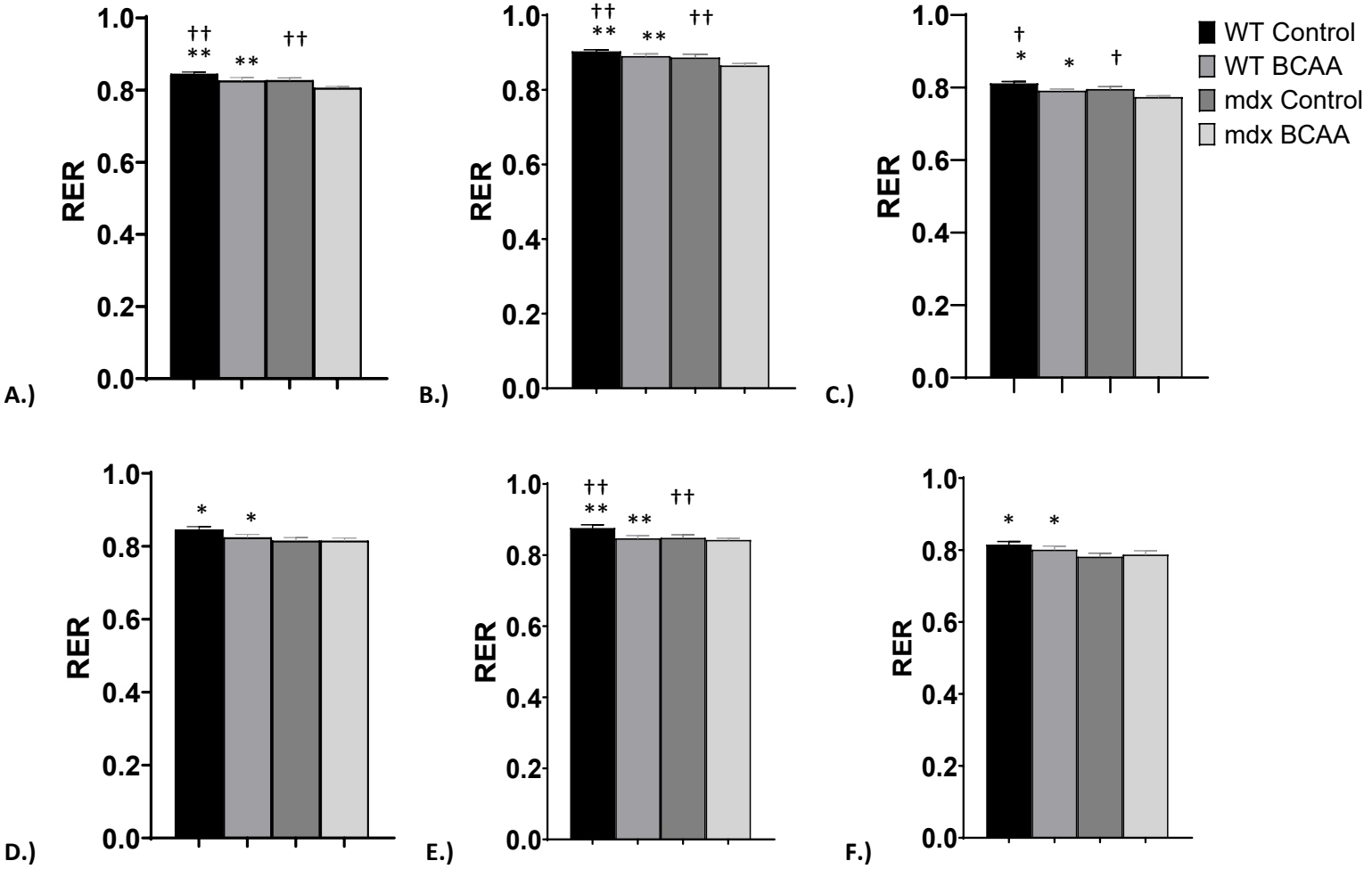

Figure 5 – Fuel oxidation at 4 and 25 weeks. Fuel oxidation was determined by indirect calorimetry using the TSE LabMaster (PhenoMaster) System as described under Methods. Average 48-hour RER; at A.) RER at 4 weeks, B.) dark cycle RER at 4 weeks, C.) light cycle RER at 4 weeks, D.) RER at 25 weeks, E.) dark cycle RER at 25 weeks, & F.) light cycle RER at 25 weeks. Symbols are: ■ WT control, ■ WT BCAA, ■ mdx Control, & ■ mdx BCAA. Standard Errors of the means are presented. Genotype effect: * $p < 0.05$; ** $p < 0.01$. Diet effect: † $p < 0.05$; †† $p < 0.01$. Data presented as standard errors of the means.

Energy expenditure

Energy expenditure (kJ/h) was determined at the beginning and end of the study and calculated using the formula $VO_2 \times [3.815 + (1.232 \times RER)] \times 4.1868$ and normalized to fat-free mass. At four weeks, *mdx* mice expended significantly more energy in both light cycles (cycle 1, $p < 0.01$; cycle 2, $p < 0.05$, data not shown) and total light energy expenditure ($p < 0.01$) (Figure 6 C). However, there were no differences in energy expenditure during any of the dark cycles or in total energy expenditure (Figure 6 A & B). There was a significant shift in energy expenditure at 25 weeks, with WT animals having higher energy expenditure in all cycles and in total energy expenditure ($p < 0.01$) (Figure 6 D – F). This drastic shift is likely attributed to the disease process, where the amount which lowers *mdx* mice activity due to damage sustained to the muscles.

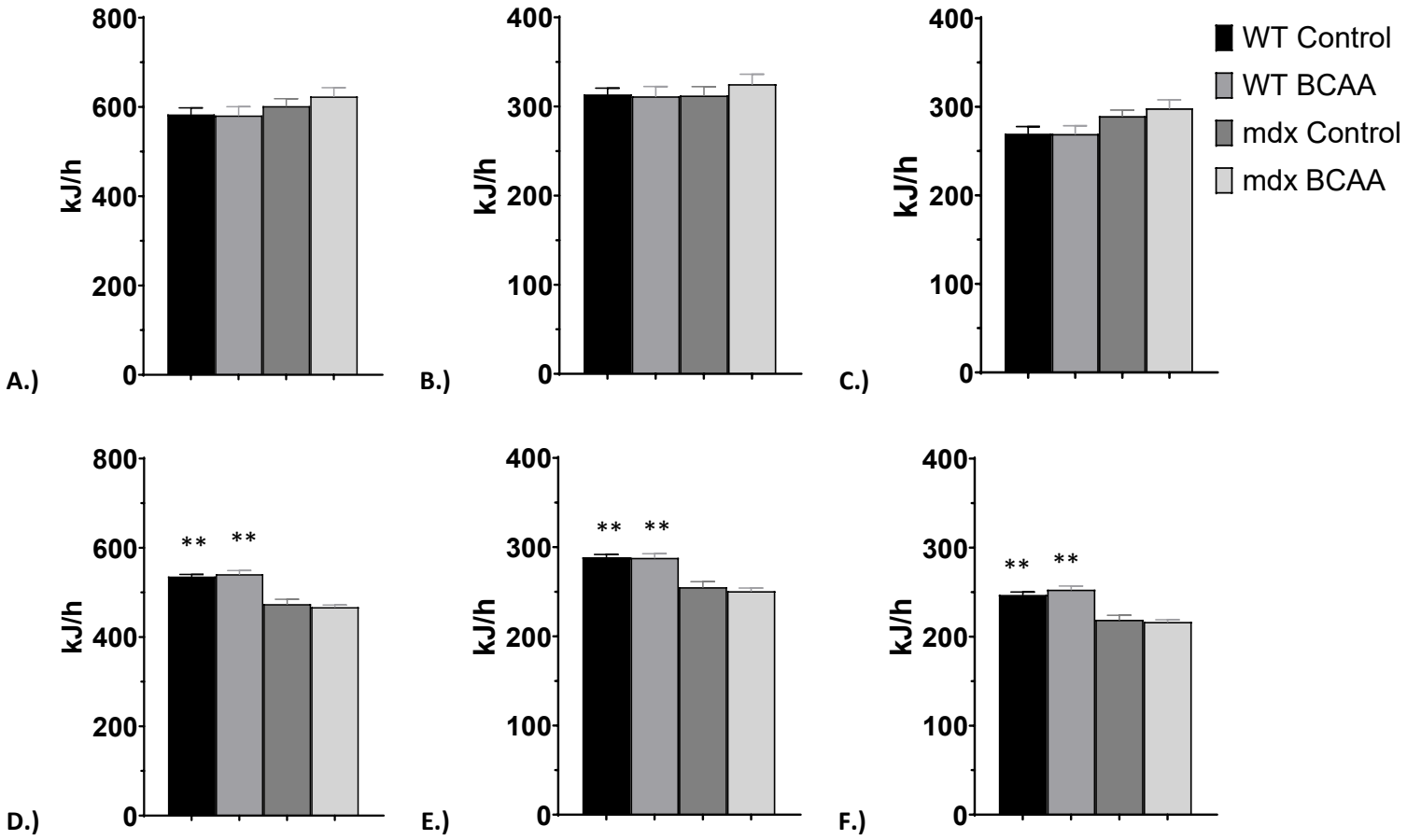

Figure 6 – Energy expenditure at 4 and 25 weeks. Energy expenditure (kJ/h) was determined at the beginning and end of the study and calculated using the formula $VO_2 \times [3.815 + (1.232 \times RER)] \times 4.1868$ and normalized to fat-free mass using the TSE LabMaster (PhenoMaster) as described under Methods. Average 48-hour energy expenditure at A.) energy expenditure at 4 weeks, B.) dark cycle energy expenditure at 4 weeks, C.) light cycle energy expenditure at 5 weeks, D.) energy expenditure at 25 weeks, E.) dark cycle energy expenditure at 25 weeks, & E.) light cycle energy expenditure at 25 weeks. Symbols are: ■ WT control, ■ WT BCAA, ■ mdx Control, & □ mdx BCAA. Standard Errors of the means are presented. Genotype effect: * $p < 0.05$; ** $p < 0.01$.

Activity monitoring

In the TSE system, cage activity was monitored by movement in the X-, Y-, and Z-planes using infrared light beams that recognize locomotor activity. At five weeks, genotype and diet differences were noted in X- and Y-plane activity and none in Z-plane activity (Figure 7). There were individual animal and cycle activity differences (Supplementary Figure 2) and diet was found to influence cage activity, with animals on the BCAA diet exhibiting more movement in the dark cycles and total activity (both, $p < 0.05$) (Figure 7 A – C). At 25 weeks, only genotype effects were noted (Figure 7 D – E). As with activity at four weeks, there was great variability in individual mouse activity and some individual cycle differences at 25 weeks (Supplementary Figure 3). The *mdx* animals have more activity in all cycles, although only significant in the light cycles and total activity ($p < 0.01$ & $p < 0.05$, respectively). In late disease progression, diet no longer influences activity and the *mdx* animals appear more active. This seems paradoxical, as one would expect *mdx* mouse activity to be reduced or limited due to disease progression.

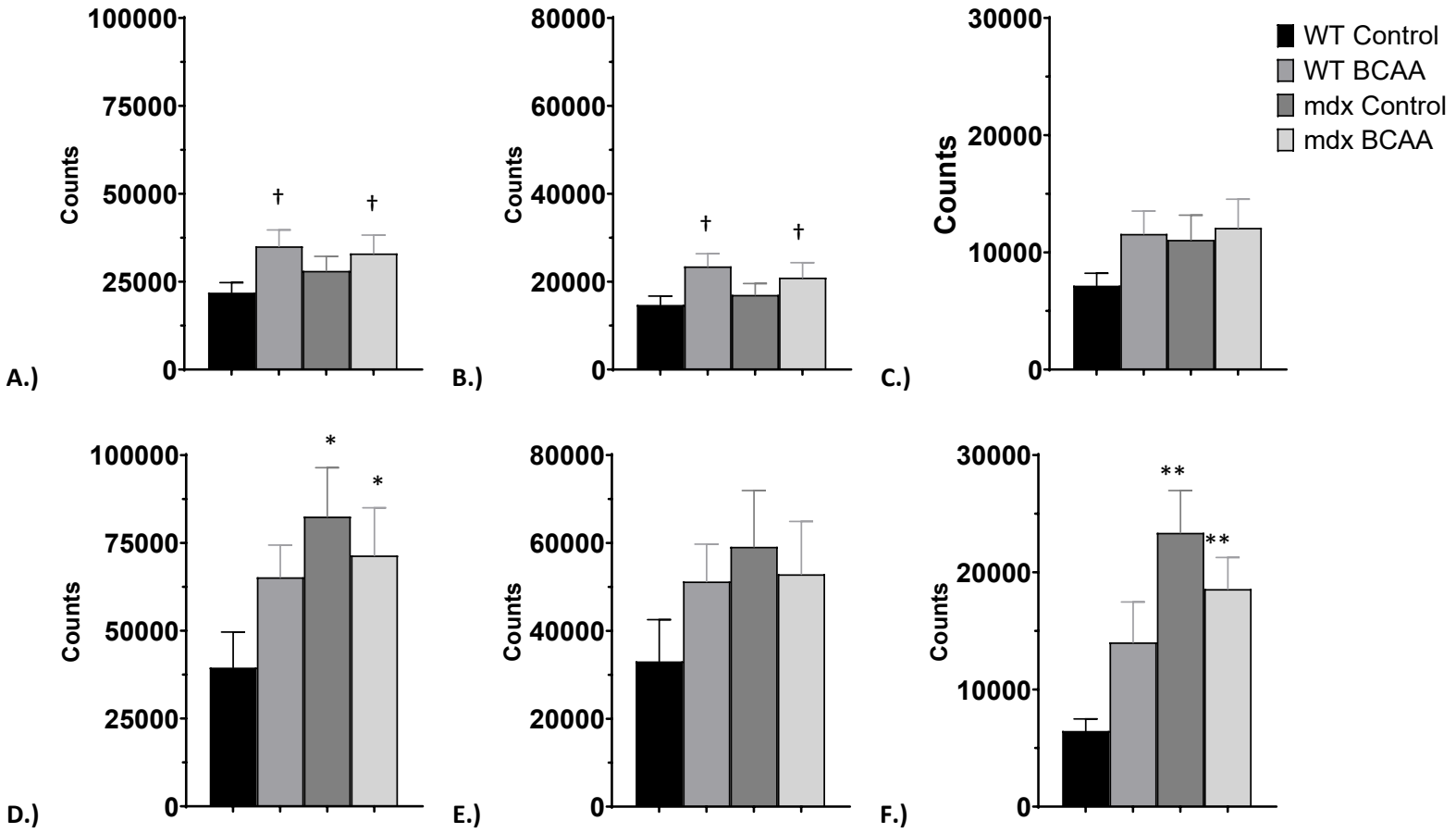

Figure 7 – Cage activity at 4 and 25 weeks. Activity was determined using the TSE LabMaster (PhenoMaster) System as described under Methods. The system tracks movement in the X-, Y-, and Z-planes using infrared light beams that recognize locomotor activity. Measurements were obtained at the beginning and end of the study during the dark and light cycles. A.) Total activity at 4 weeks, B.) dark cycle activity at 4 weeks, C.) light cycle activity at 4 weeks, D.) total activity at 25 weeks, E.) dark cycle activity at 25 weeks, & F.) light cycle activity at 25 weeks. Symbols are: ■ WT control, ▒ WT BCAA, ▒ mdx Control, & □ mdx BCAA. Genotype effect: * $p < 0.05$; ** $p < 0.01$. Diet effect: † $p < 0.05$. Data are presented as standard errors of the means.

Food consumption

Food consumption was not measured while in the TSE LabMaster system and was determined by food weight difference pre- and post-TSE. Food consumption for the duration of the study was not significantly different among groups or when normalized to body mass (Figure 8 A & B). However, there was a noticeable decrease followed by an increase in food consumption throughout the duration of the study. For example, handling of the mice for *in vivo* muscle torque assays, cheek punch for plasma, body mass, and MRI measurements resulted in decreased food and kcal consumption (Figure 8 A – C). There was no difference in kcal intake per day (Figure 8 C). After the *in vivo* protocols were complete, there was an increase in food consumption the following few days (Figure 8 A). It is likely that the stress of anesthesia and the muscle function protocols affected their eating behavior.

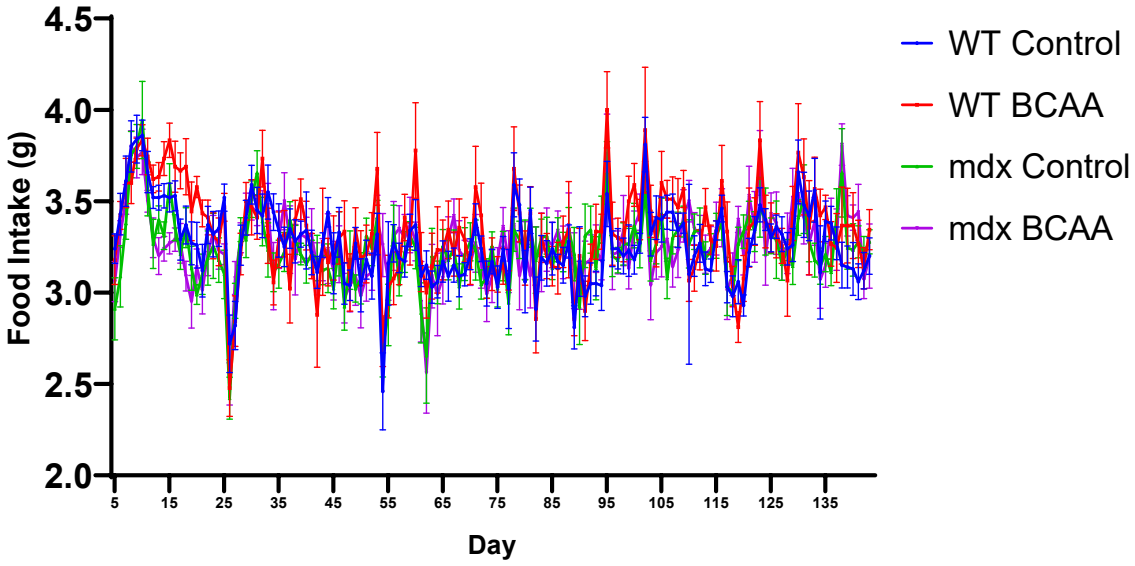

A.)

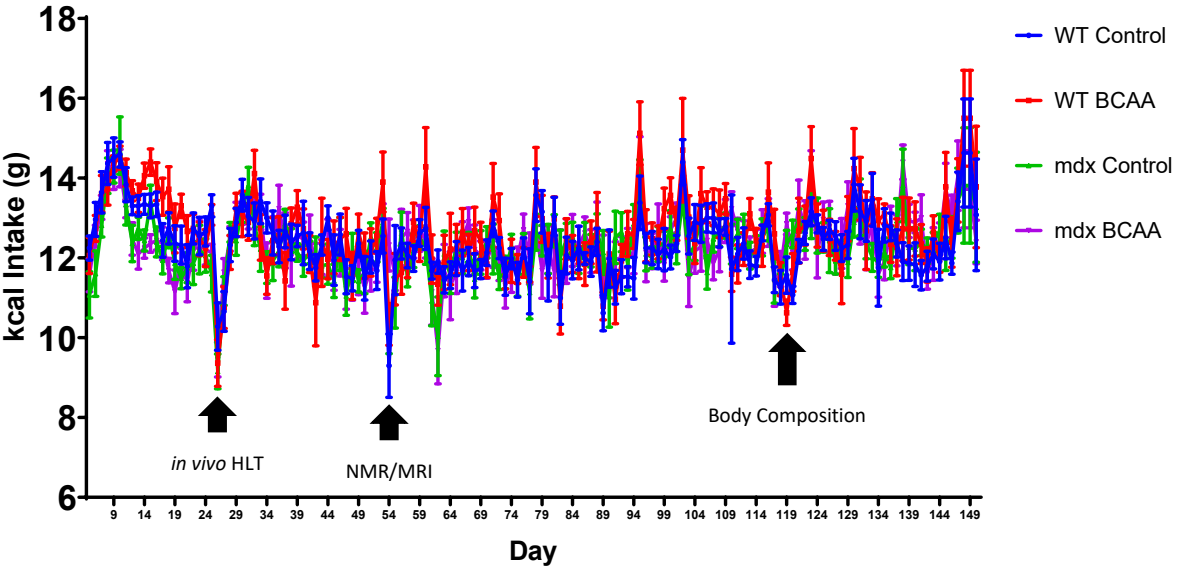

B.)

Figure 8 – Food consumption over 25 weeks. Mice had free access to water and were provided free access to food from 1600 hours to 0800 hours EST as described under Methods. Food consumption was measured daily from the weight difference between provided food (1600 hours) food at the end of the feeding cycle (0800 hours). A.) Daily BCAAs consumed normalized to body mass & B.) daily food intake. First black arrow – i*n vivo* protocol; second black arrow – body composition; third arrow physical handling of the mice. Symbols are: ● WT control, ■ WT BCAA, ▲ mdx Control, & ▼ mdx BCAA. Data provided as standard errors of the means.

Plasma amino acid profiles

Following metabolic and activity monitoring, plasma AAs were obtained at four and 25 weeks after one hour of feeding by cheek punch to determine if the diet was effective in elevating BCAAs and whether other AAs concentrations were affected. At four weeks, BCAAs were significantly elevated in the BCAA diet supplemented animals (Val, $p < 0.01$; Ile, $p < 0.01$; & Leu, $p < 0.01$) (Figure 9 A). These data show that the diet was successful in increasing plasma BCAAs. At 25 weeks, only the BCAA Leu was elevated in the BCAA diet animals ($p < 0.05$) (Figure 9 B) suggesting the animals had adapted to the high BCAA diet. Alternatively, the lack of significance in all three plasma BCAAs in the BCAA diet group could be explained by individual mouse food consumption prior to sacrifice with some mice consuming more or less of the diet.

Only genotype differences were noted for essential AAs at four and 25 weeks. At four weeks, only His ($p < 0.01$) and Arg ($p < 0.01$) were different in WT animals compared to control mice (Figure 10 A). At 25, Arg was the only essential AA found to be different, with *mdx* animals having more Arg than their WT counterparts ($p < 0.05$) (Figure 10 B). Non-essential AAs primarily showed genotype effects at four and 25 weeks – only Ala was elevated in animals on the BCAA diet compared to the control diet at four weeks ($p < 0.01$) (Figure 12 A). At four weeks, Asn ($p < 0.01$), Ser ($p < 0.01$), Gln ($p < 0.01$), and Ala ($p < 0.05$) were significantly elevated in WT animals compared to *mdx* animals (Figure 11 A). At 25 weeks, *mdx* animals had elevated Asp ($p < 0.05$), Glu ($p < 0.05$), and Gly ($p < 0.05$) (Fig 11 B). Of the non-protein AAs, Tau was significantly elevated in *mdx* animals compared to WT animals ($p < 0.01$) and β-Ala showed a diet effect diet ($p < 0.01$) at four and 25 weeks ($p < 0.01$) (Figure 12 A – D).

Tissue amino acid profiles

Tissue AAs were measured in the liver, heart, diaphragm, red muscle, and white muscle of WT and *mdx* mice at 25 weeks (Figs 13 A – E). All three BCAAs were elevated in the liver, although only Leu and Val

were significant ($p < 0.01$ & $p < 0.05$) (Figure 13 A). In the heart, all three BCAAs were elevated, although only Leu ($p < 0.01$) and Val ($p < 0.05$) were significant (Figure 13 B). In the diaphragm, animals on the BCAA diets had elevated tissue Leu ($p < 0.001$) and Val ($p < 0.01$), but not Ile ($p = 0.0644$) (Figure 13 C). Only Val exhibited a genotype effect, with the *mdx* animals having more than their WT counterparts ($p < 0.05$) (Figure 13 C). In red muscle, only Leu ($p < 0.01$) and Val ($p < 0.05$) were found to be elevated in animals on the BCAA diet (Figure 13 D). All three BCAAs were elevated in the heart of animals on the BCAA diet, although not significant (Figure 13 E). In all tissues analyzed other than white muscle, Leu and Val were the only two BCAAs to be elevated in animals on the BCAA diet compared to the control diet. Although not significant in white muscle and Ile, all three BCAAs were elevated in all tissue of animals on the BCAA diet.

Figure 13 shows results for tissue essential AAs. In the liver, only Met was elevated in *mdx* animals compared to WT animals ($p < 0.05$) (Figure 15 A). Methionine was also found to be elevated in the diaphragm of *mdx* animals compared to WT animals ($p < 0.01$) (Figure 14 C). In all muscles analyzed, His, Arg, and Lys consistently saw differences (Figure B – E). In the heart, His ($p < 0.01$) and Arg ($p < 0.05$) were significantly elevated in WT animals compared to *mdx* animals (Fig 14 B & C). Conversely, His ($p < 0.01$) and Arg ($p < 0.01$) were significantly elevated in *mdx* animals compared to control animals (Figure 14 B & C). Both the heart and diaphragm were found to have elevated Lys (both, $p < 0.05$) in animals on the control diet compared to animals o the BCAA diet (Figure 14 B & C). Histidine, Arg, and Lys also showed differences in red and white muscle. Wild type animals had significantly more Arg in red and white muscle compared to their *mdx* counterparts (red, $p < 0.01$; white, $p < 0.05$). Lysine was found to be significantly elevated in *mdx* animals compared to control animals (both, $p < 0.01$). Although only His ($p < 0.01$) and Lys ($p < 0.01$) were elevated in red muscle of animals on the control diet compared to the BCAA diet, white muscle His and Lys was elevated in animals on the control diet, although not significant (Figure 14 D & E).

Figure 14 shows results for tissue non-essential AAs. In the liver Glu ($p < 0.05$) and Gln ($p < 0.05$) were elevated in WT animals compared to *mdx* animals (Figure 15 A). Only Gly ($p < 0.01$) was elevated in *mdx* livers compared to WT animals (Figure 15 A). Glutamine was the only non-essential AA elevated in the heart of WT animals compared to *mdx* animals ($p < 0.01$) (Figure 15 B). The diaphragm showed the most differences in non-essential AAs, with *mdx* animals having significantly more Asp ($p < 0.01$), Asn ($p < 0.01$), Ser ($p < 0.01$), Gln ($p < 0.05$), Gly ($p < 0.01$), and Tyr ($p < 0.01$) compared to WT animals (Figure 15 C). In the diaphragm, only Ala was found to be elevated in animals on the BCAA diet compared to the control diet ($p < 0.05$) (Figure 15 C). In red muscle, Gln ($p < 0.01$), Ala ($p < 0.01$), and Tyr ($p < 0.01$) were found to be significantly elevated in WT animals compared to *mdx* animals, and Gly ($p < 0.05$) elevated in animals on the control diet compared to the BCAA diet (Figure 15 D). Serine ($p < 0.01$) and Tyr ($p < 0.01$) were the only two non-essential AAs elevated in WT animals compared to *mdx* animals (Figure 15 E.)

The non-protein amino acid results are shown in Figs. 16 and 17. In the liver, only genotype effects were noted, with *mdx* animals having elevated Cit ($p < 0.01$), β-Ala ($p < 0.01$), and Orn ($p < 0.01$) compared to WT animals (Figure 16 A). In the heart, only Cit was elevated in WT animals compared to *mdx* animals ($p < 0.01$) (Figure 16 B). In the diaphragm, *mdx* animals had more β-Ala than WT animals ($p < 0.05$) while WT animals had more Orn than their *mdx* counterparts ($p < 0.01$) (Figure 16 C). Ornithine was the only non-protein AA elevated in *mdx* red muscle compared to WT animals ($p < 0.05$) (Figure 16 D). No differences were noted for any non-protein AA in white muscle and no differences were noted for Tau in all tissues (Figure 16 E & 17).

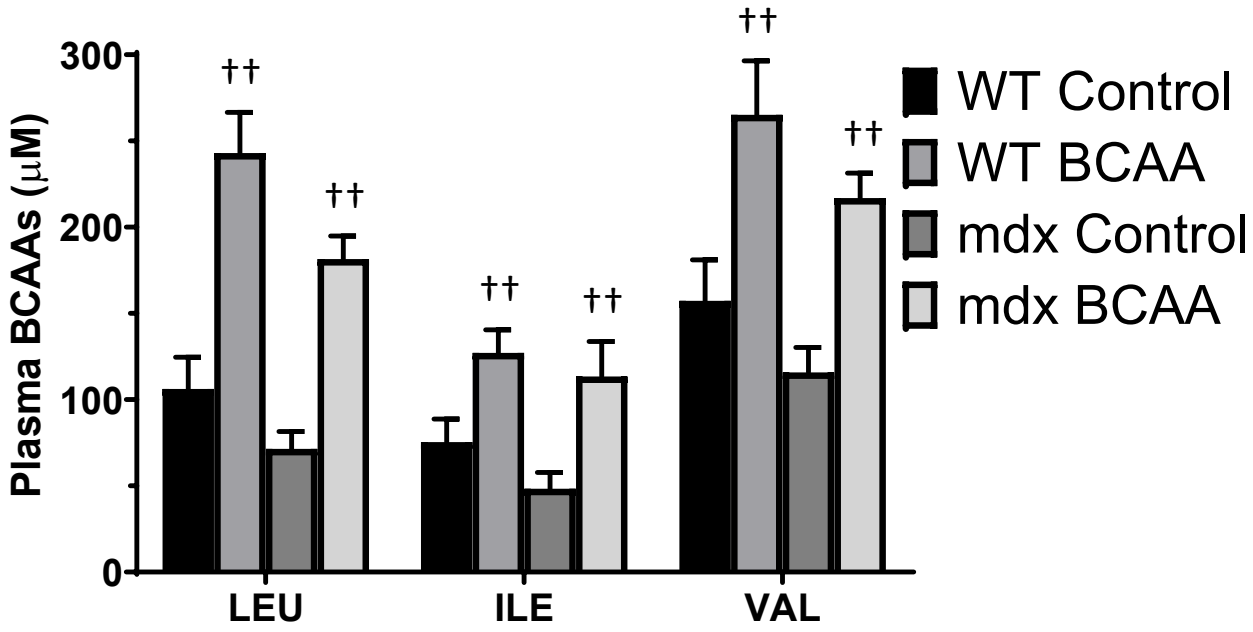

A.)

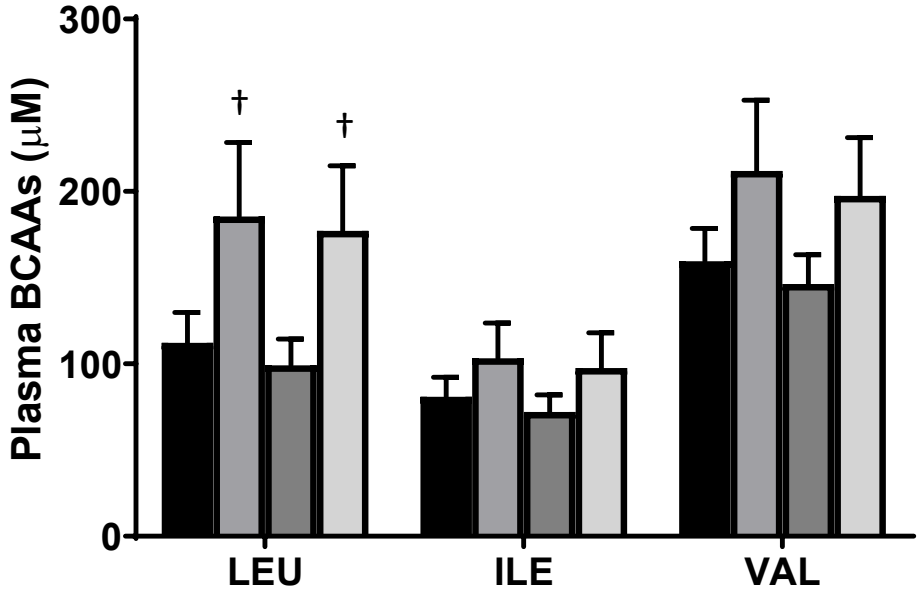

B.)

Figure 9 – Plasma BCAAs at 4 and 25 weeks. Plasma BCAAs were obtained at the beginning and end of the study using HPLC with fluoraldehyde o-phthialdehyde (OPA) derivatization as described under Methods. Plasma BCAAs at A.) 4 weeks, & B.) 25 weeks. Symbols are: ■ WT control, ▒ WT BCAA, ▒ mdx Control, & □ mdx BCAA. Diet effect: † $p < 0.05$; †† $p < 0.01$. Data are presented as standard errors of the means.

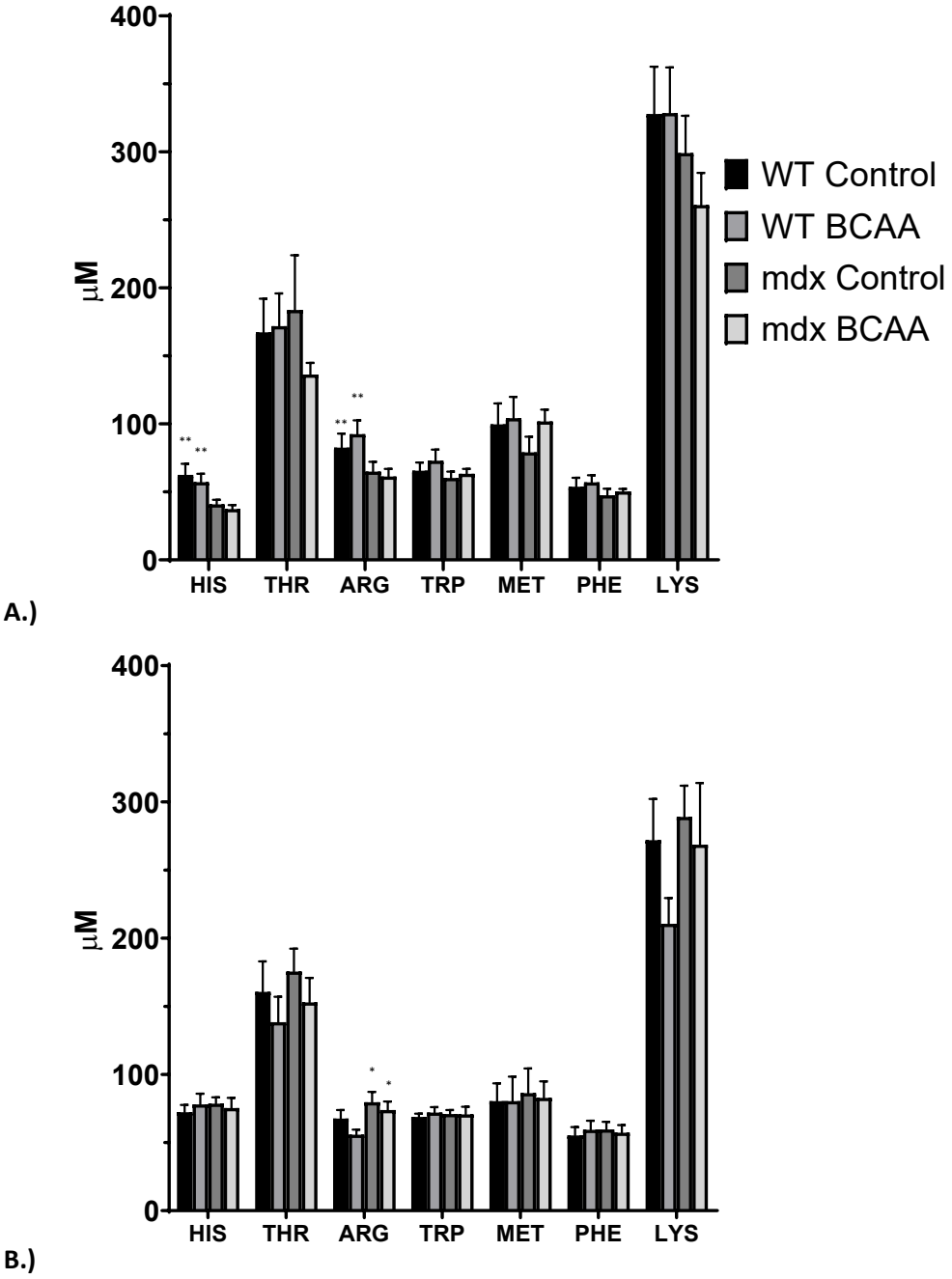

Figure 10 – Plasma essential AAs at 4 and 25 weeks. Plasma AAs were measured at the beginning and end of the study using HPLC with fluoraldehyde o-phthalialdehyde (OPA) derivatization as described under Methods. Plasma essential AAs at A.) 4 weeks, & B.) 25 weeks. Symbols are: ■ WT control, ▨ WT BCAA, ■ mdx Control, & □ mdx BCAA. Genotype effect: * $p < 0.05$; ** $p < 0.01$. Data are presented as standard errors of the means.

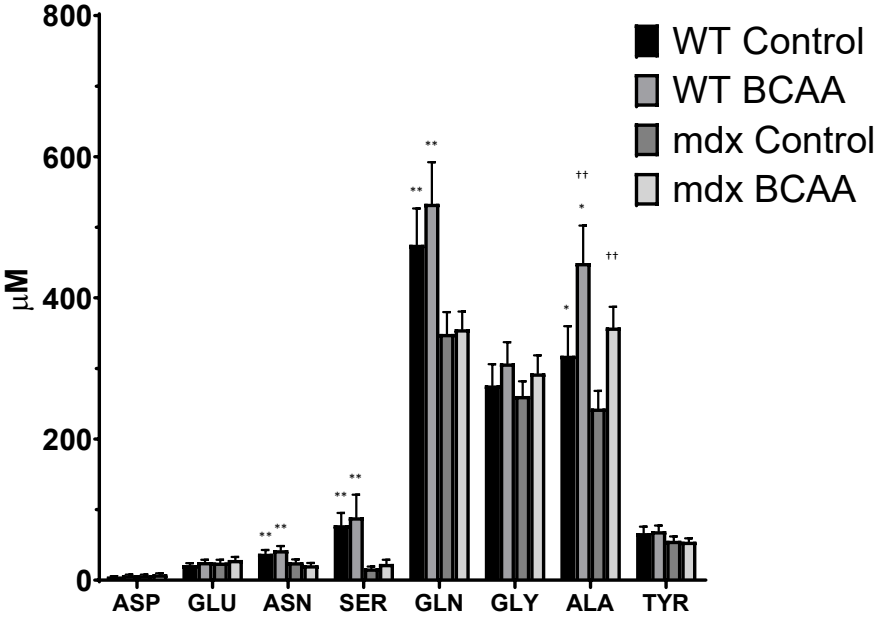

A.)

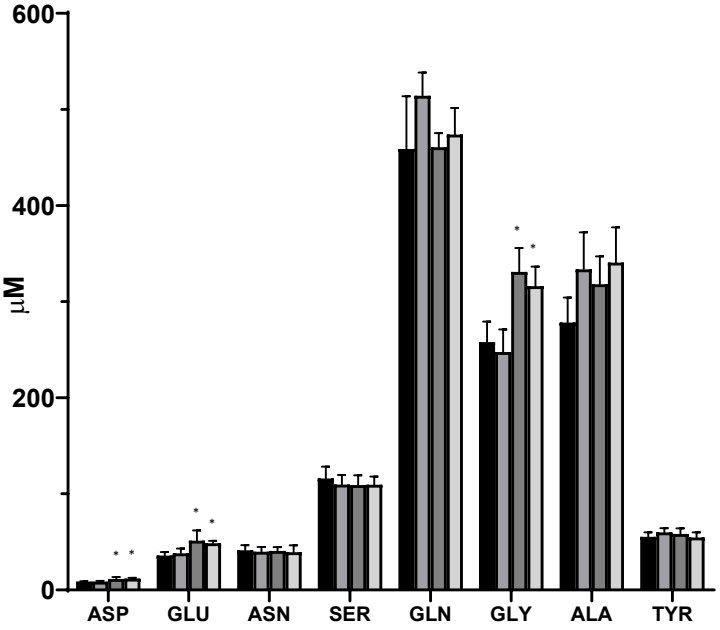

B.)

Figure 11 – Plasma non-essential AAs at 4 and 25 weeks. Plasma AAs were measured at the beginning and end of the study using HPLC with fluoraldehyde o-phthalialdehyde (OPA) derivatization as described under Methods. Plasma non-essential AAs at A.) 4 weeks, & B.) 25 weeks. Symbols are: ■ WT control, ▩ WT BCAA, ▩ mdx Control, & □ mdx BCAA. Genotype effect: * $p < 0.05$; ** $p < 0.01$. Diet effect: †† $p < 0.01$. Data are presented as standard errors of the means.

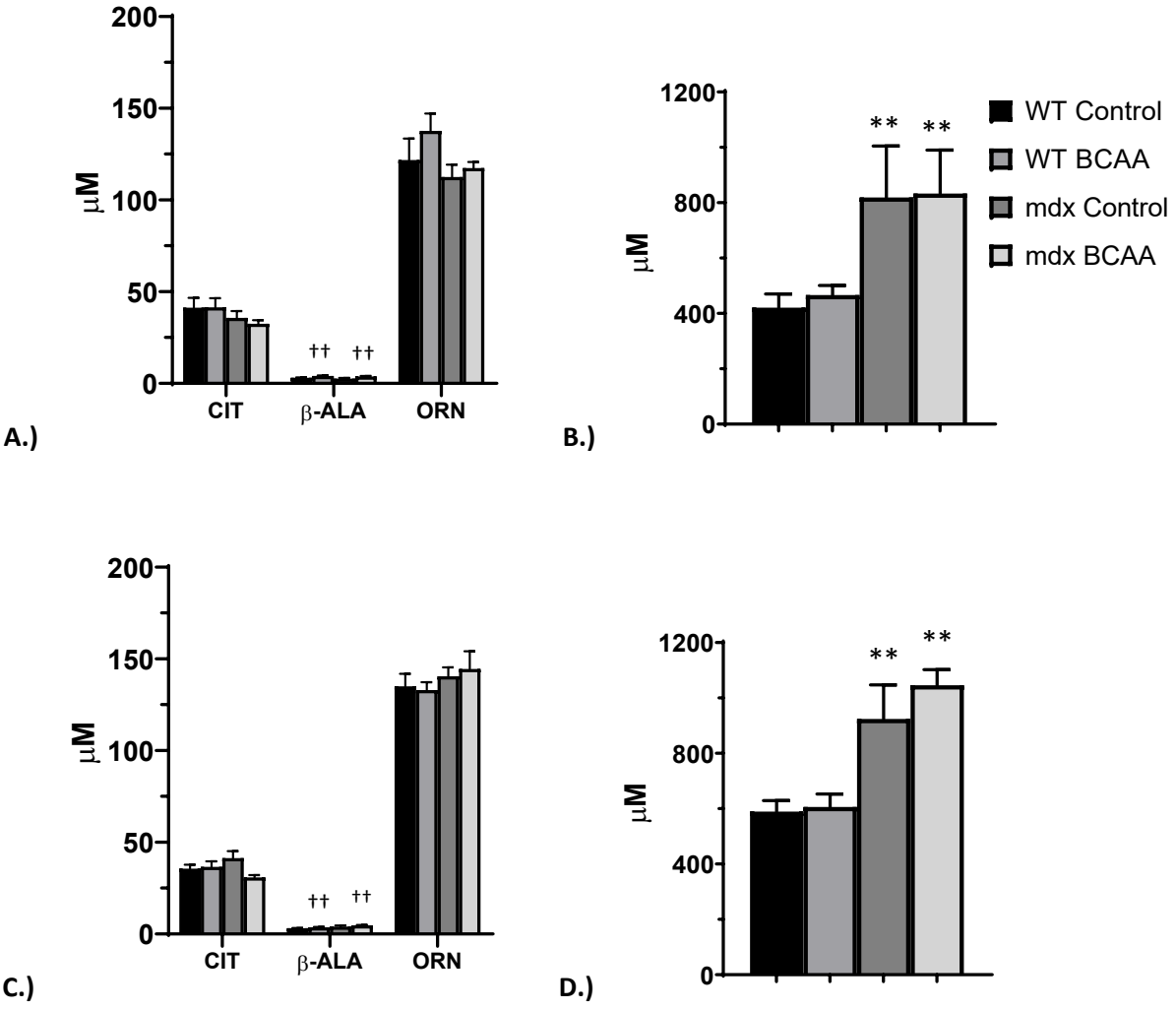

Figure 12 – Plasma non-protein AAs at 4 and 25 weeks. Plasma AAs were measured at the beginning and end of the study using HPLC with fluoraldehyde o-phthalialdehyde (OPA) derivatization as described under Methods. A.) Plasma non-protein AAs at 4 weeks, B.) plasma Tau at four weeks, C.) plasma non-protein AAs at 25 weeks, & D.) plasma Tau at 25 weeks. Symbols are: ■ WT control, ▨ WT BCAA, ▩ mdx Control, & □ mdx BCAA. Genotype effect: ** $p < 0.01$. Diet effect: †† $p < 0.01$. Data are presented as standard errors of the means.

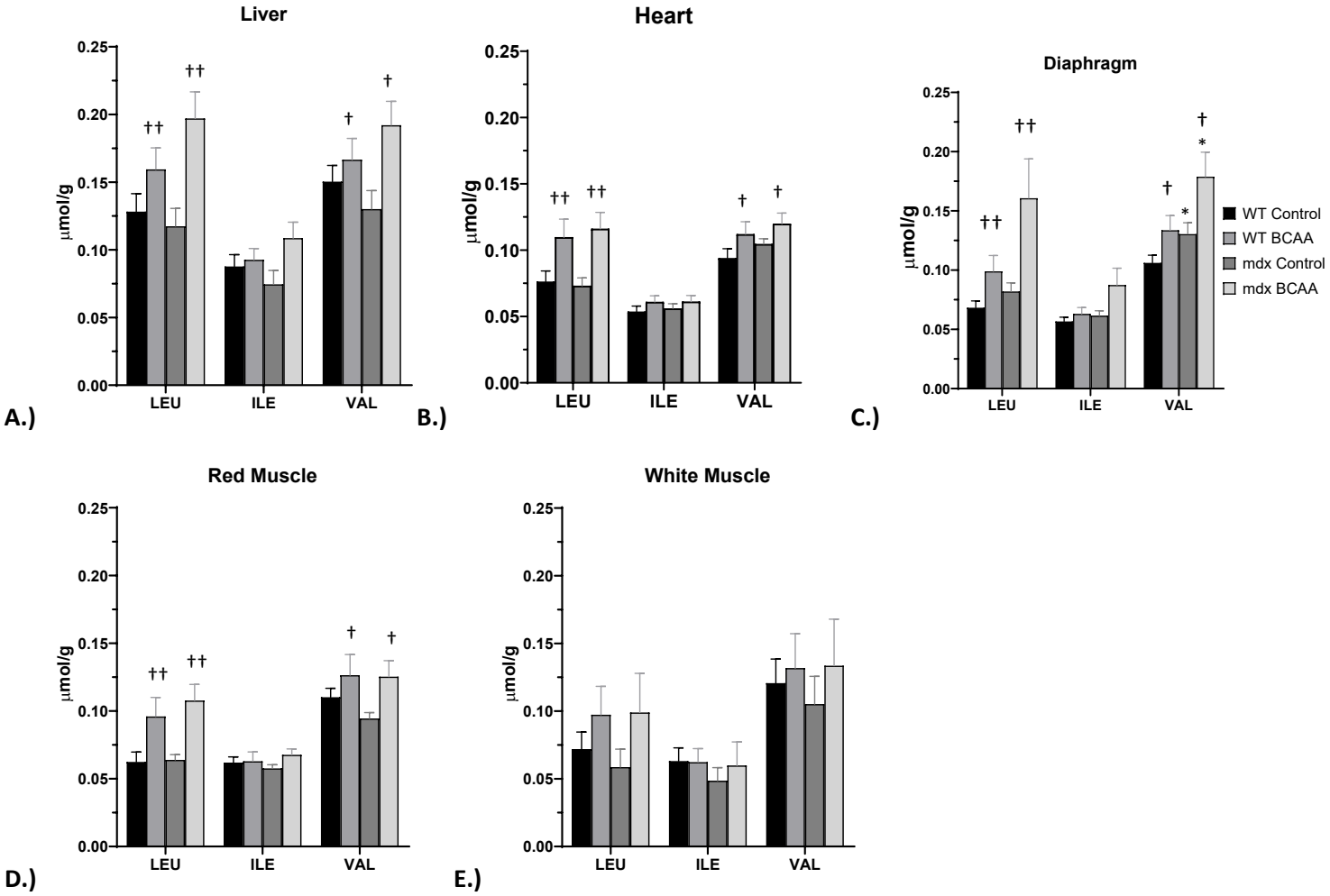

Figure 13 – Tissue BCAAs. Tissue BCAAs were measured using HPLC with fluoraldehyde o-phthalialdehyde (OPA) derivatization as described under methods. A.) Liver, B.) heart, C.) diaphragm, D.) red muscle, & E.) white muscle. Symbols are: ■ WT control, ▨ WT BCAA, ▩ mdx Control, & □ mdx BCAA. Genotype effect: * $p < 0.05$. Diet effect: † $p < 0.05$; †† $p < 0.01$. Data are presented as standard errors of the means

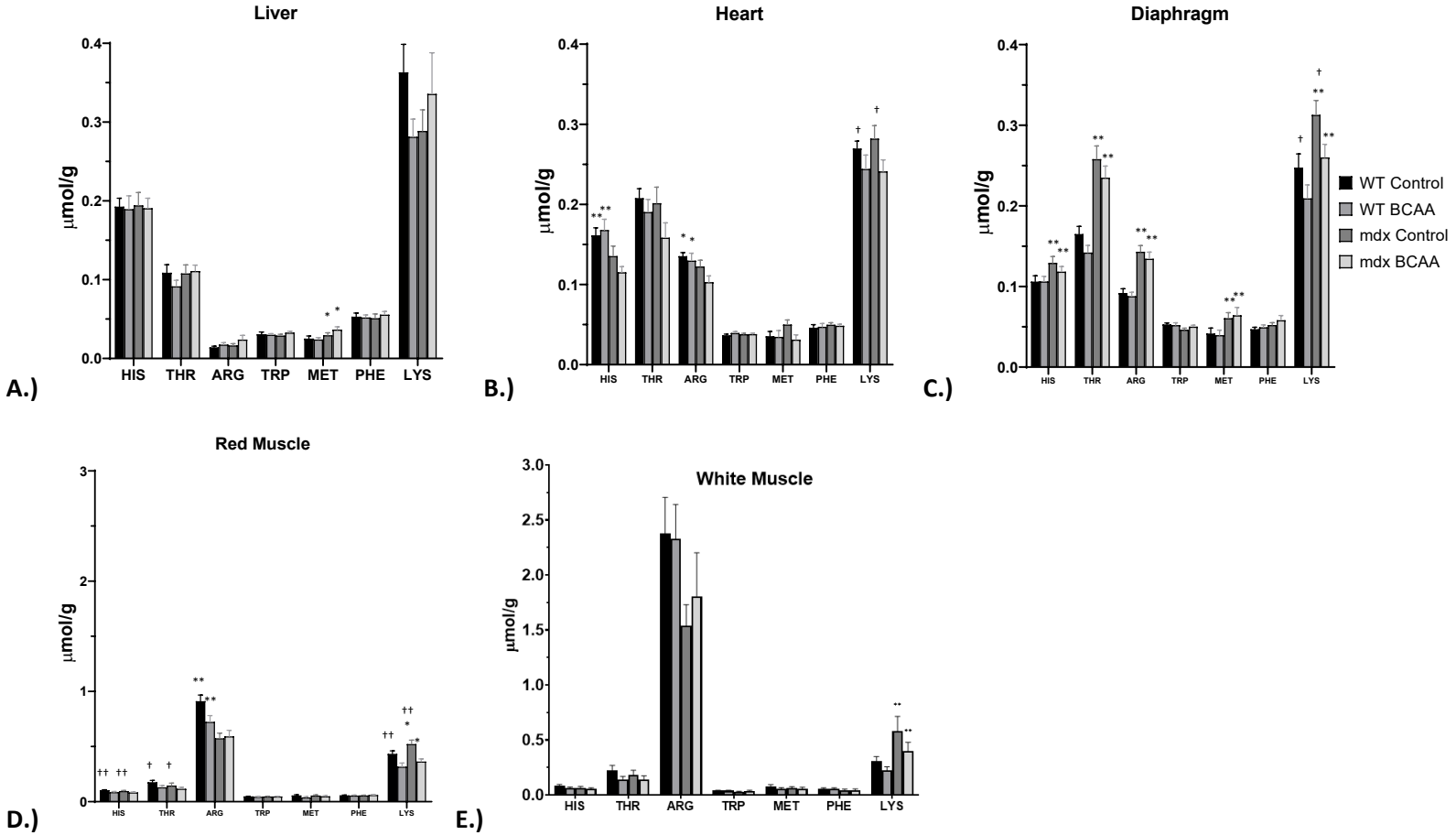

Figure 14 – Tissue essential AAs. Tissue essential AAs were measured using HPLC with fluoraldehyde o-phthalialdehyde (OPA) derivatization as described under Methods. A.) Liver, B.) heart, C.) diaphragm, D.) red muscle, & E.) white muscle. Symbols are: ■ WT control, ▨ WT BCAA, ▩ mdx Control, & □ mdx BCAA. Genotype effect: * $p < 0.05$; ** $p < 0.01$. Diet effect: † $p < 0.05$; †† $p < 0.01$. Data are presented as standard errors of the means.

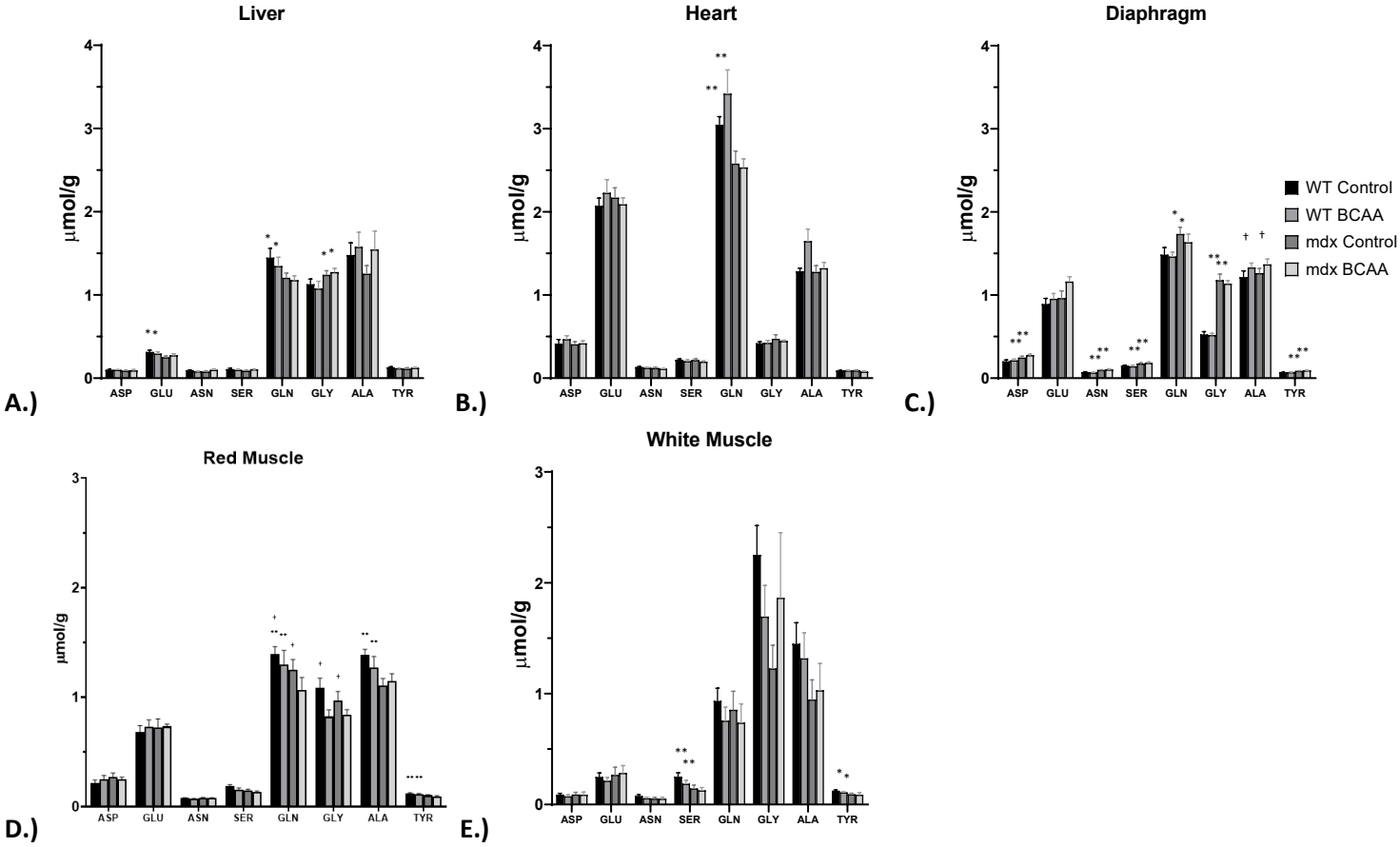

Figure 15 – Tissue non-essential AAs. Tissue non-essential AAs were measured using HPLC with fluoraldehyde o-phthalialdehyde (OPA) derivatization as described under Methods. A.) Liver, B.) heart, C.) diaphragm, D.) red muscle, & E.) white muscle. Symbols are: ■ WT control, ▩ WT BCAA, ■ mdx Control, & □ mdx BCAA. Genotype effect: * $p < 0.05$; ** $p < 0.01$. Diet effect: † $p < 0.05$. Data are presented as standard errors of the means.

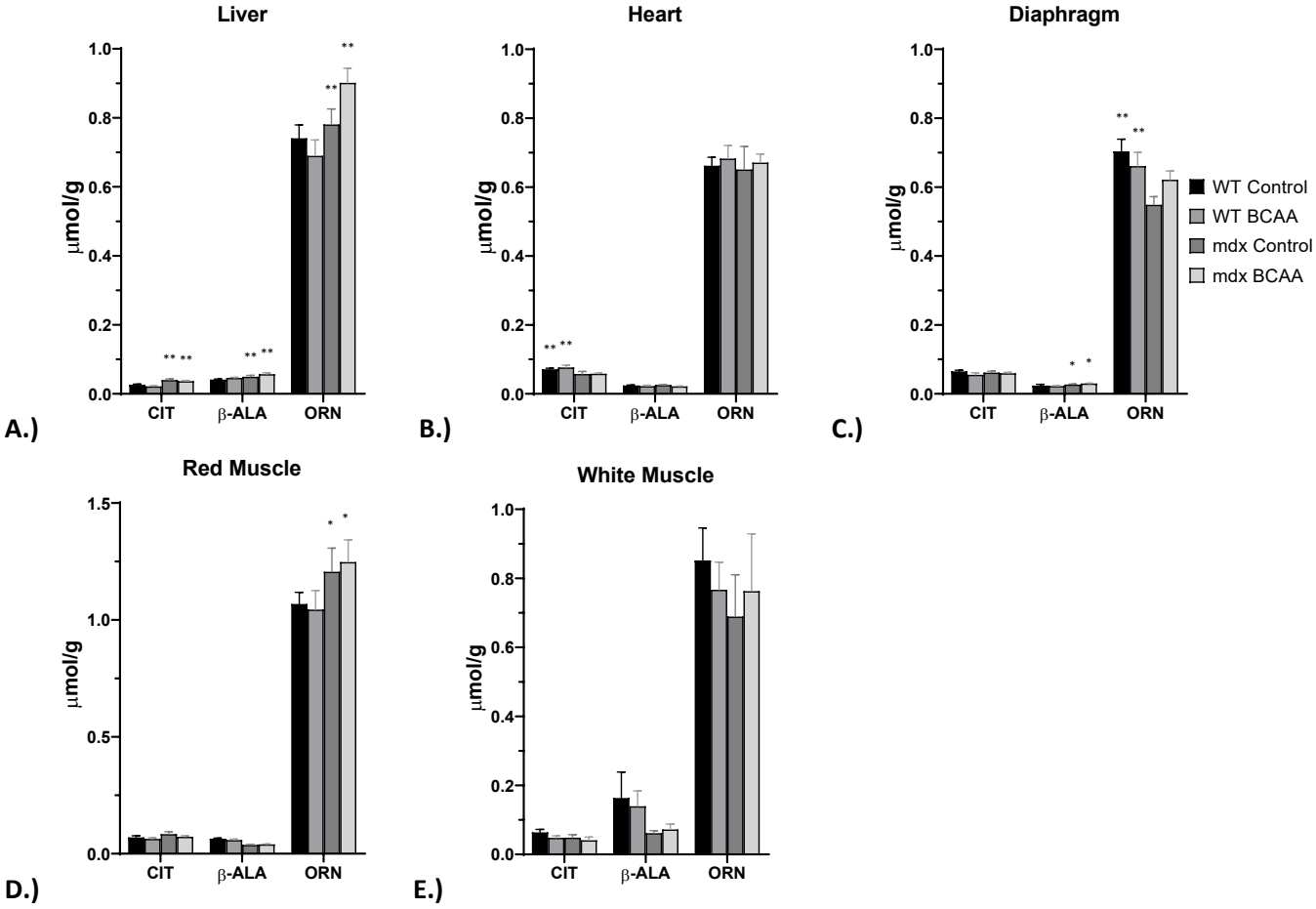

Figure 16 – Tissue non-protein AAs. Tissue non-protein AAs were measured using HPLC with fluoraldehyde o-phthalialdehyde (OPA) derivatization as described under methods. A.) Liver, B.) heart, C.) diaphragm, D.) red muscle, & E.) white muscle. Symbols are: ■ WT control, ▒ WT BCAA, ▓ mdx Control, & □ mdx BCAA. Genotype effect: * $p < 0.05$; ** $p < 0.01$. Data are presented as standard errors of the means.

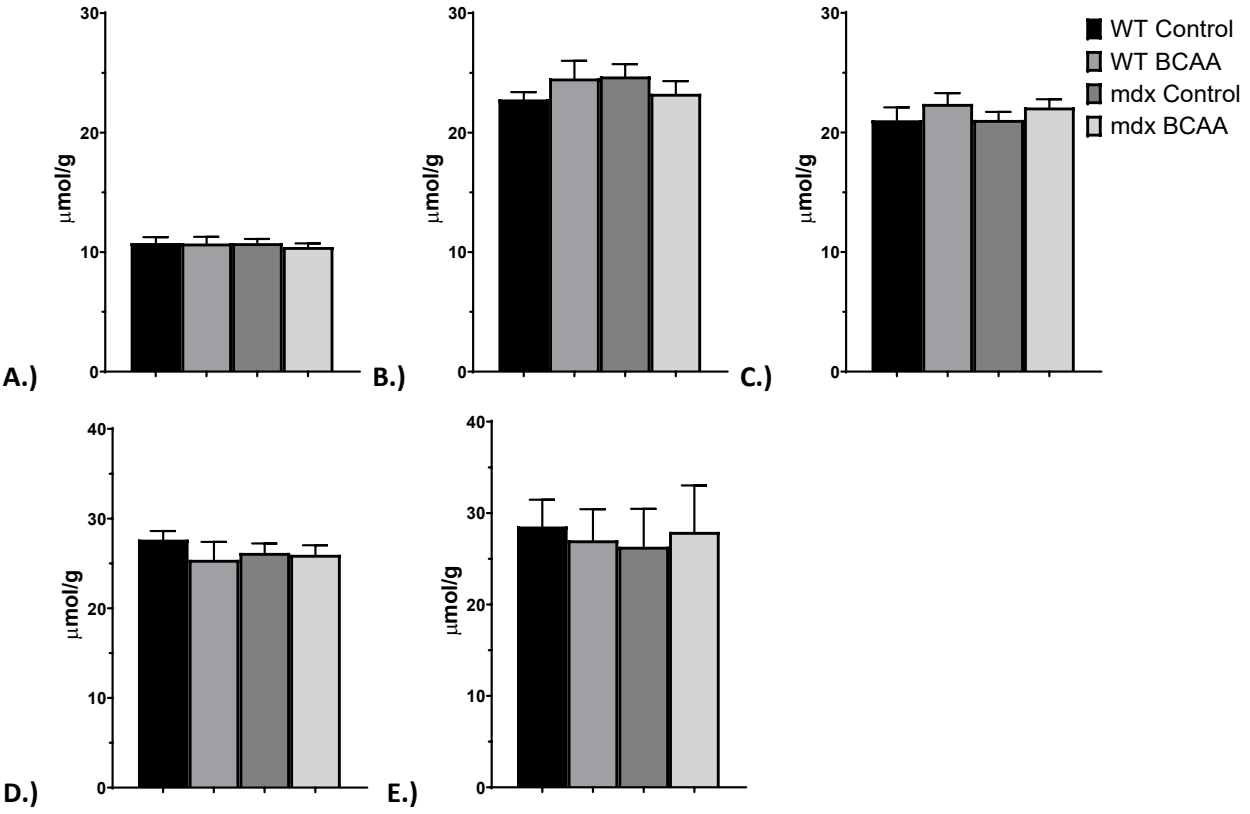

Figure 17 – Tissue taurine. Tissue Tau measured using HPLC with fluoraldehyde o-phthalialdehyde (OPA) derivatization as described under methods. A.) Liver, B.) heart, C.) diaphragm, D.) red muscle, & E.) white muscle. Symbols are: ■ WT control, ▩ WT BCAA, ▩ mdx Control, & □ mdx BCAA. Data are presented as standard errors of the means.

Muscle Function

Results for muscle torque assays are shown in Figs. 18 and 19. Initial *in vivo* muscle function assays at five weeks of age were performed to determine muscle torque and responses to activation frequencies between a twitch and tetanus. Maximal torque production was determined by tetanic contraction, where there is no increase in force with increasing frequency of stimulation. The only differences noted were by genotype, where WT mice produced significantly more torque than their *mdx* counterparts ($p < 0.01$) (Figure 18 A). Torque frequency relations plot the torque responses to activation frequencies between twitch and maximal tetanic frequencies. Unlike maximal torque production, there was a noted genotype ($p < 0.01$) and diet ($p < 0.01$) effect in torque-frequency, with WT animals producing significantly more torque compared to the *mdx* animals and animals fed the control diet producing more torque than animals on the BCAA diet (Figure 19 A). Normalization of lean mass or body mass also showed WT animals produced significantly more tetanic torque than the *mdx* animals, and animals on the control diet had significantly more torque from 50 Hz to 180 Hz) (data not shown). However, statistical tests failed to show any diet interactions between the *mdx* control and *mdx* BCAA animals or WT control and WT BCAA animals, indicating that the BCAAs did not improve muscle torque production. This

At nine weeks, there were significant differences between *mdx* and WT animal muscle torque that persisted for the duration of the study; *mdx* animals consistently produced less tetanic torque than their WT counterparts ($p < 0.01$) (Figure 18 A – F). This was also true when torque was normalized to lean mass and body mass (data not shown). Torque production at different stimulation frequencies showed that at 50 Hz of stimulation *mdx* mouse torque production was significantly less from the WT animals, which persisted for the duration of the study ($p < 0.01$) (Figure 19 A – D). Interestingly, from nine weeks until completion of the study, torque frequency curves of *mdx* animals begin to decline in the 150 to 180 Hz range of stimulation (Figure 19 B – D). Animals on the control diet produced more torque in the 50 to 180 Hz range than animals on the BCAA for the duration of the study, however, statistical tests failed to show any diet interactions between the *mdx* animals of the WT animals (Figure 19 A – D).

At 13 weeks, it became clear that the primary outcome of the *in vivo* muscle function protocols would show only a genotype effect. Wild type animals produced significantly more tetanic torque that the *mdx* animals ($p < 0.01$) (Figure 18 C). In the torque frequency analysis, WT animals produced significantly more torque than the *mdx* animals from 50 Hz to 180 Hz ($p < 0.01$). Although diet effects were noted from 50 Hz to 180 Hz, statistical tests fail to show diet effects between the *mdx* animals or the WT animals (Figure 19 C – F). Wild type animals produced significantly more tetanic torque and torque from 50 Hz to 180 Hz when normalized to lean mass and body mass (data not shown). Torque measurements at 17 and 21 weeks showed the same pattern and significance of torque production for tetanus ($p < 0.01$) and 50 Hz to 180 Hz ($p < 0.01$) in the torque frequency analysis, with WT animals producing significantly more torque than the *mdx* animals (Figure 18 D & E; Figure 19 D & E). Diet effects were noted from 50 Hz to 180 Hz, although no differences were noted between the *mdx* animals and WT animals (Figure 19 D & E). Wild type animals also produced more torque when normalized to lean mass and body mass (data not shown).

Torque measurements at the conclusion of the study continued to show the same genotype and diet effects (Figure 18 F & 19 F). Only a genotype effect was noted in tetanus, with WT animals producing significantly more torque than their *mdx* counterparts ($p < 0.01$) (Figure 18 F). Both genotype and diet effects were seen in the torque frequencies, where WT animals and animals on the control diet produced significantly more torque from 50 Hz – 180 Hz ($p < 0.01$), (Figure 19 F). Tetanus and torque frequencies from 50 Hz to 180 Hz were significantly greater in WT animals compared to control animals when normalizing to lean mass and body mass (data not shown). As with the previous torque frequencies, although there was a diet effect noted, there were no differences between *mdx* animals and WT animals.

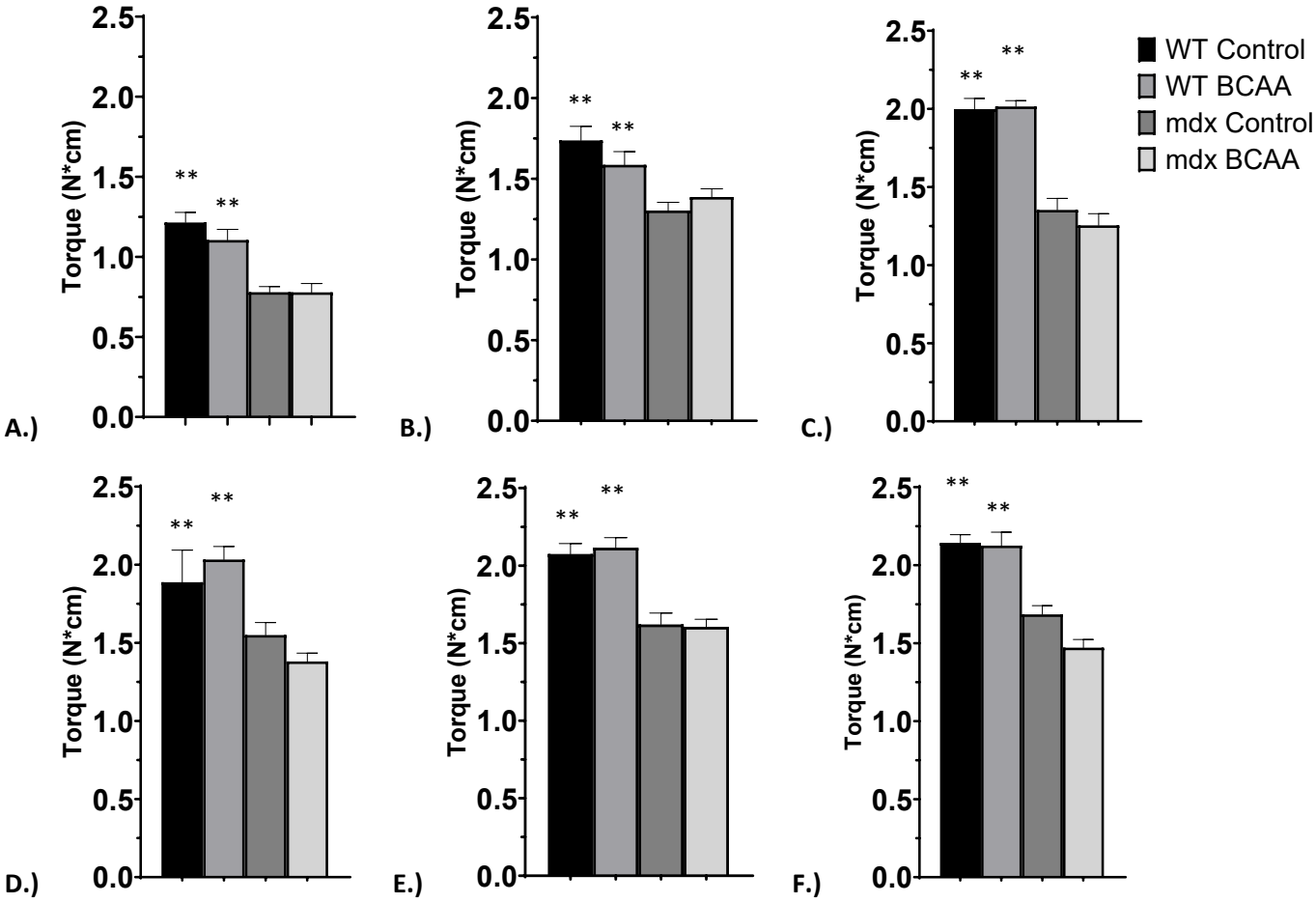

Figure 18 – Tetanic torque production from 5 to 25 weeks. Muscle function was assayed *in vivo* using Aurora Scientific 300C dual-mode muscle lever system and analyzed using DMA 3.2 and 5.211 software as described under Methods. Tetanus was achieved by 150 Hz stimulation. Tetanic force production at A.) 5 weeks, B.) 9 weeks, C.) 13 weeks, D.) 17 weeks, E.) 21 weeks, & F.) 25 weeks. Symbols are: ■ WT control, ▒ WT BCAA, ▒ mdx Control, & □ mdx BCAA. Genotype effect: ** $p < 0.01$. Data are presented as standard errors of the means.

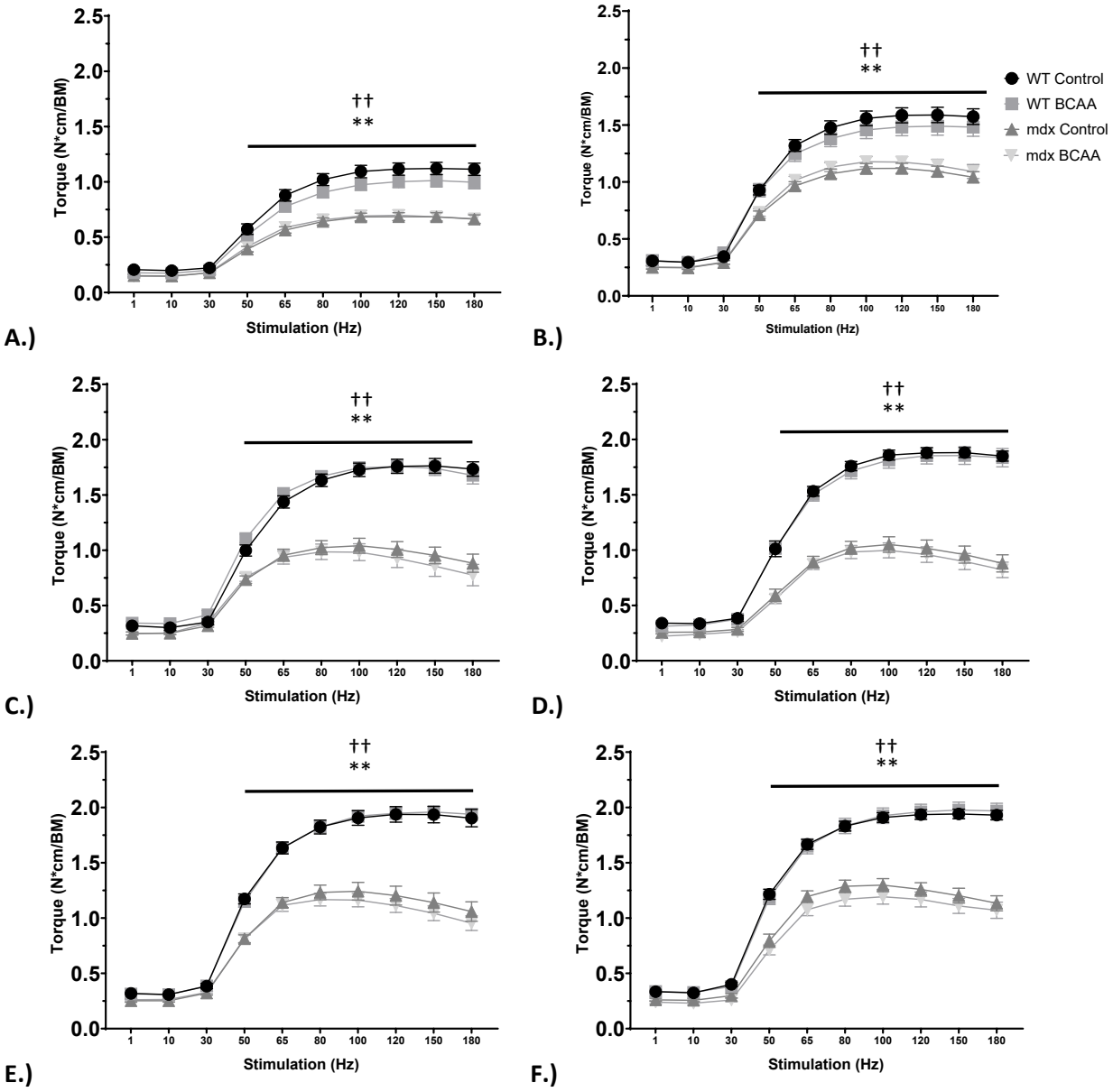

Figure 19 – Torque frequency analysis from 5 to 25 weeks. Muscle function was assayed using Aurora Scientific 300C dual-mode muscle lever system and analyzed using DMA 3.2 and 5.211 as described under Methods. Torque frequency analysis uses incremental increases in electrical stimulation to observe the torque generated upon activation. Torque frequencies were separated by 30 seconds and stimulated at 1, 10, 30, 50, 65, 80, 100, 120, 150, and 180 Hz. Torque frequency at A.) 5 weeks, B.) 9 weeks, C.) 13 weeks, D.) 17 weeks, E.) 21 weeks, & F.) 25 weeks. Symbols are: ■ WT control, □ WT BCAA, ■ mdx Control, & □ mdx BCAA. Genotype effect: ** $p < 0.01$. Diet effect: †† $p < 0.01$. Data are presented as standard errors of the means.

Tissue masses

Brain, kidney, liver, epididymal fat, lung, heart, diaphragm, quadriceps, gastrocnemius, tibialis anterior, and extensor digitorum longus were removed and wet organ or tissue mass in grams was used to determine if genotype and diet had any effect on organ and tissue mass. Animals on the control diet had larger brains than animals on the BCAA diet ($p < 0.05$) (Figure 20 A). Wild-type animals were found to have larger kidneys ($p < 0.05$) and more epidydimal fat ($p < 0.01$) than the *mdx* animals, although the *mdx* animals had significantly larger livers ($p < 0.05$) (Figure 20 B – D). Progressive decline in respiratory function is a major part of disease progression in DMD, with the diaphragm and the lungs being the primary ventilatory structures, however, there was no differences in lung mass between WT & *mdx* animals ($p = 0.328$), but *mdx* diaphragm mass was significantly greater the WT animals ($p < 0.01$) (Figure 20 E & F). This result suggests that the damage sustained to the diaphragm results in fibrosis of the tissue, impairing its proper physiological function and potentially resulting in respiratory complications. Neither genotype or diet affected heart mass (Figure 20 G). Progressive skeletal muscle wasting is the most prominent feature of DMD, resulting in inflammation and fibrosis of the muscle. Although NMR cannot detect fibrosis in tissues, fibrotic tissue has more mass than functioning muscle tissue and all *mdx* mice muscles had significantly larger mass, including: quadriceps ($p < 0.01$), gastrocnemius ($p < 0.01$), tibialis anterior ($p < 0.01$), and extensor digitorum longus ($p < 0.01$) (Figure 20 H – K).

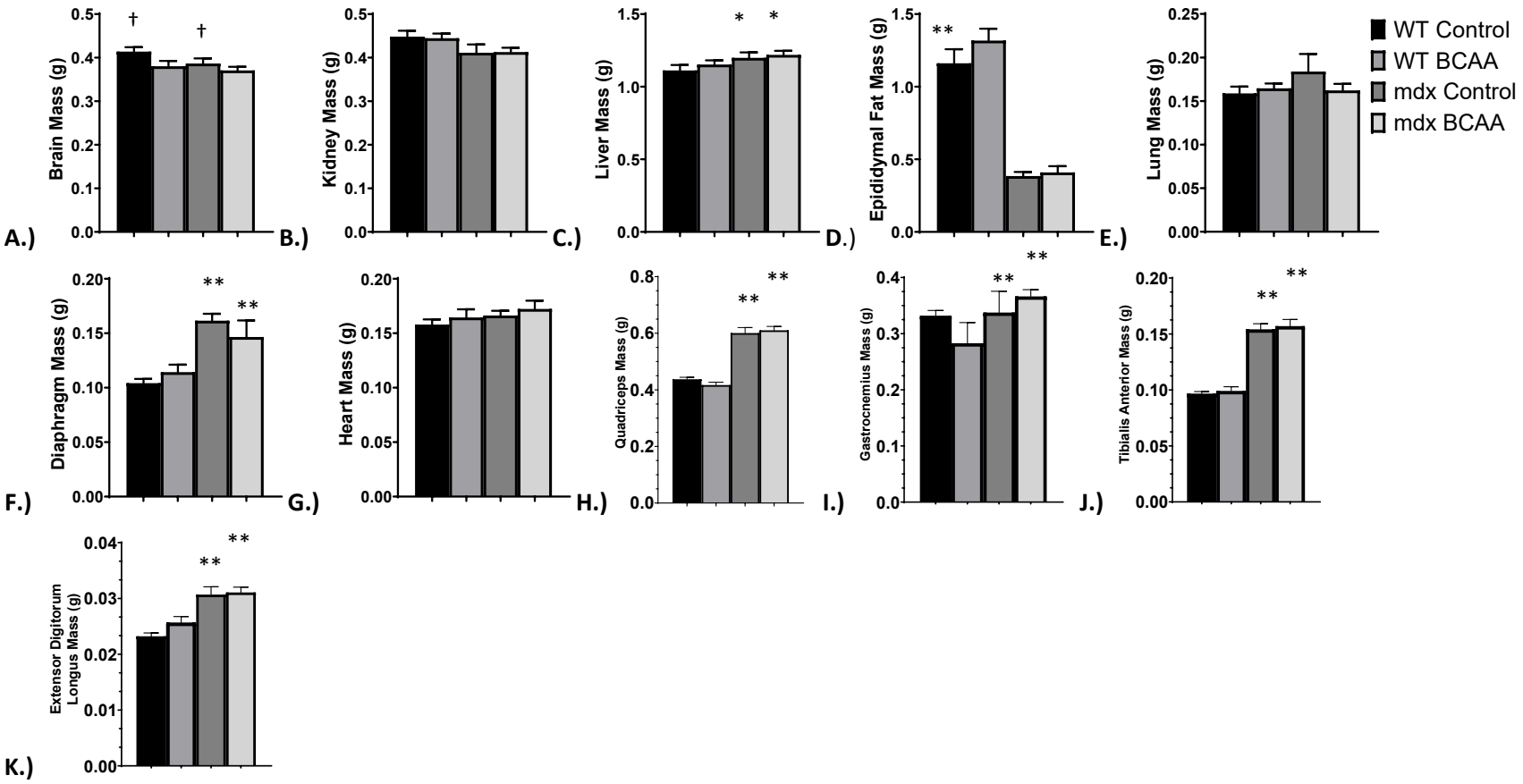

Figure 20 – Tissue masses. Tissue masses were obtained from tissue wet weight. Contralateral tissues were combined for total wet weight. A.) Brain, B.) kidney, C.) liver, D.) epididymal fat pad, E.) lungs, F.) heart, G.) diaphragm, H.) quadriceps, I.) gastrocnemius, J.) tibialis anterior mass, & K.) extensor digitorum longus mass. Symbols are: ■ WT control, ▒ WT BCAA, ▒ mdx Control, & □ mdx BCAA. Genotype effect: * $p < 0.05$; ** $p < 0.01$. Diet effect: † $p < 0.05$. Data are presented as standard errors of the means.

mTORC1 effectors

Liver

Activation of the mTORC1 pathway was determined by measuring Ribosomal Protein S6 (S6) and eukaryotic translation initiation factor 4E-binding protein (4E-BP1) and their phosphorylated forms. There were no significant differences in total S6 nor phosphorylated S6 (p-S6) among groups; wild-type (WT) animals had more total p-S6 than their *mdx* counterparts, although not significant (Figure 21 A). Statistical differences were not reached because of the large variation in the WT animals. The ratio of p-S6 to S6 showed the same pattern of WT animals having a greater ratio of p-S6 to S6 as well as a greater variability, although not significant (Figure 21 A). Total 4E-BP1 and phosphorylated 4E-BP1 (p-4E-BP1) were not significantly different among groups, although BCAA animals have more p-4E-BP1 than their control diet counterparts (Figure 21 B). Interestingly, the ratio of p-4E-BP1 to 4E-BP1 appeared to be greater in WT animals compared to *mdx* animals (Figure 21 B).

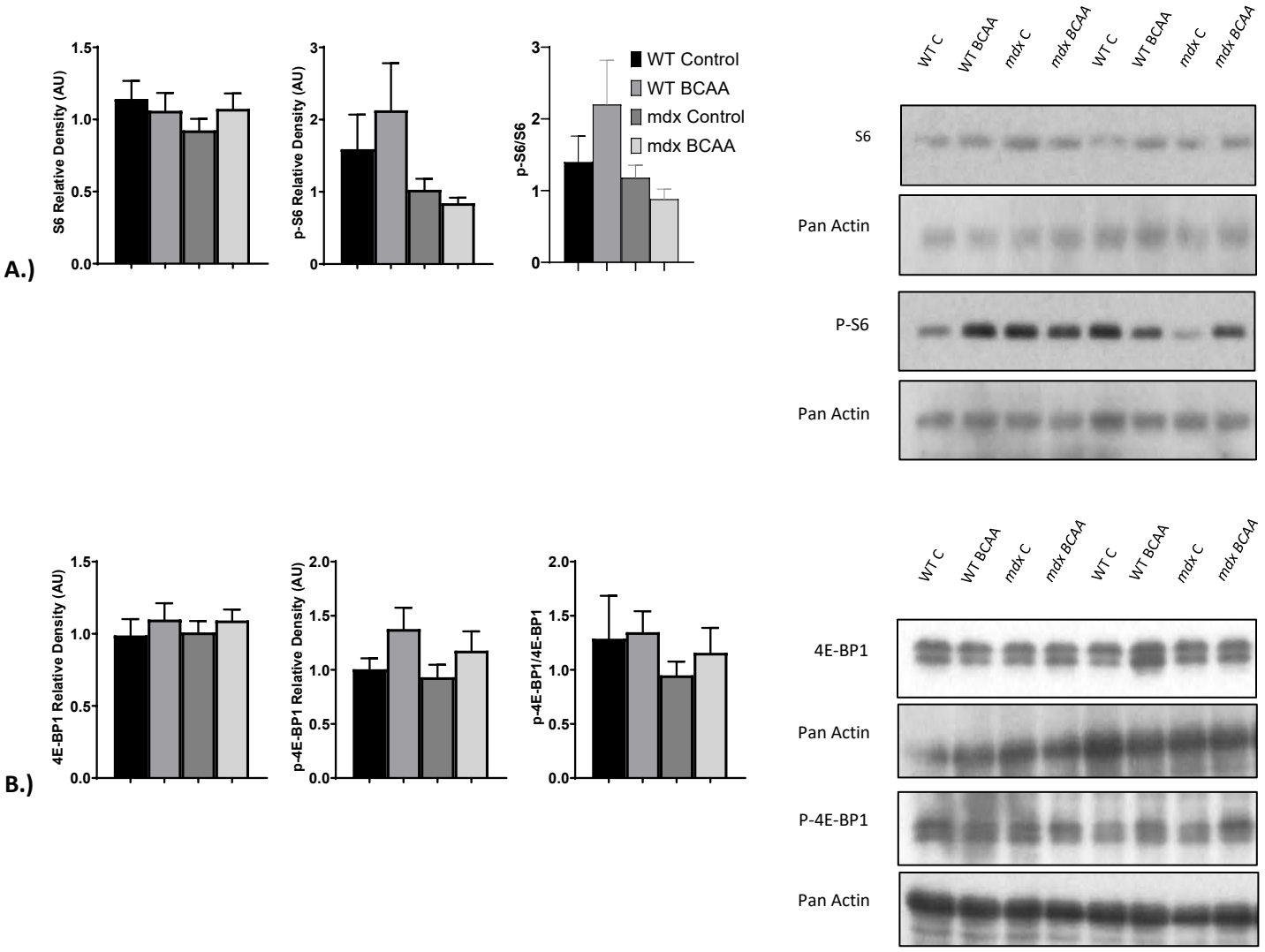

Figure 21 – Liver Western blots. mTORC1 effectors was determined by Western blot analysis at 25 weeks as described under Methods. Wild type (WT) and mdx animals were provided either a control diet or a diet with elevated BCAAs for 25 weeks. A.) Proteins S6 and p-S6, B.) Proteins 4E-BP1 and p-4E-BP1. Symbols are: ■ WT control, □ WT BCAA, ■ mdx Control, & □ mdx BCAA. Data are presented as standard errors of the means.

Red Muscle

There was significantly more S6 and p-S6 in WT animals compared to *mdx* animals ($p < 0.01$) (Figure 22 A). However, there was no significant difference in p-S6 to S6 ratio ($p = 0.0503$), although WT animals have more p-S6 to S6, but with much more variation in the ratio of p-S6 to S6 content (Figure 22 A). A genotype effect was noted for 4E-BP1 and p-4E-BP1 content, with WT animals having more compared to their *mdx* counterparts ($p < 0.05$ & $p < 0.01$, respectively) (Figure 22 B). Although WT animals have a greater ratio than their *mdx* counterparts, there were no differences seen in the ratio of p-4E-BP1 to 4E-BP1, (Figure 22 B). There were no differences in total E1α content, but there was significantly more p-E1α in WT animals compared to *mdx* animals ($p < 0.01$) (Figure 22 C).

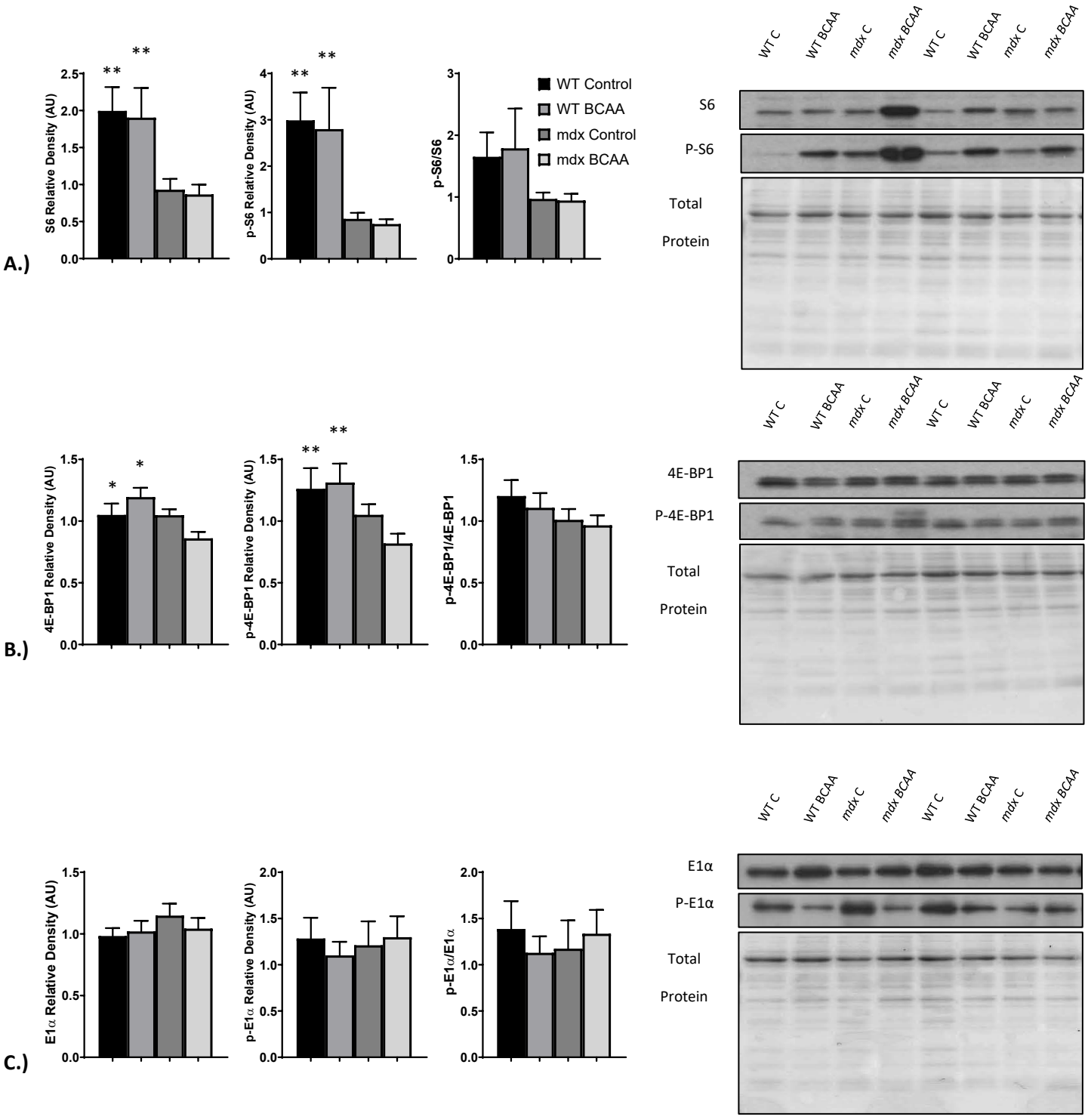

Figure 22 – Red muscle Western blots. mTORC1 effectors and BCKDCs E1α and p-E1α was determined by Western blot analysis as described under Methods. Wild type (WT) and mdx animals were provided either a control diet or a diet with elevated BCAAs for 25 weeks. A.) Proteins S6 and p-S6, B.) proteins 4E-BP1 and p-4E-BP1, & C.) Proteins E1α and p-E1α. Symbols are: ■ WT control, ▩ WT BCAA, ▩ mdx Control, & □ mdx BCAA. Genotype effect: * $p < 0.05$; ** $p < 0.01$. Data are presented as standard errors of the means.

White Muscle

There was significantly more total S6 ($p < 0.05$) and p-S6 ($p < 0.01$) in the WT animals compared to their *mdx* counterparts (Figure 23 A). However, there were no differences among groups; as with the liver, WT animals exhibited a large variation in total S6. Wild type animals also had significantly more p-S6 to S6 ratio ($p < 0.05$) (Figure 23 A). The *mdx* animals on the BCAA diets also have greater S6 and p-S6 content, although not significant (Figure 23 A). There was also a genotype effect noted in the ratio of p-S6 to S6 ($p < 0.05$), although no diet effect was noted (Figure 23 A). A genotype effect was noted in total 4E-BP1 content; WT animals had significantly more 4E-BP1 ($p < 0.05$), p-4E-BP1 ($p < 0.01$), and the ratio of p-4E-BP1 to 4E-BP1 ($p < 0.01$) (Figure 23 B). The ration of p-E1α to E1α also showed only a genotype effect, where WT animals had a greater ratio of p-E1α to E1α ($p < 0.01$) (Figure 23 C).

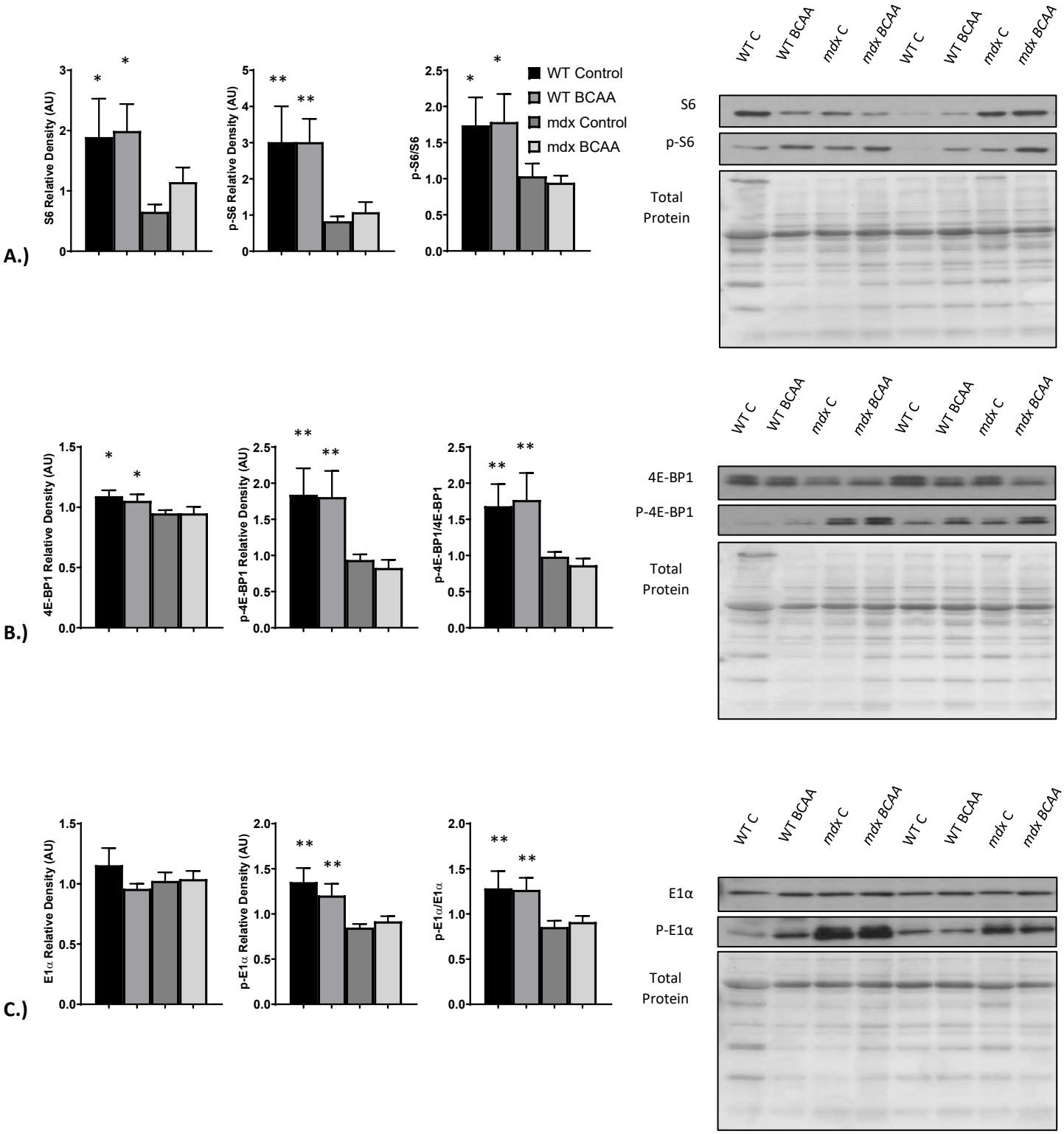

Figure 23 – White muscle Western blots. mTORC1 effectors and BCKDCs E1α and p-E1α was determined by Western blot analysis as described under methods. Wild type (WT) and mdx animals were provided either a control diet or a diet with elevated BCAAs for 25 weeks. A.) Proteins S6 and p-S6, B.) proteins 4E-BP1 and p-4E-BP1, & C.) Proteins E1α and p-E1α. Symbols are: ■ WT control, ▨ WT BCAA, ▩ mdx Control, & □ mdx BCAA. Genotype effect: * $p < 0.05$; ** $p < 0.01$. Data are presented as standard errors of the means

Autophagy

Atrogin 1 was used as a marker for autophagy. There were no differences in atrogin 1 in liver, red muscle, and white muscle (data not shown).

Tissue Hydroxyproline

Hydroxyproline (HOP) is a major component of collagen and is used as a marker for fibrosis in tissues. A significant problem in the progression of DMD is the replacement of functional muscle tissue with collagen, reducing muscle function with disease progression. Tissues most affected by fibrosis in DMD are the diaphragm, heart, and skeletal muscle. Tissue HOP was determined in the diaphragm, heart, red muscle, and white muscle. Genotype differences were the only interaction noted, and no diet effect was observed, with the *mdx* mice having significantly more HOP in the diaphragm, heart, and white muscle (all, $p < 0.01$) (Figure 24 A – D). Interestingly, there was no significant difference in HOP content in red muscle ($p = 0.0523$), indicating that DMD may affect one type of muscle more than another (Figure 24 A – D).

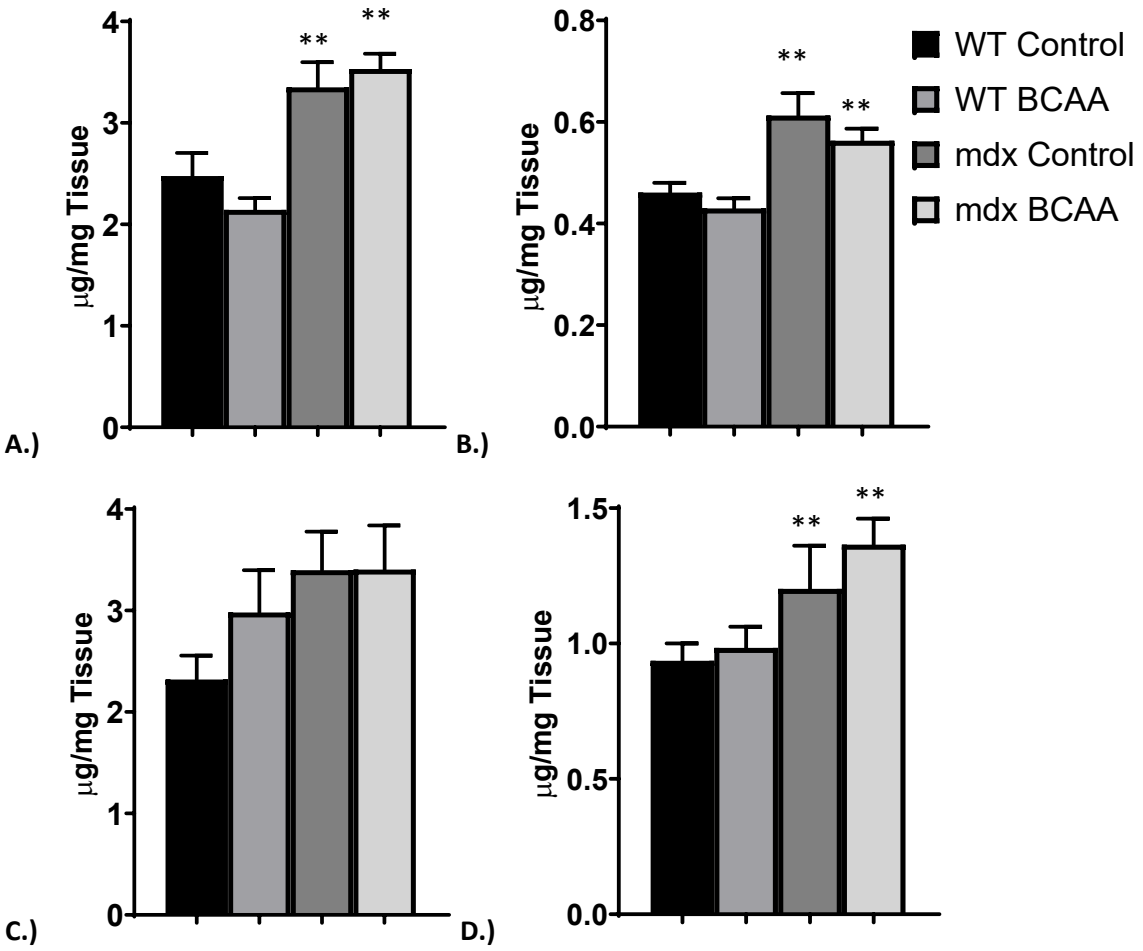

Figure 24 – Tissue hydroxyproline. Hydroxyproline (HOP) is a major structural component of collagen used as an indicator for fibrosis. Hydroxyproline was obtained from the diaphragm, heart, red, and white muscle. A.) Diaphragm, B.) heart, C.) red muscle, & D.) white muscle. Symbols are: ■ WT control, ▨ WT BCAA, ▩ mdx Control, & □ mdx BCAA. Genotype effect: ** $p < 0.01$. Data are presented as standard errors of the means.

References

1 Mah, J. K. *et al.* A systematic review and meta-analysis on the epidemiology of Duchenne and Becker muscular dystrophy. *Neuromuscul Disord* **24**, 482-491, doi:10.1016/j.nmd.2014.03.008 (2014).

2 Bladen, C. L. *et al.* The TREAT-NMD DMD Global Database: analysis of more than 7,000 Duchenne muscular dystrophy mutations. *Hum Mutat* **36**, 395-402, doi:10.1002/humu.22758 (2015).

3 Davoodi, J., Markert, C. D., Voelker, K. A., Hutson, S. M. & Grange, R. W. Nutrition strategies to improve physical capabilities in Duchenne muscular dystrophy. *Phys Med Rehabil Clin N Am* **23**, 187-199, xii-xiii, doi:10.1016/j.pmr.2011.11.010 (2012).

4 Reinig, A. M., Mirzaei, S. & Berlau, D. J. Advances in the Treatment of Duchenne Muscular Dystrophy: New and Emerging Pharmacotherapies. *Pharmacotherapy* **37**, 492-499, doi:10.1002/phar.1909 (2017).

5 Bushby, K. *et al.* Diagnosis and management of Duchenne muscular dystrophy, part 1: diagnosis, and pharmacological and psychosocial management. *Lancet Neurol* **9**, 77-93, doi:10.1016/S1474-4422(09)70271-6 (2010).

6 Le Guiner, C. *et al.* Long-term microdystrophin gene therapy is effective in a canine model of Duchenne muscular dystrophy. *Nat Commun* **8**, 16105, doi:10.1038/ncomms16105 (2017).

7 Mendell, J. R. *et al.* A phase 1/2a follistatin gene therapy trial for becker muscular dystrophy. *Mol Ther* **23**, 192-201, doi:10.1038/mt.2014.200 (2015).

8 Hakim, C. H. *et al.* AAV CRISPR editing rescues cardiac and muscle function for 18 months in dystrophic mice. *JCI Insight* **3**, doi:10.1172/jci.insight.124297 (2018).

9 Min, Y. L. *et al.* CRISPR-Cas9 corrects Duchenne muscular dystrophy exon 44 deletion mutations in mice and human cells. *Sci Adv* **5**, eaav4324, doi:10.1126/sciadv.aav4324 (2019).

10 Mah, J. K. Current and emerging treatment strategies for Duchenne muscular dystrophy. *Neuropsychiatr Dis Treat* **12**, 1795-1807, doi:10.2147/NDT.S93873 (2016).

11 Ousterout, D. G. *et al.* Multiplex CRISPR/Cas9-based genome editing for correction of dystrophin mutations that cause Duchenne muscular dystrophy. *Nat Commun* **6**, 6244, doi:10.1038/ncomms7244 (2015).

12 Hotta, A. Genome Editing Gene Therapy for Duchenne Muscular Dystrophy. *J Neuromuscul Dis* **2**, 343-355, doi:10.3233/JND-150116 (2015).

13 Kimball, S. R., Shantz, L. M., Horetsky, R. L. & Jefferson, L. S. Leucine regulates translation of specific mRNAs in L6 myoblasts through mTOR-mediated changes in availability of eIF4E and phosphorylation of ribosomal protein S6. *J Biol Chem* **274**, 11647-11652 (1999).

14 Kimball, S. R. & Jefferson, L. S. Signaling pathways and molecular mechanisms through which branched-chain amino acids mediate translational control of protein synthesis. *J Nutr* **136**, 227S-231S (2006).

15 Anthony, J. C. *et al.* Leucine stimulates translation initiation in skeletal muscle of postabsorptive rats via a rapamycin-sensitive pathway. *J Nutr* **130**, 2413-2419 (2000).

16 Matthews, E., Brassington, R., Kuntzer, T., Jichi, F. & Manzur, A. Y. Corticosteroids for the treatment of Duchenne muscular dystrophy. *Cochrane Database Syst Rev*, CD003725, doi:10.1002/14651858.CD003725.pub4 (2016).

17 Dubowitz, V. Screening for Duchenne muscular dystrophy. *Arch Dis Child* **51**, 249-251 (1976).

18 Parsons, E. P., Clarke, A. J. & Bradley, D. M. Developmental progress in Duchenne muscular dystrophy: lessons for earlier detection. *Eur J Paediatr Neurol* **8**, 145-153, doi:10.1016/j.ejpn.2004.01.009 (2004).

19 Ross, L. F. & Clarke, A. J. A Historical and Current Review of Newborn Screening for Neuromuscular Disorders From Around the World: Lessons for the United States. *Pediatr Neurol* **77**, 12-22, doi:10.1016/j.pediatrneurol.2017.08.012 (2017).
20 Zakaria, R., Allen, K. J., Koplin, J. J., Roche, P. & Greaves, R. F. Advantages and Challenges of Dried Blood Spot Analysis by Mass Spectrometry Across the Total Testing Process. *EJIFCC* **27**, 288-317 (2016).
21 McMillan, H. J., Gregas, M., Darras, B. T. & Kang, P. B. Serum transaminase levels in boys with Duchenne and Becker muscular dystrophy. *Pediatrics* **127**, e132-136, doi:10.1542/peds.2010-0929 (2011).
22 Scriver, C. R. *The metabolic & molecular bases of inherited disease*. 8th edn, (McGraw-Hill, 2001).
23 Falzarano, M. S., Scotton, C., Passarelli, C. & Ferlini, A. Duchenne Muscular Dystrophy: From Diagnosis to Therapy. *Molecules* **20**, 18168-18184, doi:10.3390/molecules201018168 (2015).
24 Hegde, M. R. *et al.* Microarray-based mutation detection in the dystrophin gene. *Hum Mutat* **29**, 1091-1099, doi:10.1002/humu.20831 (2008).
25 Bovolenta, M. *et al.* A novel custom high density-comparative genomic hybridization array detects common rearrangements as well as deep intronic mutations in dystrophinopathies. *BMC Genomics* **9**, 572, doi:10.1186/1471-2164-9-572 (2008).
26 Chen, W. J. *et al.* Molecular analysis of the dystrophin gene in 407 Chinese patients with Duchenne/Becker muscular dystrophy by the combination of multiplex ligation-dependent probe amplification and Sanger sequencing. *Clin Chim Acta* **423**, 35-38, doi:10.1016/j.cca.2013.04.006 (2013).
27 Bovolenta, M., Scotton, C., Falzarano, M. S., Gualandi, F. & Ferlini, A. Rapid, comprehensive analysis of the dystrophin transcript by a custom micro-fluidic exome array. *Hum Mutat* **33**, 572-581, doi:10.1002/humu.22017 (2012).
28 Vaz-Drago, R., Custodio, N. & Carmo-Fonseca, M. Deep intronic mutations and human disease. *Hum Genet* **136**, 1093-1111, doi:10.1007/s00439-017-1809-4 (2017).
29 Davies, K. E. & Nowak, K. J. Molecular mechanisms of muscular dystrophies: old and new players. *Nat Rev Mol Cell Biol* **7**, 762-773, doi:10.1038/nrm2024 (2006).
30 Blake, D. J., Weir, A., Newey, S. E. & Davies, K. E. Function and genetics of dystrophin and dystrophin-related proteins in muscle. *Physiol Rev* **82**, 291-329, doi:10.1152/physrev.00028.2001 (2002).
31 Bhat, H. F. *et al.* ABC of multifaceted dystrophin glycoprotein complex (DGC). *J Cell Physiol*, doi:10.1002/jcp.25982 (2017).
32 Rahimov, F. & Kunkel, L. M. The cell biology of disease: cellular and molecular mechanisms underlying muscular dystrophy. *J Cell Biol* **201**, 499-510, doi:10.1083/jcb.201212142 (2013).
33 Chelly, J. *et al.* Dystrophin gene transcribed from different promoters in neuronal and glial cells. *Nature* **344**, 64-65, doi:10.1038/344064a0 (1990).
34 Pilgram, G. S., Potikanond, S., Baines, R. A., Fradkin, L. G. & Noordermeer, J. N. The roles of the dystrophin-associated glycoprotein complex at the synapse. *Mol Neurobiol* **41**, 1-21, doi:10.1007/s12035-009-8089-5 (2010).
35 Nowak, K. J. & Davies, K. E. Duchenne muscular dystrophy and dystrophin: pathogenesis and opportunities for treatment. *EMBO Rep* **5**, 872-876, doi:10.1038/sj.embor.7400221 (2004).
36 Allen, D. G., Whitehead, N. P. & Froehner, S. C. Absence of Dystrophin Disrupts Skeletal Muscle Signaling: Roles of Ca2+, Reactive Oxygen Species, and Nitric Oxide in the Development of Muscular Dystrophy. *Physiol Rev* **96**, 253-305, doi:10.1152/physrev.00007.2015 (2016).
37 Williamson, R. A. *et al.* Dystroglycan is essential for early embryonic development: disruption of Reichert's membrane in Dag1-null mice. *Hum Mol Genet* **6**, 831-841 (1997).

38 Di Stasio, E. *et al.* Structural and functional analysis of the N-terminal extracellular region of beta-dystroglycan. *Biochem Biophys Res Commun* **266**, 274-278, doi:10.1006/bbrc.1999.1803 (1999).
39 Laval, S. H. & Bushby, K. M. Limb-girdle muscular dystrophies--from genetics to molecular pathology. *Neuropathol Appl Neurobiol* **30**, 91-105, doi:10.1111/j.1365-2990.2004.00555.x (2004).
40 Oak, S. A., Russo, K., Petrucci, T. C. & Jarrett, H. W. Mouse alpha1-syntrophin binding to Grb2: further evidence of a role for syntrophin in cell signaling. *Biochemistry* **40**, 11270-11278 (2001).
41 Adams, M. E. *et al.* Absence of alpha-syntrophin leads to structurally aberrant neuromuscular synapses deficient in utrophin. *J Cell Biol* **150**, 1385-1398 (2000).
42 Crosbie, R. H., Heighway, J., Venzke, D. P., Lee, J. C. & Campbell, K. P. Sarcospan, the 25-kDa transmembrane component of the dystrophin-glycoprotein complex. *J Biol Chem* **272**, 31221-31224 (1997).
43 Grady, R. M. *et al.* Role for alpha-dystrobrevin in the pathogenesis of dystrophin-dependent muscular dystrophies. *Nat Cell Biol* **1**, 215-220, doi:10.1038/12034 (1999).
44 Laboratory, T. J. C57BL/10ScSn-Dmdmdx/J mouse strain datasheet - 001801. (2017).
45 Gumerson, J. D. & Michele, D. E. The dystrophin-glycoprotein complex in the prevention of muscle damage. *J Biomed Biotechnol* **2011**, 210797, doi:10.1155/2011/210797 (2011).
46 Dutzmann, J., Bauersachs, J. & Sedding, D. G. Evidence for the use of mineralocorticoid receptor antagonists in the treatment of coronary artery disease and post-angioplasty restenosis. *Vascul Pharmacol*, doi:10.1016/j.vph.2017.12.065 (2017).
47 Raman, S. V. *et al.* Eplerenone for early cardiomyopathy in Duchenne muscular dystrophy: a randomised, double-blind, placebo-controlled trial. *Lancet Neurol* **14**, 153-161, doi:10.1016/S1474-4422(14)70318-7 (2015).
48 Raman, S. V. *et al.* Eplerenone for early cardiomyopathy in Duchenne muscular dystrophy: results of a two-year open-label extension trial. *Orphanet J Rare Dis* **12**, 39, doi:10.1186/s13023-017-0590-8 (2017).
49 Bushby, K. *et al.* Diagnosis and management of Duchenne muscular dystrophy, part 2: implementation of multidisciplinary care. *Lancet Neurol* **9**, 177-189, doi:10.1016/S1474-4422(09)70272-8 (2010).
50 Russo, V. *et al.* ACE inhibition to slow progression of myocardial fibrosis in muscular dystrophies. *Trends Cardiovasc Med*, doi:10.1016/j.tcm.2017.12.006 (2017).
51 Ponikowski, P. *et al.* 2016 ESC Guidelines for the diagnosis and treatment of acute and chronic heart failure: The Task Force for the diagnosis and treatment of acute and chronic heart failure of the European Society of Cardiology (ESC)Developed with the special contribution of the Heart Failure Association (HFA) of the ESC. *Eur Heart J* **37**, 2129-2200, doi:10.1093/eurheartj/ehw128 (2016).
52 Timpani, C. A., Hayes, A. & Rybalka, E. Therapeutic strategies to address neuronal nitric oxide synthase deficiency and the loss of nitric oxide bioavailability in Duchenne Muscular Dystrophy. *Orphanet J Rare Dis* **12**, 100, doi:10.1186/s13023-017-0652-y (2017).
53 Hammers, D. W. *et al.* Tadalafil Treatment Delays the Onset of Cardiomyopathy in Dystrophin-Deficient Hearts. *J Am Heart Assoc* **5**, doi:10.1161/JAHA.116.003911 (2016).
54 Consalvi, S. *et al.* Preclinical studies in the mdx mouse model of duchenne muscular dystrophy with the histone deacetylase inhibitor givinostat. *Mol Med* **19**, 79-87, doi:10.2119/molmed.2013.00011 (2013).
55 Medicine, U. S. N. L. o. *https://clinicaltrials.gov*, <https://clinicaltrials.gov/> (2019).
56 Morales, M. G. *et al.* Reducing CTGF/CCN2 slows down mdx muscle dystrophy and improves cell therapy. *Hum Mol Genet* **22**, 4938-4951, doi:10.1093/hmg/ddt352 (2013).

57 Bhat, H. F., Baba, R. A., Adams, M. E. & Khanday, F. A. Role of SNTA1 in Rac1 activation, modulation of ROS generation, and migratory potential of human breast cancer cells. *Br J Cancer* **110**, 706-714, doi:10.1038/bjc.2013.723 (2014).
58 Shimizu-Motohashi, Y. *et al.* Restoring Dystrophin Expression in Duchenne Muscular Dystrophy: Current Status of Therapeutic Approaches. *J Pers Med* **9**, doi:10.3390/jpm9010001 (2019).
59 Wang, Z. *et al.* Adeno-associated virus serotype 8 efficiently delivers genes to muscle and heart. *Nat Biotechnol* **23**, 321-328, doi:10.1038/nbt1073 (2005).
60 Gregorevic, P. *et al.* rAAV6-microdystrophin preserves muscle function and extends lifespan in severely dystrophic mice. *Nat Med* **12**, 787-789, doi:10.1038/nm1439 (2006).
61 Yue, Y. *et al.* Safe and bodywide muscle transduction in young adult Duchenne muscular dystrophy dogs with adeno-associated virus. *Hum Mol Genet* **24**, 5880-5890, doi:10.1093/hmg/ddv310 (2015).
62 Bowles, D. E. *et al.* Phase 1 gene therapy for Duchenne muscular dystrophy using a translational optimized AAV vector. *Mol Ther* **20**, 443-455, doi:10.1038/mt.2011.237 (2012).
63 Mendell, J. R. *et al.* Dystrophin immunity in Duchenne's muscular dystrophy. *N Engl J Med* **363**, 1429-1437, doi:10.1056/NEJMoa1000228 (2010).
64 Okada, T. & Takeda, S. Current Challenges and Future Directions in Recombinant AAV-Mediated Gene Therapy of Duchenne Muscular Dystrophy. *Pharmaceuticals (Basel)* **6**, 813-836, doi:10.3390/ph6070813 (2013).
65 Davies, J. & Davis, B. D. Misreading of ribonucleic acid code words induced by aminoglycoside antibiotics. The effect of drug concentration. *J Biol Chem* **243**, 3312-3316 (1968).
66 Barton-Davis, E. R., Cordier, L., Shoturma, D. I., Leland, S. E. & Sweeney, H. L. Aminoglycoside antibiotics restore dystrophin function to skeletal muscles of mdx mice. *J Clin Invest* **104**, 375-381, doi:10.1172/JCI7866 (1999).
67 Wagner, K. R. *et al.* Gentamicin treatment of Duchenne and Becker muscular dystrophy due to nonsense mutations. *Ann Neurol* **49**, 706-711 (2001).
68 Malik, V. *et al.* Gentamicin-induced readthrough of stop codons in Duchenne muscular dystrophy. *Ann Neurol* **67**, 771-780, doi:10.1002/ana.22024 (2010).
69 Bushby, K. *et al.* Ataluren treatment of patients with nonsense mutation dystrophinopathy. *Muscle Nerve* **50**, 477-487, doi:10.1002/mus.24332 (2014).
70 McDonald, C. M. *et al.* Ataluren in patients with nonsense mutation Duchenne muscular dystrophy (ACT DMD): a multicentre, randomised, double-blind, placebo-controlled, phase 3 trial. *Lancet* **390**, 1489-1498, doi:10.1016/S0140-6736(17)31611-2 (2017).
71 Kinali, M. *et al.* Local restoration of dystrophin expression with the morpholino oligomer AVI-4658 in Duchenne muscular dystrophy: a single-blind, placebo-controlled, dose-escalation, proof-of-concept study. *Lancet Neurol* **8**, 918-928, doi:10.1016/S1474-4422(09)70211-X (2009).
72 van Deutekom, J. C. *et al.* Local dystrophin restoration with antisense oligonucleotide PRO051. *N Engl J Med* **357**, 2677-2686, doi:10.1056/NEJMoa073108 (2007).
73 Voit, T. *et al.* Safety and efficacy of drisapersen for the treatment of Duchenne muscular dystrophy (DEMAND II): an exploratory, randomised, placebo-controlled phase 2 study. *Lancet Neurol* **13**, 987-996, doi:10.1016/S1474-4422(14)70195-4 (2014).
74 Mendell, J. R. *et al.* Eteplirsen for the treatment of Duchenne muscular dystrophy. *Ann Neurol* **74**, 637-647, doi:10.1002/ana.23982 (2013).
75 Khan, N. *et al.* Eteplirsen Treatment Attenuates Respiratory Decline in Ambulatory and Non-Ambulatory Patients with Duchenne Muscular Dystrophy. *J Neuromuscul Dis* **6**, 213-225, doi:10.3233/JND-180351 (2019).
76 Mendell, J. R. *et al.* Myoblast transfer in the treatment of Duchenne's muscular dystrophy. *N Engl J Med* **333**, 832-838, doi:10.1056/NEJM199509283331303 (1995).

77 Srivastava, N. K., Annarao, S. & Sinha, N. Metabolic status of patients with muscular dystrophy in early phase of the disease: In vitro, high resolution NMR spectroscopy based metabolomics analysis of serum. *Life Sci* **151**, 122-129, doi:10.1016/j.lfs.2016.01.032 (2016).
78 Skuk, D. *et al.* Dystrophin expression in myofibers of Duchenne muscular dystrophy patients following intramuscular injections of normal myogenic cells. *Mol Ther* **9**, 475-482 (2004).
79 Sampaolesi, M. *et al.* Mesoangioblast stem cells ameliorate muscle function in dystrophic dogs. *Nature* **444**, 574-579, doi:10.1038/nature05282 (2006).
80 Cossu, G. *et al.* Intra-arterial transplantation of HLA-matched donor mesoangioblasts in Duchenne muscular dystrophy. *EMBO Mol Med* **8**, 1470-1471, doi:10.15252/emmm.201607129 (2016).
81 Dellavalle, A. *et al.* Pericytes of human skeletal muscle are myogenic precursors distinct from satellite cells. *Nat Cell Biol* **9**, 255-267, doi:10.1038/ncb1542 (2007).
82 Long, C. *et al.* Correction of diverse muscular dystrophy mutations in human engineered heart muscle by single-site genome editing. *Sci Adv* **4**, eaap9004, doi:10.1126/sciadv.aap9004 (2018).
83 Lim, K. R. Q., Yoon, C. & Yokota, T. Applications of CRISPR/Cas9 for the Treatment of Duchenne Muscular Dystrophy. *J Pers Med* **8**, doi:10.3390/jpm8040038 (2018).
84 Long, C. *et al.* Prevention of muscular dystrophy in mice by CRISPR/Cas9-mediated editing of germline DNA. *Science* **345**, 1184-1188, doi:10.1126/science.1254445 (2014).
85 Amoasii, L. *et al.* Single-cut genome editing restores dystrophin expression in a new mouse model of muscular dystrophy. *Sci Transl Med* **9**, doi:10.1126/scitranslmed.aan8081 (2017).
86 Sweatt, A. J. *et al.* Branched-chain amino acid catabolism: unique segregation of pathway enzymes in organ systems and peripheral nerves. *Am J Physiol Endocrinol Metab* **286**, E64-76, doi:10.1152/ajpendo.00276.2003 (2004).
87 Sengupta, S., Peterson, T. R. & Sabatini, D. M. Regulation of the mTOR complex 1 pathway by nutrients, growth factors, and stress. *Mol Cell* **40**, 310-322, doi:10.1016/j.molcel.2010.09.026 (2010).
88 Jackman, S. R. *et al.* Branched-Chain Amino Acid Ingestion Stimulates Muscle Myofibrillar Protein Synthesis following Resistance Exercise in Humans. *Front Physiol* **8**, 390, doi:10.3389/fphys.2017.00390 (2017).
89 Chantranupong, L. *et al.* The Sestrins interact with GATOR2 to negatively regulate the amino-acid-sensing pathway upstream of mTORC1. *Cell Rep* **9**, 1-8, doi:10.1016/j.celrep.2014.09.014 (2014).
90 Wolfson, R. L. *et al.* Sestrin2 is a leucine sensor for the mTORC1 pathway. *Science* **351**, 43-48, doi:10.1126/science.aab2674 (2016).
91 Wolfson, R. L. & Sabatini, D. M. The Dawn of the Age of Amino Acid Sensors for the mTORC1 Pathway. *Cell Metab* **26**, 301-309, doi:10.1016/j.cmet.2017.07.001 (2017).
92 Saxton, R. A. & Sabatini, D. M. mTOR Signaling in Growth, Metabolism, and Disease. *Cell* **168**, 960-976, doi:10.1016/j.cell.2017.02.004 (2017).
93 Garza-Lombo, C. & Gonsebatt, M. E. Mammalian Target of Rapamycin: Its Role in Early Neural Development and in Adult and Aged Brain Function. *Front Cell Neurosci* **10**, 157, doi:10.3389/fncel.2016.00157 (2016).
94 Sarbassov, D. D., Ali, S. M. & Sabatini, D. M. Growing roles for the mTOR pathway. *Curr Opin Cell Biol* **17**, 596-603, doi:10.1016/j.ceb.2005.09.009 (2005).
95 Weber, J. D. & Gutmann, D. H. Deconvoluting mTOR biology. *Cell Cycle* **11**, 236-248, doi:10.4161/cc.11.2.19022 (2012).
96 Laplante, M. & Sabatini, D. M. mTOR signaling at a glance. *J Cell Sci* **122**, 3589-3594, doi:10.1242/jcs.051011 (2009).

97 Bar-Peled, L. & Sabatini, D. M. SnapShot: mTORC1 signaling at the lysosomal surface. *Cell* **151**, 1390-1390 e1391, doi:10.1016/j.cell.2012.11.038 (2012).
98 Zoncu, R. *et al.* mTORC1 Senses Lysosomal Amino Acids Through an Inside-Out Mechanism That Requires the Vacuolar H+-ATPase. *Science* **334**, 678-683, doi:10.1126/science.1207056 (2011).
99 Bar-Peled, L., Schweitzer, L. D., Zoncu, R. & Sabatini, D. M. Ragulator is a GEF for the rag GTPases that signal amino acid levels to mTORC1. *Cell* **150**, 1196-1208, doi:10.1016/j.cell.2012.07.032 (2012).
100 Archer, J. D., Vargas, C. C. & Anderson, J. E. Persistent and improved functional gain in mdx dystrophic mice after treatment with L-arginine and deflazacort. *FASEB J* **20**, 738-740, doi:10.1096/fj.05-4821fje (2006).
101 Hankard, R. G., Hammond, D., Haymond, M. W. & Darmaun, D. Oral glutamine slows down whole body protein breakdown in Duchenne muscular dystrophy. *Pediatr Res* **43**, 222-226, doi:10.1203/00006450-199804001-01321 (1998).
102 Stewart, P. M., Walser, M. & Drachman, D. B. Branched-chain ketoacids reduce muscle protein degradation in Duchenne muscular dystrophy. *Muscle Nerve* **5**, 197-201, doi:10.1002/mus.880050304 (1982).
103 Sperringer, J. E. & Grange, R. W. In Vitro Assays to Determine Skeletal Muscle Physiologic Function. *Methods Mol Biol* **1460**, 271-291, doi:10.1007/978-1-4939-3810-0_19 (2016).
104 Weir, J. B. New methods for calculating metabolic rate with special reference to protein metabolism. *J Physiol* **109**, 1-9 (1949).
105 Wu, G. & Knabe, D. A. Free and protein-bound amino acids in sow's colostrum and milk. *J Nutr* **124**, 415-424, doi:10.1093/jn/124.3.415 (1994).
106 Heydemann, A., Huber, J. M., Demonbreun, A., Hadhazy, M. & McNally, E. M. Genetic background influences muscular dystrophy. *Neuromuscul Disord* **15**, 601-609, doi:10.1016/j.nmd.2005.05.004 (2005).
107 Capogrosso, R. F. *et al.* Contractile efficiency of dystrophic mdx mouse muscle: in vivo and ex vivo assessment of adaptation to exercise of functional end points. *J Appl Physiol (1985)* **122**, 828-843, doi:10.1152/japplphysiol.00776.2015 (2017).
108 Banks, G. B., Chamberlain, J. S. & Froehner, S. C. Truncated dystrophins can influence neuromuscular synapse structure. *Mol Cell Neurosci* **40**, 433-441, doi:10.1016/j.mcn.2008.12.011 (2009).
109 Ghedini, P. C. *et al.* Increased expression of acetylcholine receptors in the diaphragm muscle of MDX mice. *Muscle Nerve* **38**, 1585-1594, doi:10.1002/mus.21183 (2008).
110 De Luca, A. *et al.* Enhanced dystrophic progression in mdx mice by exercise and beneficial effects of taurine and insulin-like growth factor-1. *J Pharmacol Exp Ther* **304**, 453-463, doi:10.1124/jpet.102.041343 (2003).
111 Handschin, C. & Spiegelman, B. M. The role of exercise and PGC1alpha in inflammation and chronic disease. *Nature* **454**, 463-469, doi:10.1038/nature07206 (2008).
112 Banfi, S. *et al.* Supplementation with a selective amino acid formula ameliorates muscular dystrophy in mdx mice. *Sci Rep* **8**, 14659, doi:10.1038/s41598-018-32613-w (2018).
113 Blomstrand, E., Eliasson, J., Karlsson, H. K. & Kohnke, R. Branched-chain amino acids activate key enzymes in protein synthesis after physical exercise. *J Nutr* **136**, 269S-273S, doi:10.1093/jn/136.1.269S (2006).
114 Moberg, M. *et al.* Activation of mTORC1 by leucine is potentiated by branched-chain amino acids and even more so by essential amino acids following resistance exercise. *Am J Physiol Cell Physiol* **310**, C874-884, doi:10.1152/ajpcell.00374.2015 (2016).

115 Karlsson, H. K. *et al.* Branched-chain amino acids increase p70S6k phosphorylation in human skeletal muscle after resistance exercise. *Am J Physiol Endocrinol Metab* **287**, E1-7, doi:10.1152/ajpendo.00430.2003 (2004).
116 Radley-Crabb, H. G. *et al.* Dystropathology increases energy expenditure and protein turnover in the mdx mouse model of duchenne muscular dystrophy. *PLoS One* **9**, e89277, doi:10.1371/journal.pone.0089277 (2014).
117 Lindsay, A., Larson, A. A., Verma, M., Ervasti, J. M. & Lowe, D. A. Isometric resistance training increases strength and alters histopathology of dystrophin-deficient mouse skeletal muscle. *J Appl Physiol (1985)* **126**, 363-375, doi:10.1152/japplphysiol.00948.2018 (2019).
118 Call, J. A., McKeehen, J. N., Novotny, S. A. & Lowe, D. A. Progressive resistance voluntary wheel running in the mdx mouse. *Muscle Nerve* **42**, 871-880, doi:10.1002/mus.21764 (2010).
119 May, M. E. & Buse, M. G. Effects of branched-chain amino acids on protein turnover. *Diabetes Metab Rev* **5**, 227-245 (1989).
120 Chua, B., Siehl, D. L. & Morgan, H. E. Effect of leucine and metabolites of branched chain amino acids on protein turnover in heart. *J Biol Chem* **254**, 8358-8362 (1979).
121 Maki, T. *et al.* Branched-chain amino acids reduce hindlimb suspension-induced muscle atrophy and protein levels of atrogin-1 and MuRF1 in rats. *Nutr Res* **32**, 676-683, doi:10.1016/j.nutres.2012.07.005 (2012).
122 Whitehead, N. P., Kim, M. J., Bible, K. L., Adams, M. E. & Froehner, S. C. A new therapeutic effect of simvastatin revealed by functional improvement in muscular dystrophy. *Proc Natl Acad Sci U S A* **112**, 12864-12869, doi:10.1073/pnas.1509536112 (2015).
123 Chen, Y. W. *et al.* Early onset of inflammation and later involvement of TGFbeta in Duchenne muscular dystrophy. *Neurology* **65**, 826-834, doi:10.1212/01.wnl.0000173836.09176.c4 (2005).
124 Schill, K. E. *et al.* Muscle damage, metabolism, and oxidative stress in mdx mice: Impact of aerobic running. *Muscle Nerve* **54**, 110-117, doi:10.1002/mus.25015 (2016).
125 Hartel, J. V., Granchelli, J. A., Hudecki, M. S., Pollina, C. M. & Gosselin, L. E. Impact of prednisone on TGF-beta1 and collagen in diaphragm muscle from mdx mice. *Muscle Nerve* **24**, 428-432 (2001).
126 Roberts, N. W., Holley-Cuthrell, J., Gonzalez-Vega, M., Mull, A. J. & Heydemann, A. Biochemical and Functional Comparisons of mdx and Sgcg(-/-) Muscular Dystrophy Mouse Models. *Biomed Res Int* **2015**, 131436, doi:10.1155/2015/131436 (2015).
127 Gosselin, L. E., Williams, J. E., Personius, K. & Farkas, G. A. A comparison of factors associated with collagen metabolism in different skeletal muscles from dystrophic (mdx) mice: impact of pirfenidone. *Muscle Nerve* **35**, 208-216, doi:10.1002/mus.20681 (2007).
128 Pistilli, E. E. *et al.* Targeting the activin type IIB receptor to improve muscle mass and function in the mdx mouse model of Duchenne muscular dystrophy. *Am J Pathol* **178**, 1287-1297, doi:10.1016/j.ajpath.2010.11.071 (2011).
129 Zhou, L. & Lu, H. Targeting fibrosis in Duchenne muscular dystrophy. *J Neuropathol Exp Neurol* **69**, 771-776, doi:10.1097/NEN.0b013e3181e9a34b (2010).
130 Klingler, W., Jurkat-Rott, K., Lehmann-Horn, F. & Schleip, R. The role of fibrosis in Duchenne muscular dystrophy. *Acta Myol* **31**, 184-195 (2012).
131 Verhaart, I. E. C. *et al.* A modified diet does not ameliorate muscle pathology in a mouse model for Duchenne muscular dystrophy. *PLoS One* **14**, e0215335, doi:10.1371/journal.pone.0215335 (2019).
132 Smriga, M., Kameishi, M. & Torii, K. Exercise-dependent preference for a mixture of branched-chain amino acids and homeostatic control of brain serotonin in exercising rats. *J Nutr* **136**, 548S-552S, doi:10.1093/jn/136.2.548S (2006).

133 Hinkle, R. T. *et al.* Treatment with a corticotrophin releasing factor 2 receptor agonist modulates skeletal muscle mass and force production in aged and chronically ill animals. *BMC Musculoskelet Disord* **12**, 15, doi:10.1186/1471-2474-12-15 (2011).

134 Mokhtarian, A., Decrouy, A., Chinet, A. & Even, P. C. Components of energy expenditure in the mdx mouse model of Duchenne muscular dystrophy. *Pflugers Arch* **431**, 527-532, doi:10.1007/bf02191899 (1996).

Chapter Four

Discussion

In this study, we report that a chronic dietary supplementation of elevated BCAAs does not attenuate muscle torque loss in the *mdx* mouse. The elevated BCAA diet also had no effect on decreasing fibrosis markers, increasing protein synthesis effectors, or decrease autophagy markers in *mdx* mouse tissues. The *mdx* mouse (C57BL/10ScSn-Dmd^{mdx}/J) is the most common animal model for DMD, with a C-to-T transition that results in a premature stop codon in exon 23[44]. Dystrophin is an intracellular rod-shaped protein, localized to the inner surface of the sarcolemma and is highly expressed at costameres, proteins that anchor the sarcomere to the cell membrane, particularly at the myotendinous junction (MTJ) and the neuromuscular junction (NJM) and is thought to protects muscle during mechanical stress as well being involved in cellular signaling[29,31,32]. Muscles lacking dystrophin have increased susceptibility to damage caused by normal muscle contractions[29,107].

Neurological and morphologic changes have been previously described in the *mdx* mouse, including fibrosis of the muscle and NMJ morphologies and pathologies resulting in progressive declines in muscle force and torque over the course of the lifespan[107-109]. It has been established that *in vivo* limb force weakness in exercised non-anesthetized *mdx* mice is a function of neuronal and physiological systems and that in anesthetized *mdx* mice, muscular weakness is related to time-dependent exercise-induced impairment in neuromuscular function[107,110,111]. Although these studies used a treadmill exercise protocol, Capogrosso *et al.* also noted that the exercised *mdx* mice became significantly weaker than sedentary *mdx* mice[107]. Although our study did not include an exercise component, our results also show a significant difference between WT and *mdx* mouse hind limb torque production over 25 weeks. In recent work by Banfi *et al.,* endurance run time on a treadmill was increased by approximately 20% in *mdx* animals on a BCAA diet and amelioration of tetanic force at high stimulation frequencies[112]. In contrast, this study does not show any amelioration of tetanic torque loss in the *mdx* mouse with a chronic elevated BCAA diet. It

was expected that the elevated BCAA diet would improve tetanic torque production and improve torque responses to increasing stimulation frequencies; specifically, it was expected that the absolute tetanic contraction would produce more torque with animals on the BCAA diet and that there would be improvements in torque production at the different stimulation frequencies. Although not tested, providing an exercise protocol with an elevated BCAA diet in conjunction with a pharmacological intervention early in the disease process may be beneficial in the DMD patient.

Phosphorylation of mTORC1 protein synthesis effector S6 results in increased protein and nucleotide synthesis and phosphorylation of 4E-BP1 results in its dissociation from eIF4E to promote cap-dependent translation[113-115]. The BCAAs are well established in increasing S6 and 4E-BP1 phosphorylation and significantly increases in conjunction with exercise[113-115]. Although the BCAAs were elevated in plasma at four and 25 weeks and all tissues, the BCAAs did not increase S6 or 4E-BP1 total content or their phosphorylated forms in liver, red skeletal muscle, or white skeletal muscle. However, studies by Blomstrand, Moberg, and Karlsson all report increases in S6 and 4E-BP1 phosphorylation 60 to 90 minutes post exercise that decline to basal levels over time, although not performed in the *mdx* mouse[113-115]. Although we do not report any increases in phosphorylated protein synthesis effectors, total protein and muscle protein synthesis may be occurring as S6 and 4E-BP1 are phosphorylated in a time-dependent manner post exercise. Although total protein synthesis and turnover were not tested for in this study, juvenile and adult *mdx* mice have increased total protein synthesis and whole-body protein turnover compared to control animals[116]. The *mdx* mouse has greater grip strength and specific tetanic force with wheel running and resistance training isometric torque protocols have also shown to increase contractile function of muscles[117,118]. It is possible that concomitantly providing a BCAA diet with an endurance or resistance training protocol would increase protein synthesis effectors, as Banfi *et al.* report improvements in *mdx* muscle strength with BCAA supplementation[112]. Some considerations and limitations for DMD patients and BCAA-mediated protein synthesis is the need for a stressor and the physical capabilities of the patient, which are limited with increasing age and disease progression.

The BCAAs are known promote muscle protein synthesis and inhibit autophagy by activation of the mTORC1 complex[97,113-115,119]. In rat hearts, Leu administration alone decreases the negative nitrogen balance, inhibits protein degradation, further reduces protein degradation in the presence of insulin, and reduces protease activity[120]. In this study, we report increases in all three BCAAs in the plasma at four and 25 weeks as well as increases in tissues of animals on the BCAA diet, however no increases in protein synthesis effectors in any tissues or decreases in autophagy marker atrogin1, which has been shown to be reduced (along with MuRF1) in hindlimb suspension-induced muscle atrophy[121]. Atrogin-1, a ubiquitin-protein ligase that stimulates protein breakdown, has recently been shown to be consistently lower in DMD than in normal muscle and does not increase throughout disease progression[122,123]. It is possible that mTORC1 autophagy effectors ATG13, ULK1, and FIP200 are decreased with BCAA supplementation, although not tested in this study.

Hydroxyproline assays are used to determine the amount of collagen in tissues and is used as a measure of fibrosis in tissues[124,125]. Biochemical and histological assays for HOP and collagen in *mdx* mouse tissues illustrates that the *mdx* genotype has significantly more HOP and fibrotic infiltration into muscle tissues than their WT counterparts[124-128]. In line with muscle function decreases in torque production with exercise, exercised *mdx* animals have increased HOP content in muscle tissues than sedentary *mdx* controls and WT animals[124,129,130]. Cellular signaling may play a role in tissue fibrosis, as recently Pistilli *et al.* inhibited ActRIIB signaling, a transmembrane protein for TGF-β receptor family and myostatin, in the *mdx* mouse and significantly decreased HOP content and collagen infiltration in immunostained *mdx* muscle[128]. Although we did not perform any histological analyses on the tissues, we report significant increases in HOP content in all muscles tested other than red muscle that are in line with previous reports on HOP content. However, we separated red skeletal muscle from white skeletal muscle for HOP analysis and did not perform HOP analysis on individual skeletal muscles, which could explain the difference seen in the separated red skeletal muscle HOP content. In line with our study, Verhaart *et al.* recently noted that a modified diet of 5.4% BCAAs did not ameliorate fibrosis or calcification of the gastrocnemius and

diaphragm[131]. The work by Verhaart *et al*. was a 12-week protocol and our data suggest that the fibrosis is not reduced even with chronic dietary supplementation of BCAAs up to 25 weeks of age[131]. It is possible that if both studies were for the duration of the *mdx* mouse's life and BCAA diet intervention earlier in the lifecycle, there may have been some beneficial effects in reducing fibrosis with increasing age.

One interesting finding in this study was that at four weeks, the BCAAs significantly increased dark cycle activity that disappeared by 25 weeks. One possibility for the initial differences in cage activity could be related to circadian rhythms. Rats fed a fortified BCAA diet have an increased volume of physical activity within four days and that administering the BCAAs before a forced-exercise protocol decreased serotonin release in the lateral hypothalamus and the amygdala compared to control animals[132]. Signaling may also play a role in activity as *mdx* animals given a corticotropin releasing factor 2 receptor agonist (CRF2R) in conjunction with glucocorticoids prevents the loss of and recovery of diaphragm specific force as well as significant changes in gene expression for circadian rhythm control genes and decreased expression of locomotor output cycles kaput (CLOCK) and aryl hydrocarbon receptor nuclear translocator-like (ARNTL/BMAL1/MOP3) genes[133]. Work by Radley-Crabb *et al.* looked at juvenile and adult *mdx* cage activity and noted that juvenile and adult *mdx* mice have significantly less horizontal and vertical cage activity than WT controls[116]. Our results show that the only genotype effect for cage activity in juvenile mice is that the *mdx* animals have significantly more horizontal activity in the light cycles. We also report that the BCAAs increased horizontal and vertical activity at four weeks and that adult *mdx* mice were significantly more active in all cycles at 25 weeks.

Energy expenditure saw some unique findings when compared to cage activity. Radley-Crabb *et al*. do note that juvenile *mdx* animals have increased energy expenditure and protein turnover due to the inability to regulate their intake to meet their metabolic needs, contributing to the disease phenotype and smaller stature and that the energy expenditure as an adult mouse was no different than *mdx* animals, in contrast to this study[116]. Mokhtarian *et al.* note that the thermic effect of feeding is approximately 32% greater in *mdx* mice than control animals and alterations in glucose and lipid oxidation, which could be contributing to the

increased energy expenditure seen in this study[134]. In this study, we note differences in juvenile and adult *mdx* animal energy expenditure in that the BCAAs increase activity in the dark cycles and *mdx* animals have more activity in the light cycles.

In this study, we found that at four weeks, WT animals and animals on the control diet having higher RER values that persisted for the duration of the study. Reports by Radley-Crabb *et al*. report RQ values of approximately 0.91 for juvenile *mdx* animals that increases to 0.95 in adult *mdx* animals and 0.92 for juvenile WT animals that increases to 0.96 in adult WT animals[116]. In this study RER was used in place a RQ, where RER is an indirect measurement of CO_2 production to O_2 consumed, and values ranged between 0.79 and 0.82 for both *mdx* and WT animals. The use of indirect calorimetry (RER vs RQ) as well as the Radley-Crabb protocol only looking at a single 24-hour period compared to the 48-hour periods used in this study may account for the differences in fuel oxidation ratios[116]. Radley-Crabb *et al.* suggest that there is a strong correlation between energy expenditure and that energy intake indicated protein catabolism is negligible in RER, although we do report minimal changes with the BCAA diet[116]. In this study, the elevated BCAA diet lowers RER slightly, indicating that the BCAAs may be being oxidized as they are more prevalent in the diet and they are being oxidized, which is refuted by Radley-Crabb, who suggest that a high level of carbohydrates can occur with high levels of protein catabolism[116].

Conclusions

In this study, we characterized the *mdx* mouse and illustrated that an elevated BCAA diet does not attenuate muscle torque loss in the *mdx* mouse. The *mdx* mouse phenotype was not improved with the elevated BCAA diet and no improvements in torque production were noted for the duration of the study. We characterize plasma and tissue AAs in the *mdx* mouse and the differences between the *mdx* mouse and the WT control. Many AAs found to be elevated in *mdx* mouse plasma and tissues are AAs essential in the formation of protein kinases, antioxidant enzymes, and fatty acid transporters. The elevated BCAA diet increased cage activity at four weeks but had no effect by 25 weeks. We also demonstrate that *mdx* mice are consistently

more active in the X- and Y-planes in the light cycles. The BCAA diet increases X- and Y-plane activity in the dark cycles at four weeks, but not at 25 weeks. Although not significant, animals on the BCAA diet have more Z-plane activity in both the light and dark cycles at four weeks; by 25 weeks, animals on the control diet have more Z-plane activity, although not significant. The RER values in *mdx* animals and animals on the BCAA diet are more indicative of a more mixed fuel usage than WT animals and animals on the control diet, however the closeness of the RER values questions physiological significance. mTORC1 effectors S6 and 4E-BP1 were not elevated in any *mdx* tissue or any animals on the BCAA diet, indicating no upregulation of protein synthesis effectors with an elevated BCAA diet. Tissue content of phosphorylated E1α subunit of BCKDC was only elevated in WT animals in white muscle. The BCAA diet also did not decrease autophagy marker atrogin-1 in all tissues tested.

Future research

This research provides evidence that chronic administration of an elevated BCAA diet does not attenuate the loss of muscle function or strength loss in the *mdx* mouse. These data illustrated the significant difference in phenotypic characteristics and muscle function of *mdx* mice from a very early age that persists throughout the lifetime. Although this research did not show any amelioration of muscle function and strength loss in the *mdx* mouse, there are many avenues of future research in the effect an elevated BCAA diet has on dystrophic mice. The following areas of research needed to be addressed:

1.) Determine if an elevated BCAA diet provided at weaning will attenuate muscle function and strength loss in the *mdx* mouse. Future research should also concomitantly administer glucocorticoids with an elevated BCAA diet for the attenuation of muscle function and strength loss in the *mdx* mouse.

2.) Determine if an elevated BCAA diet with a weight training or stress protocol will improve muscle strength in the *mdx* mouse.

3.) Determine the effect the dystrophic phenotype has on *mdx* mouse cage activity over the lifetime. Future research should determine if the *mdx* mouse is more active in the light hours than WT animals over the course of the lifetime. Research should also determine the differences in X- and Y-plane activity compared to Z-plane activity over the course of the lifetime.

4.) Determine the effect an elevated BCAA diet has on mouse cage activity over the lifetime. Research should also determine the effect an elevated BCAA diet has on X- and Y-plane activity compared to Z-plane activity over the course of the lifetime. Future research should determine the effect an elevated BCAA diet has on dark and light cycle activity over the course of the lifetime.

5.) Determine the effect a chronic BCAA diet has on BCAA adaptation. Future research should collect urine BCAAs, BCKAs, and nitrogen to determine if the chronic elevation on BCAAs results in catabolism or elimination of excess AAs.

6.) Determine BCAA metabolism in *mdx* mouse tissues. Future research should determine the effects and elevated BCAA diet have on E1α and p-E1α of BCKDC in the liver, $BCAT_m$ in extrahepatic tissues, and $BCAT_c$ neuronal tissues.

7.) Determine the effect BCAAs have on the dystrophic phenotype on cardiac, skeletal, and smooth muscle. Single-fiber studies should look at the impact on type I, IIa, IIb, IIx, cardiac, and smooth muscle fibers.

8.) Determine if the BCAAs increase total muscle protein synthesis, myofibrillar protein synthesis, and total protein turnover in the *mdx* mouse.

9.) Determine if the BCAAs reduce autophagy by decreasing mTORC1-effector autophagy markers ATG13, ULK1, and FIP200.

Contributions

Dr. Susan Hutson: Co-lead investigator, study design, laboratory materials, & laboratory equipment

Dr. Robert Grange: Co-lead investigator, study design, laboratory materials, & laboratory equipment

Dr. Adele Addington: Study design, maintenance of mouse colonies, body composition analysis, plasma & tissue amino acid analysis, hydroxyproline analysis, metabolic & activity analysis, & Western blot analysis.

Dr. Greg Rodden: Maintenance of mouse colonies, *in vivo* muscle function analysis, body composition analysis, & tissue collection.

Erin Shelton: Maintenance of mouse colonies, *in vivo* muscle function analysis, body composition analysis, & tissue collection.

Haiyan Zhang: Metabolic & activity analysis

Dr. Mostafa Ali: Metabolic & activity analysis

Virginia Tech Integrated Life Sciences Operations & Animal Husbandry

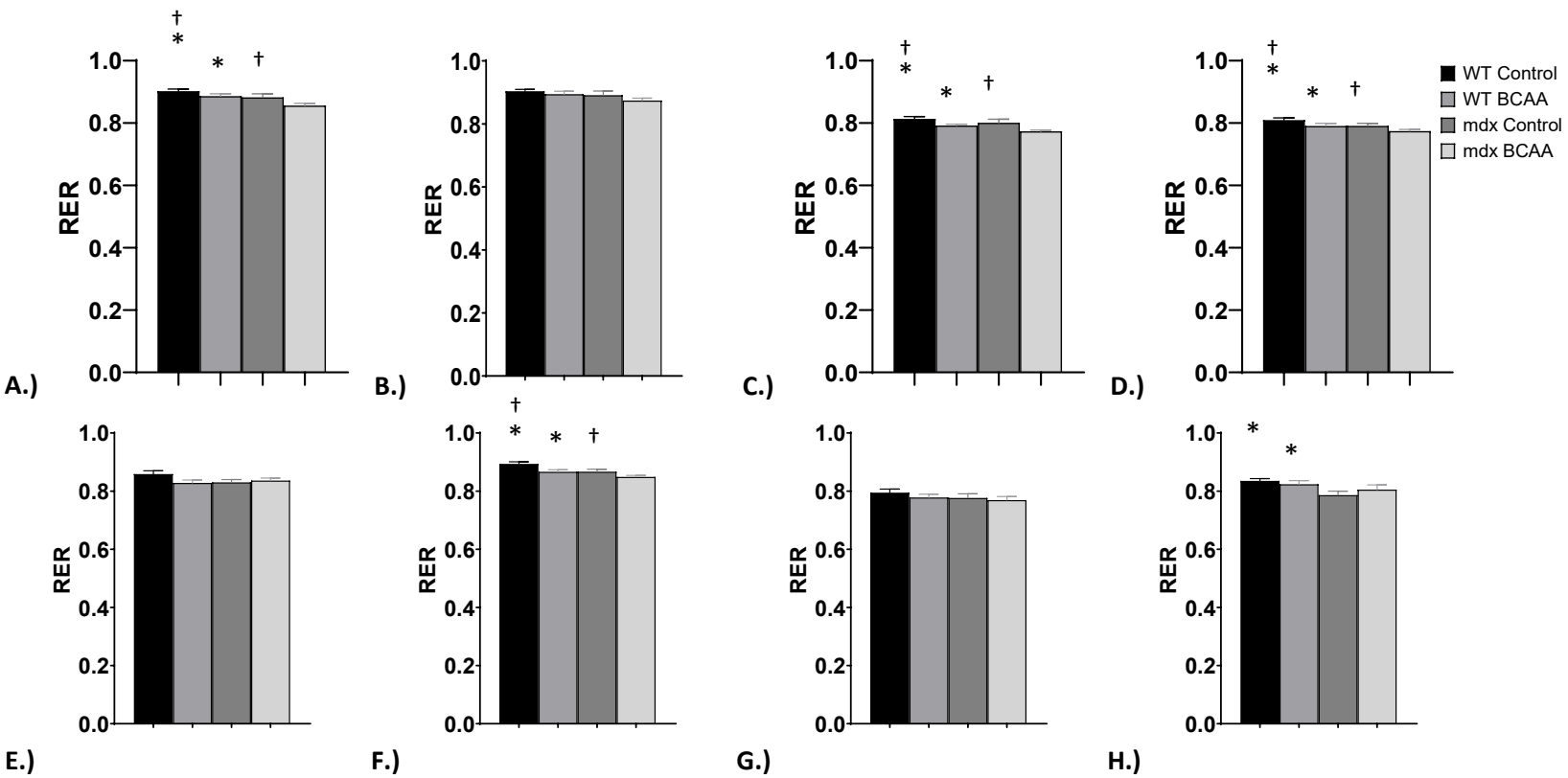

Supplementary Figure 1 – Fuel oxidation at four and 25 weeks. Fuel oxidation was determined by indirect calorimetry using the TSE LabMaster (PhenoMaster) System as described under Methods. Average 48 hour RER; at A.) dark cycle 1 RER at 4 weeks, B.) dark cycle 2 at RER at 4 weeks, C.) light cycle 1 RER at 4 weeks, D.) light cycle 2 RER at 4 week, E.) dark cycle 1 RER at 25 weeks, F.) dark cycle 2 RER at 25 weeks, G.) light cycle 1 RER at 25 weeks, & H.) light cycle 2 RER at 25 weeks. Symbols are: ■ WT control, ▩ WT BCAA, ▩ mdx Control, & □ mdx BCAA. Standard Errors of the means are presented. Genotype effect: * $p < 0.05$. Data presented as standard errors of the means.

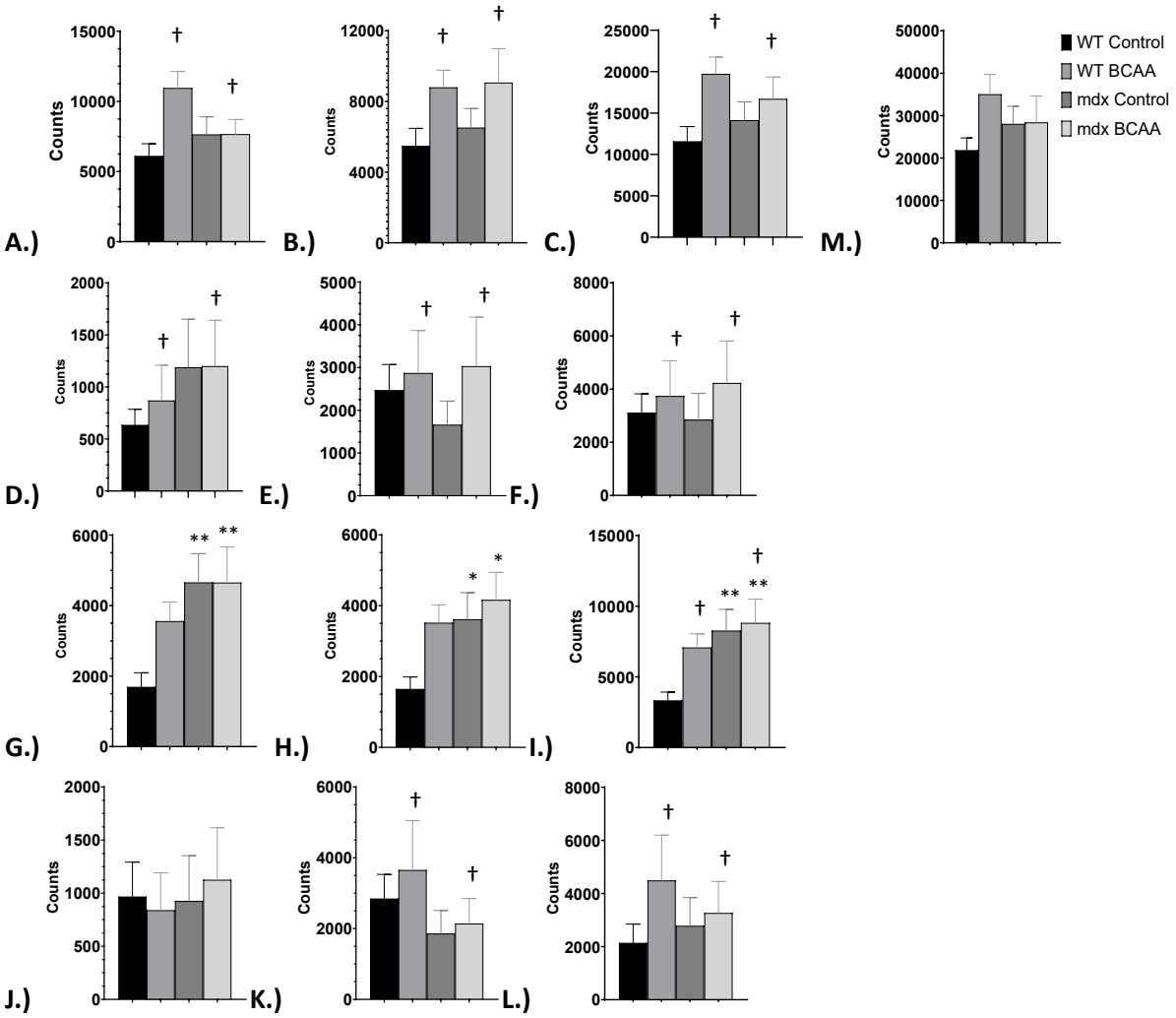

Supplementary Figure 2 – Cage activity at four weeks. Activity was determined using the TSE LabMaster (PhenoMaster) System as described under Methods. The system tracks movement in the X-, Y-, and Z-planes using infrared light beams that recognize locomotor activity. Measurements were obtained at the beginning and end of the study during the dark and light cycles. A.) dark cycle 1 X + Y plane activity, B.) dark cycle 2 X + Y plane activity, C.) dark cycle total X + Y plane activity, D.) dark cycle 1 Z plane activity, E.) dark cycle 2 Z plane activity, F.) dark cycle total Z plane activity, G.) light cycle 1 X + Y plane activity, H.) light cycle 2 X + Y plane activity, I.) light cycle total X + Y plane activity, J.) light cycle 1 Z plane activity, K.) light cycle 2 Z plane activity, L.) light cycle total activity, M.) total activity. Symbols are: ■ WT control, ▩ WT BCAA, ▩ mdx Control, & □ mdx BCAA. Genotype effect: * $p < 0.05$, ** $p < 0.01$. Diet effect: † $p < 0.05$. Standard Errors of the means are presented.

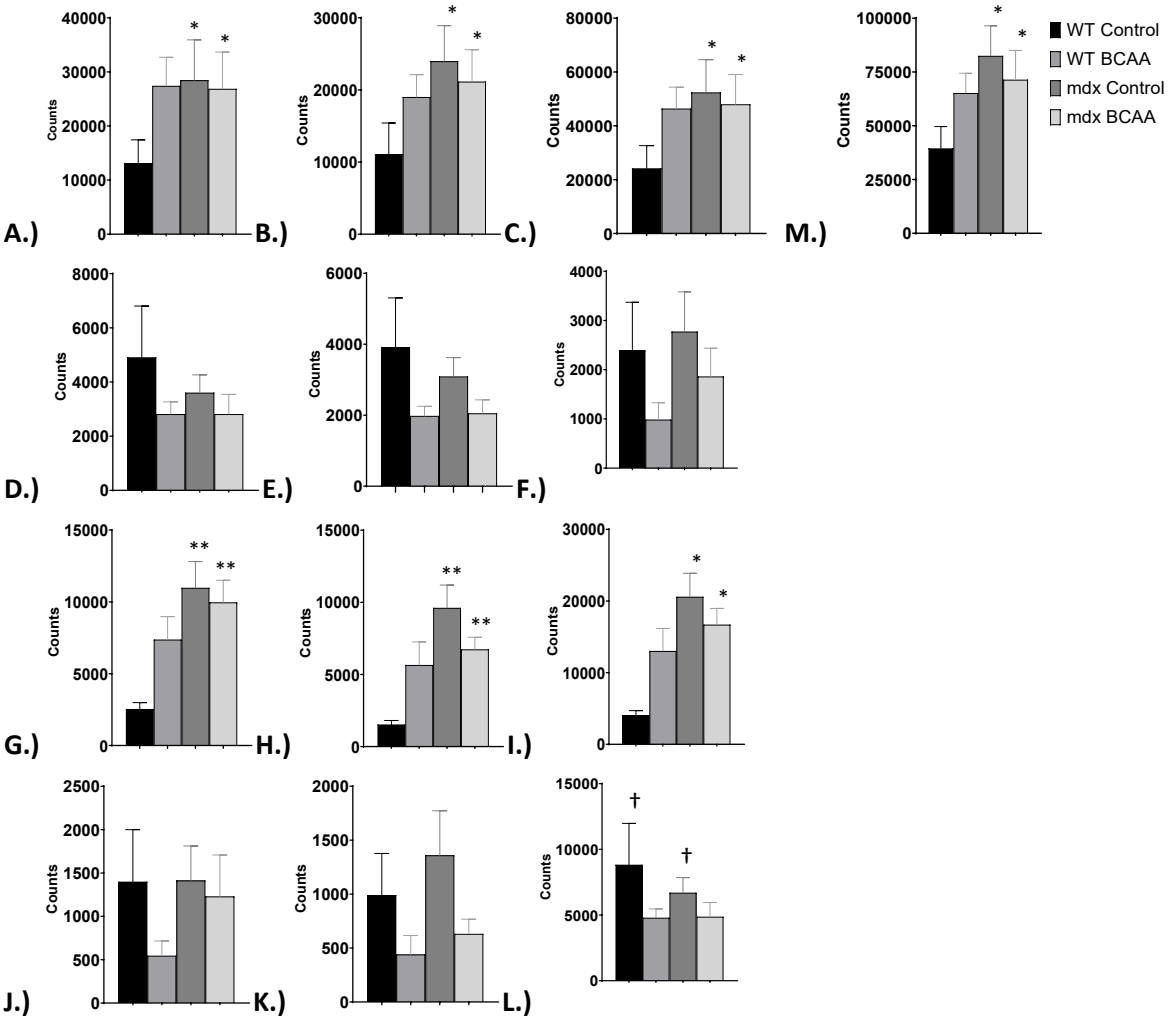

Supplementary Figure 3 – Cage activity at 25 weeks. Activity was determined using the TSE LabMaster (PhenoMaster) System as described under Methods. The system tracks movement in the X-, Y-, and Z-planes using infrared light beams that recognize locomotor activity. Measurements were obtained at the beginning and end of the study during the dark and light cycles. A .) dark cycle 1 X + Y plane activity, B.) dark cycle 2 X + Y plane activity, C.) dark cycle total X + Y plane activity, D.) dark cycle 1 Z plane activity, E.) dark cycle 2 Z plane activity, F.) dark cycle total Z plane activity, G.) light cycle 1 X + Y plane activity, H.) light cycle 2 X + Y plane activity, I.) light cycle total X + Y plane activity, J.) light cycle 1 Z plane activity, K.) light cycle 2 Z plane activity, L.) light cycle total activity, M.) total activity. Symbols are: ■ WT control, ▩ WT BCAA, ▩ mdx Control, & □ mdx BCAA. Genotype effect: * $p < 0.05$. Diet effect: † $p < 0.05$. Standard Errors of the means are presented.